

Stem cell therapy for myocardial infarction

Amber D. Moelker

ISBN 978-90-9021804-5

Printed by PrintPartners Ipskamp

©2007, A. D. Moelker, All rights reserved. No part of this publication may be reproduced, stored in a retrieval system of any nature, or transmitted in any form by any means, electronic, mechanical, photocopying, recording or otherwise, without the written permission of the author.

Stem cell therapy for myocardial infarction

Stamcel therapie voor een myocardi infarct

PROEFSCHRIFT

ter verkrijging van
de graad Doctor aan de Erasmus Universiteit
op gezag van de Rector Magnificus,

Prof. dr. S.W.J. Lamberts

en volgens besluit van het College voor Promoties
de openbare verdediging zal plaatsvinden op

Woensdag 6 Juni 2007 om 11.45 uur

door

Amber Dahvynya Moelker
geboren te Rotterdam



Promotiecommissie

Promotoren: Prof. dr. W. J. van der Giessen
Prof. dr. D. J. Duncker

Overige leden: Prof. dr. P.J. de Feyter
Prof. dr. A. van der Laarse
Prof. dr. J.J. Piek

Financial support by the Netherlands Heart Foundation for the publication of this thesis is gratefully acknowledged.

To those who inspired me

Contents

1.	Introduction	8
<i>Imaging</i>		
2.	Baks T, Cademartiri F, Moelker AD, et al. Assessment of acute reperfused myocardial infarction with 64-slice delayed enhancement computed tomography. Am J Roentgenology. 2007 Feb;188(2):W135-7	18
3.	Baks T, Cademartiri F, Moelker AD, et al. Multislice computed tomography and magnetic resonance imaging for the assessment of reperfused acute myocardial infarction. J Am Coll Cardiol. 2006 Jul 4;48(1):144-52.	26
<i>Assesment of Efficacy</i>		
4.	Moelker AD, Wever K, et al. Umbilical cord blood derived stem cells. EuroIntervention. 2007; 2(Suppl B):1-4.	40
5.	Moelker AD, Baks T, Wever K, et al. Intracoronary Delivery of Umbilical Cord Blood Derived Unrestricted Somatic Stem Cells is Not Suitable to Improve LV Function after Myocardial Infarction in Swine. JMCC. 2007	48
6.	Moelker AD, Baks T, van den Bos EJ, et al. Reduction in infarct size, but no functional improvement after bone marrow cell administration in a porcine model of reperfused myocardial infarction. Eur Heart J. 2006 Dec;27(24):3057-64.	66
<i>Technical issues</i>		
7.	Moelker AD, de Jong M, et al. Grafting of bone marrow derived mononuclear cells is not enhanced by flow limiting injection in a porcine model of myocardial infarction.	82
8.	Moelker AD, de Jong M, et al. Intracoronary injection of cultured bone marrow cells causes micro infarctions in contrast to freshly isolated cells in a porcine model of myocardial infarction.	92
<i>Cell tracking</i>		
9.	Van den Bos EJ, Baks T, Moelker AD, et al. Magnetic resonance imaging of haemorrhage within reperfused myocardial infarcts: possible interference with iron oxide-labelled cell tracking? Eur Heart J. 2006 Jul;27(13):1620-6.	102
10.	Summary and general discussion	116
11.	Samenvatting	120
12.	Over de auteur	124
13.	Dankwoord	126
14.	Colour section	128

Chapter 1

Introduction

Amber D. Moelker, MSc

Department of Experimental Cardiology, Thoraxcenter, Erasmus MC, Rotterdam, the Netherlands

Introduction

Epidemiology of heart failure

Coronary artery disease is still one of the leading causes of morbidity and mortality in western society¹. In The Netherlands (www.hartstichting.nl) 32% of all deaths are caused by heart and vascular diseases. This translates in more than 44.000 people per year, of which 24% died after a myocardial infarction. In The Netherlands in 2005, 66 patients per day were hospitalized due to a myocardial infarction of which only 11% died during hospitalization. In contrast, in 1972 21% of the hospitalized patients died in the hospital after a myocardial infarction. The incidence of a myocardial infarction in The Netherlands is estimated at 2.3 per 1000 persons.

Myocardial infarction causes abrupt loss of left ventricular synergy and global dysfunction. After myocardial infarction, the decreased left ventricular function results in a decreased ejection fraction and cardiac output due to the loss of cardiomyocytes. Rapid neurohumoral activation and early ventricular chamber dilatation contribute to restoring stroke volume despite the depressed ejection fraction. Continued neurohumoral activation provokes late remodeling of the remote non-infarcted myocardium, characterized by a progressively increasing left ventricular volume/mass ratio that leads to further remodeling. Due to dilation caused by remodeling, end systolic and diastolic volumes are increased after infarction.

Heart failure is a progressive disorder of left ventricular remodeling. Heart failure from post-infarction remodeling due to the dysfunctional scar tissue causes continuous abnormal loading conditions. Left ventricular remodeling is a dynamic process that is driven by a number of factors. During remodeling, the left ventricle becomes dilated, changes shape, and undergoes morphologic and physiologic alterations at the cellular level². This results eventually in depressed left ventricular contractility. Pathologically, there is extensive fibrosis with abnormally structured myocardial cells that are disarrayed². Apoptosis (programmed cell death) becomes more active, resulting in additional loss of myocardial cells. It is the combination of these pathologic changes that deforms the structure of the heart and impairs the dynamics of the left ventricle.

Patients with coronary artery disease, who survive a myocardial infarction, are at an increased risk of developing heart failure. The extent of left ventricular systolic and diastolic dysfunction is associated with clinical symptoms and cardiovascular mortality. In The Netherlands ~200.000 patients suffer from heart failure, and the number of patients increases with 10% every year. In general, the prognosis of patients with heart failure is poor; 70% of patients is still alive one year after diagnosis of heart failure and 35% is still alive five years after the diagnosis. Although medical care (of acute myocardial infarction) has considerably improved over the last decades, this paradoxically resulted in a higher prevalence of patients with heart failure³. This paradox is partly because the population is getting older⁴ but also because of the reduced number of people who die after myocardial infarction. Unfortunately, those people end up with heart failure, which decreases life expectancy and quality of life⁵; People with heart failure may experience breathlessness and coughing. Due to edema they experience swelling of the feet, ankles, legs or abdomen. People with heart failure may also experience heart palpitations. Therefore these patients would benefit

enormously from an improvement in cardiac function, which results in an improvement in symptoms. An improvement in cardiac function improves the prognosis of these patients⁶.

Conventional pharmacological treatment of heart failure

The more common forms of heart failure, those due to damage that has accumulated over time, cannot be cured, but they can be stabilized by lifestyle changes, medication or surgery. Lifestyle changes like quitting smoking, losing weight, avoiding alcohol and caffeine, eating a low-saturated-fat low-sodium diet, exercising and reducing stress can help to alleviate symptoms, slow the disease's progression and improve everyday life. Medication can also be used to slow the progression of heart failure.

ACE inhibitors (angiotensin-converting-enzyme inhibitors) are now considered first-choice treatment and are the cornerstone of heart failure drug therapy⁷. ACE inhibitors limit the formation of angiotensin II. Angiotensin II causes small blood vessels to constrict, which raises blood pressure and places more stress on the heart. ACE inhibitors prevent cardiac hypertrophy⁸, prevent fibrosis and decrease afterload and preload. In stead of ACE inhibitors, Angiotensin II receptor blockers can be prescribed. Diuretics are prescribed for almost all patients who have volume overload in the body and swelling of the tissues. This helps to relieve the heart's workload, since there is less fluid and at lower preload to pump throughout the body. Digoxin increases the force of the heart's contractions. This relieves heart failure symptoms, especially when the patient is not responding to ACE inhibitors and diuretics. Beta-blockers are prescribed to most patients to reduce heart rate and lower blood pressure. They also inhibit ventricular remodeling and reduce the risk of arrhythmias and sudden death⁹.

At this moment there is no sufficient treatment for patient with end-stage heart failure. Medical therapy can attenuate remodeling and improve survival but does not change the size of the scar. Drug treatment does not lead to sufficient recovery of left ventricular function. Unfortunately, angioplasty or bypass surgery does not reverse the damage in the myocardium after infarction. Transplantable donor hearts are scarce, and left ventricular assist devices can prolong patient lives only for several weeks or months. Therefore, there is an urgent demand for a new therapy to treat patients suffering from heart failure after a myocardial infarction.

Stem cell therapy

Several animals such as planarian platworms and amphibians have the ability to regrow missing body parts with speed and precision. This remarkable physiological process is called regeneration. Salamanders for example can regenerate lost body parts¹⁰, like a limb, by dedifferentiation of specialized cells into stem cells. Subsequently, these cells proliferate and will eventually differentiate into the specialized cells of the regenerated organ. This second process is similar to what happens in the blastula of embryos. Zebrafish are able to regenerate their heart completely.¹¹ Humans have lost most of their regenerative capacity, except for wound healing and liver regeneration after partial hepatectomy. The human heart was always thought to be a terminally differentiated organ, however almost ten years ago it became clear that cardiomyocytes can divide¹². It became clear that this even

happened after myocardial infarction¹³. The hope that patients who suffer from myocardial infarction can be treated with stem cells is based on this remarkable regeneration ability of animals¹⁴, on observations of bone marrow transplants in patients suffering from leukemia, and on the recently discovered plasticity of the human heart. The presence of donor bone marrow cells in the hearts of patients that underwent a bone marrow transplantation¹⁵ suggests that bone marrow might play a role in repairing the myocardium and vasculature.

Experimental studies in rodents showed a great potential of stem cells in the regeneration of infarcted myocardium¹⁶. Injection of stem cell therapy after experimental myocardial infarction in rodents caused an improvement of left ventricular function and regeneration of the infarcted myocardium by newly formed myocytes and blood vessels¹⁷. In the last decade more than 100 experimental studies that have used stem cells to regenerate the myocardium after infarction have been published. Initially they all invariably demonstrated a positive effect on left ventricular function and infarct size after injection. Therefore, these positive results in experimental studies suggest that stem cell therapy could offer a therapy for patients suffering from myocardial infarction and may prevent the development of heart failure.

To date several clinical trials have been completed¹⁸⁻²⁷, which all used bone marrow or blood derived cells to treat patients after acute myocardial infarction. In these trials, there are differences in selection and *in vitro* processing of the bone marrow derived cells. There are also differences in inclusion criteria between the trials, differences in the timing of cell injection, follow-up time and choice of endpoints²⁸⁻³⁰. Although left ventricular function increases in most trials after stem cell therapy, this was not the case for all trials²¹⁻²³. The BOOST-update²⁶ showed that the initial benefit of mononuclear cell injection after acute myocardial infarction was lost over time compared to the controls. Therefore, the long-term efficacy of stem cell therapy needs to be determined. Furthermore, the mechanistic basis of the improvement observed in cardiac function in clinical trials is not explained in these studies.

There are many questions that need to be answered before stem cell therapy can be applied as a standard treatment for patients³¹.

Cell type

It remains unclear which cell³², in which numbers, will lead to the optimal recovery of left ventricular function after myocardial infarction. A variety of cell types have been identified, each with distinct characteristics with varying potency to repair infarcted myocardium and with different advantages and disadvantages³³. Bone marrow or blood is an easily available and safe cell source containing several side populations which have been used in previous studies, e.g. hematopoietic cells³⁴, endothelial progenitor cells³⁵, CD133+ (Cellular Differentiation nomenclature) cells¹⁸ and mesenchymal stems³⁶. A potential disadvantage of bone marrow derived cells is that they are harvested from a diseased person. It has been demonstrated that bone marrow cells from patients suffering from heart failure have decreased proliferation, migration and differentiation capacity³⁷. The major advantage of bone marrow or

blood derived cells is that they can be easily injected intracoronary and it is an autologous cell source²⁸.

Although the intramyocardial injection of skeletal myoblasts³⁸ can lead to replacement of scar tissue by myotubes, these cells fail to electromechanically couple to resident myocytes *in vivo*³⁵. In patients, this potentially induces arrhythmias³⁹, and therefore, these cells are currently only implanted in patients with an internal defibrillator.

The use of embryonic stem cells raises ethical difficulties, however these cells have a great potential to differentiate into cardiomyocytes and integrate structurally with recipient myocytes. However, there are concerns about the tumorigenicity of embryonic stem cells⁴⁰. Therefore, embryonic stem cells are not yet ready to be tested in clinical trials.

Recently, several populations of resident cardiac stem/progenitor cells have been identified⁴¹. More research need to be performed before it will become clear whether these cells can be easily isolated, expanded and injected in patients or activated in-situ to replace scar tissue.

Timing and route of administration

Timing of cell injection⁴² after infarction and the route of cell administration⁴³ could influence the potential capacity of stem cells to regenerate the myocardium. Several modes of cell administration have been investigated, including intramyocardial, intravenous, transendocardial and epicardial as well as intracoronary injection^{43,44}. The major advantage of intracoronary injection is the wide infusion of the cells in the infarct area. In contrast, intravenous injection is thought to cause less sufficient homing of the injected cells to the site of injury. This is in contrast to intramyocardial injection, where cells are only distributed in the injected tissue. However, it is not clear yet which injection method will lead to optimal recovery of left ventricular infarct size after myocardial infarction.

It should be investigated whether the route of administration or the injection of certain cell types can cause micro infarctions, which has been demonstrated in dogs⁴⁵.

Mechanism of cardiac regeneration

Although all initial preclinical stem cell studies showed a beneficial effect of stem cell therapy, to date, there also are several clinical and preclinical studies with neutral or even negative effects of stem cell therapy. Taken together all the reports on the effect of stem cells after myocardial infarction, these findings are sometimes confusing and contradicting⁴⁶.

So far, the mechanism of cardiac regeneration remains unclear. Even the regenerative capacity of, for example, zebrafish is not fully understood yet. Until the mechanism of regeneration of myocardium after infarction is understood in experimental models, further optimised stem therapy cannot be applied yet to patients in routine clinical practice.

Determination of the effects of stem cell therapy

To evaluate the effect and efficacy of stem cell therapy on the heart after infarction several imaging modalities can be used to assess left ventricular function and infarct size. In clinical trials, magnetic resonance imaging is predominantly performed to evaluate cardiac function before and after stem cell injection⁴⁷. Cardiac volumes, myocardial mass, global function, regional function and infarct size can be measured non-invasively with magnetic resonance to evaluate the effect of stem cell therapy.

Cell labeling is a method to track cells after injection and to investigate the fate of the injected cells. Tracking can be performed directly *in vivo* using magnetic resonance imaging or single-photon emission computed tomography for example, but cells can also be tracked *ex vivo* using histology. Immunohistochemistry makes it possible to determine the phenotype of the injected cells. This will help understanding the mechanism of cardiac regeneration.

Aim of the present thesis

The aim of this thesis is to validate non-invasive imaging techniques for infarct size measurement, to assess safety and efficacy of several stem cell sources and to explore a method to track the cells *in vivo*.

This thesis addresses the promising novel stem cell treatment for patients suffering from myocardial infarction using a large, more translational, animal model. Previous studies in rodents all induced a myocardial infarction by permanent ligation of a coronary artery, and therefore the route of administration of stem cells was limited to intramyocardial¹⁶ or intravenous⁴⁸ injection. However in patients, the standard therapy for myocardial infarction as described in the guidelines is reperfusion therapy, preferably by percutaneous coronary intervention. Furthermore, in most clinical trials, bone marrow or blood derived stem cells were injected intracoronary in patients with acute myocardial infarction. To evaluate the potential of stem cell therapy, we investigated the effect of intracoronary stem cell injection in a porcine pre-clinical model of myocardial infarction followed by reperfusion which closely mimics clinical settings.

Chapters two and three describe the imaging techniques used to assess left ventricular function and infarct size in our model. In chapter two infarct size measurement by multislice computed tomography is compared with histology. In chapter three infarct size is assessed by both computed tomography and magnetic resonance imaging.

In chapters four to six the effects of stem cell therapy on left ventricular function and infarct size after myocardial infarction are described. To address these effects, we used magnetic resonance imaging to study several different stem cells. The initial experiences with human umbilical cord blood derived cells in animal models is reviewed in chapter four, while the effects of human umbilical cord blood derived unrestricted somatic stem cells on the porcine left ventricular function after myocardial infarction has been described in chapter five. In chapter six, the effect of autologous unselected bone marrow is compared with mononuclear cells isolated from the bone marrow.

In chapters five and six we injected cells intracoronary at a normal arterial flow rate, while clinical trials used the method of intermittent balloon occlusion. Therefore we investigated in chapter seven whether there are differences in cell engraftment

after cell injection during normal/uninterrupted coronary blood flow and after injection during intermittent balloon occlusion.

Since we observed in chapter five that cultured umbilical cord blood derived cells caused micro infarctions after intracoronary injection, we hypothesized that this could also occur after the injection of cultured bone marrow derived cells. In chapter eight the differences between injections of cultured bone marrow derived mononuclear cells and freshly isolated mononuclear cells are addressed.

To investigate the fate of injected cells *in vivo*, injected cells need to be recognized after injection. Autologous cells are not easy to track *in vivo*. In chapter nine iron-oxide labeling is evaluated as a possible marker for stem cell tracking after injection.

References

1. Kay D, Blue A, Pye P, et al. Heart failure: improving the continuum of care. *Care Manag J*. Summer 2006;7(2):58-63.
2. Francis GS, McDonald K, Chu C, et al. Pathophysiologic aspects of end-stage heart failure. *Am J Cardiol*. Jan 19 1995;75(3):11A-16A.
3. Eriksson H. Heart failure: a growing public health problem. *J Intern Med*. Feb 1995;237(2):135-141.
4. Longer survival, more cases, boost heart failure population. *Harv Heart Lett*. May 2006;16(9):7.
5. Masoudi FA, Rumsfeld JS, Havranek EP, et al. Age, functional capacity, and health-related quality of life in patients with heart failure. *J Card Fail*. Oct 2004;10(5):368-373.
6. Heywood JT, Elatre W, Pai RG, et al. Simple clinical criteria to determine the prognosis of heart failure. *J Cardiovasc Pharmacol Ther*. Sep 2005;10(3):173-180.
7. Tiyyagura SR, Pinney SP. Left ventricular remodeling after myocardial infarction: past, present, and future. *Mt Sinai J Med*. Oct 2006;73(6):840-851.
8. van Kats JP, Duncker DJ, Haitsma DB, et al. Angiotensin-converting enzyme inhibition and angiotensin II type 1 receptor blockade prevent cardiac remodeling in pigs after myocardial infarction: role of tissue angiotensin II. *Circulation*. Sep 26 2000;102(13):1556-1563.
9. Domanski MJ, Krause-Steinrauf H, Massie BM, et al. A comparative analysis of the results from 4 trials of beta-blocker therapy for heart failure: BEST, CIBIS-II, MERIT-HF, and COPERNICUS. *J Card Fail*. Oct 2003;9(5):354-363.
10. Brockes JP. Amphibian limb regeneration: rebuilding a complex structure. *Science*. Apr 4 1997;276(5309):81-87.
11. Poss KD. Getting to the heart of regeneration in zebrafish. *Semin Cell Dev Biol*. Nov 24 2006.
12. Anversa P, Kajstura J. Ventricular myocytes are not terminally differentiated in the adult mammalian heart. *Circ Res*. Jul 13 1998;83(1):1-14.
13. Beltrami AP, Urbanek K, Kajstura J, et al. Evidence that human cardiac myocytes divide after myocardial infarction. *N Engl J Med*. Jun 7 2001;344(23):1750-1757.
14. Bongso A, Richards M. History and perspective of stem cell research. *Best Pract Res Clin Obstet Gynaecol*. Dec 2004;18(6):827-842.
15. Deb A, Wang S, Skelding KA, et al. Bone marrow-derived cardiomyocytes are present in adult human heart: A study of gender-mismatched bone marrow transplantation patients. *Circulation*. Mar 11 2003;107(9):1247-1249.
16. Orlic D, Kajstura J, Chimenti S, et al. Bone marrow cells regenerate infarcted myocardium. *Nature*. Apr 5 2001;410(6829):701-705.
17. Tang J, Xie Q, Pan G, et al. Mesenchymal stem cells participate in angiogenesis and improve heart function in rat model of myocardial ischemia with reperfusion. *Eur J Cardiothorac Surg*. Aug 2006;30(2):353-361.
18. Bartunek J, Vanderheyden M, Vandekerckhove B, et al. Intracoronary injection of CD133-positive enriched bone marrow progenitor cells promotes cardiac recovery after recent myocardial infarction: feasibility and safety. *Circulation*. Aug 30 2005;112(9 Suppl):I178-183.

19. Chen SL, Fang WW, Ye F, et al. Effect on left ventricular function of intracoronary transplantation of autologous bone marrow mesenchymal stem cell in patients with acute myocardial infarction. *Am J Cardiol*. Jul 1 2004;94(1):92-95.
20. Fernandez-Aviles F, San Roman JA, Garcia-Frade J, et al. Experimental and clinical regenerative capability of human bone marrow cells after myocardial infarction. *Circ Res*. Oct 1 2004;95(7):742-748.
21. Janssens S, Dubois C, Bogaert J, et al. Autologous bone marrow-derived stem-cell transfer in patients with ST-segment elevation myocardial infarction: double-blind, randomised controlled trial. *Lancet*. Jan 14 2006;367(9505):113-121.
22. Kuethe F, Richartz BM, Sayer HG, et al. Lack of regeneration of myocardium by autologous intracoronary mononuclear bone marrow cell transplantation in humans with large anterior myocardial infarctions. *Int J Cardiol*. Oct 2004;97(1):123-127.
23. Lunde K, Solheim S, Aakhus S, et al. Intracoronary injection of mononuclear bone marrow cells in acute myocardial infarction. *N Engl J Med*. Sep 21 2006;355(12):1199-1209.
24. Schachinger V, Assmus B, Britten MB, et al. Transplantation of progenitor cells and regeneration enhancement in acute myocardial infarction: final one-year results of the TOPCARE-AMI Trial. *J Am Coll Cardiol*. Oct 19 2004;44(8):1690-1699.
25. Strauer BE, Brehm M, Zeus T, et al. Repair of infarcted myocardium by autologous intracoronary mononuclear bone marrow cell transplantation in humans. *Circulation*. Oct 8 2002;106(15):1913-1918.
26. Meyer GP, Wollert KC, Lotz J, et al. Intracoronary bone marrow cell transfer after myocardial infarction: eighteen months' follow-up data from the randomized, controlled BOOST (BOne marrOw transfer to enhance ST-elevation infarct regeneration) trial. *Circulation*. Mar 14 2006;113(10):1287-1294.
27. Schachinger V, Erbs S, Elsasser A, et al. Intracoronary bone marrow-derived progenitor cells in acute myocardial infarction. *N Engl J Med*. Sep 21 2006;355(12):1210-1221.
28. Ang KL, Shenje LT, Srinivasan L, et al. Repair of the damaged heart by bone marrow cells: from experimental evidence to clinical hope. *Ann Thorac Surg*. Oct 2006;82(4):1549-1558.
29. Haider H. Bone marrow cells for cardiac regeneration and repair: current status and issues. *Expert Rev Cardiovasc Ther*. Jul 2006;4(4):557-568.
30. Allan R, Kass M, Glover C, et al. Cellular transplantation: future therapeutic options. *Curr Opin Cardiol*. Mar 2007;22(2):104-110.
31. Nanjundappa A, Raza JA, Dieter RS, et al. Cell transplantation for treatment of left-ventricular dysfunction due to ischemic heart failure: from bench to bedside. *Expert Rev Cardiovasc Ther*. Jan 2007;5(1):125-131.
32. Hampton T. Search is on for cells that repair heart. *Jama*. Dec 6 2006;296(21):2541.
33. Murry CE, Reinecke H, Pabon LM. Regeneration gaps: observations on stem cells and cardiac repair. *J Am Coll Cardiol*. May 2 2006;47(9):1777-1785.
34. Thompson CA, Reddy VK, Srinivasan A, et al. Left ventricular functional recovery with percutaneous, transvascular direct myocardial delivery of bone marrow-derived cells. *J Heart Lung Transplant*. Sep 2005;24(9):1385-1392.
35. Katritsis DG, Sotiropoulou PA, Karvouni E, et al. Transcoronary transplantation of autologous mesenchymal stem cells and endothelial progenitors into infarcted human myocardium. *Catheter Cardiovasc Interv*. Jul 2005;65(3):321-329.
36. Amado LC, Saliaris AP, Schuleri KH, et al. Cardiac repair with intramyocardial injection of allogeneic mesenchymal stem cells after myocardial infarction. *Proc Natl Acad Sci U S A*. Aug 9 2005;102(32):11474-11479.
37. Vasa M, Fichtlscherer S, Aicher A, et al. Number and migratory activity of circulating endothelial progenitor cells inversely correlate with risk factors for coronary artery disease. *Circ Res*. Jul 6 2001;89(1):E1-7.
38. Hagege AA, Marolleau JP, Vilquin JT, et al. Skeletal myoblast transplantation in ischemic heart failure: long-term follow-up of the first phase I cohort of patients. *Circulation*. Jul 4 2006;114(1 Suppl):I108-113.
39. Abraham MR, Hare JM. Is skeletal myoblast transplantation proarrhythmic? The jury is still out. *Heart Rhythm*. Apr 2006;3(4):462-463.
40. Trounson A. Human embryonic stem cells: mother of all cell and tissue types. *Reprod Biomed Online*. 2002;4 Suppl 1:58-63.

Chapter 1

41. Lyngbaek S, Schneider M, Hansen JL, et al. Cardiac regeneration by resident stem and progenitor cells in the adult heart. *Basic Res Cardiol*. Mar 2007;102(2):101-114.
42. Bartunek J, Wijns W, Heyndrickx GR, et al. Timing of intracoronary bone-marrow-derived stem cell transplantation after ST-elevation myocardial infarction. *Nat Clin Pract Cardiovasc Med*. Mar 2006;3 Suppl 1:S52-56.
43. Sherman W, Martens TP, Viles-Gonzalez JF, et al. Catheter-based delivery of cells to the heart. *Nat Clin Pract Cardiovasc Med*. Mar 2006;3 Suppl 1:S57-64.
44. Freyman T, Polin G, Osman H, et al. A quantitative, randomized study evaluating three methods of mesenchymal stem cell delivery following myocardial infarction. *Eur Heart J*. Mar 1 2006.
45. Vulliet PR, Greeley M, Halloran SM, et al. Intra-coronary arterial injection of mesenchymal stromal cells and microinfarction in dogs. *Lancet*. Mar 6 2004;363(9411):783-784.
46. Metharom P, Doyle B, Caplice NM. Clinical trials in stem cell therapy: pitfalls and lessons for the future. *Nat Clin Pract Cardiovasc Med*. Feb 2007;4 Suppl 1:S96-99.
47. Gibbons RJ, Araoz PA, Williamson EE. The year in cardiac imaging. *J Am Coll Cardiol*. Dec 5 2006;48(11):2324-2339.
48. Schuster MD, Kocher AA, Seki T, et al. Myocardial neovascularization by bone marrow angioblasts results in cardiomyocyte regeneration. *Am J Physiol Heart Circ Physiol*. Sep 2004;287(2):H525-532.

Chapter 2

Assessment of Acute Reperfused Myocardial Infarction with Delayed Enhancement 64-MDCT

Timo Baks, MD,*† Filippo Cademartiri, MD, PhD,*† Amber D. Moelker, MSc,* Willem J. van der giessen, MD, PhD,* Gabriel P. Krestin, MD, PhD,† Dirk J. Duncker, MD, PhD,* Pim J. de Feyter, MD, PhD, FACC*†

From the *Department of Cardiology, Thoraxcenter, and the †Department of Radiology, Erasmus University Medical Center, Rotterdam, the Netherlands

Abstract

Objective The purpose of this study was to evaluate the utility of delayed enhancement 64-MDCT in the assessment of myocardial infarct size in a porcine model of acute reperfused myocardial infarction. CT can be used for noninvasive assessment of coronary artery stenosis, but to our knowledge, evaluation of myocardial viability in the subacute phase of acute myocardial infarction has not been validated. We performed delayed enhancement imaging on six domestic swine 5 days after reperfused acute myocardial infarction and assessed the relation between delayed enhancement patterns in vivo and the extent of viable and nonviable myocardium at postmortem histochemical analysis.

Conclusion Delayed enhancement imaging with 64-MDCT can be used for accurate assessment of the size of reperfused acute myocardial infarcts.

Introduction

MDCT is used for the evaluation of coronary artery disease and has high diagnostic accuracy in the detection of coronary artery stenosis^{1,2}. The diagnostic value of MDCT for assessment of myocardial viability in the subacute phase of acute myocardial infarction is unclear. Studies^{3,4} have shown that MDCT during the first pass after administration of an iodinated contrast agent results in low tissue contrast between infarcted and uninfarcted myocardium and that total infarct size appears to be underestimated. A delayed enhancement imaging protocol as used in MRI may be an alternative approach. Excellent tissue contrast with MRI is obtained 10–30 minutes after administration of gadolinium derivatives, because this type of contrast agent accumulates in the infarcted tissue. The pharmacokinetic behavior of gadolinium chelates is somewhat similar to that of iodinated contrast agents⁵. We performed delayed enhancement MDCT in a porcine model of reperfused acute myocardial infarction to investigate whether reperfused infarct size can be assessed accurately with delayed enhancement MDCT.

Materials and Methods

Animal Model

Six Yorkshire-Landrace pigs (age, 2–3 months; weight, 22 kg) were subjected to coronary angiography followed by balloon occlusion of the left circumflex coronary artery. Reperfusion was obtained by deflation of the balloon after 2 hours of ischemia. The study complied with the regulations of the animal care committee of the Erasmus Medical Center and the “Guide for the Care and Use of Laboratory Animals” (National Institutes of Health, 1996). Animals were sedated (ketamine 20 mg/kg intramuscularly and midazolam 1 mg/kg intramuscularly), anesthetized (thiopental, 12 mg/kg IV), intubated, and mechanically ventilated (mixture of oxygen and nitrogen, 1:2). Anesthesia was maintained with fentanyl (12.5 µg/kg/h).

CT

Five days after induction of myocardial infarction, all swine were anesthetized as described earlier and subjected to MDCT. Mean heart rate decreased from approximately 80 to 45 ± 9 beats per minute (BPM) after administration of zatebradine (10 mg/kg IV). A 64-MDCT scanner (Sensation 64, Siemens Medical Solutions) was used for imaging with the following characteristics: number of detector rows, 32×2 (oversampling in the z-axis obtained with flying focal spot); number of slices per rotation, 64; individual detector width, 0.6 mm; gantry rotation time, 330 milliseconds; effective temporal resolution, 165 milliseconds. Delayed enhancement imaging was performed 15 minutes after administration of 80 mL of iodinated contrast agent (iomeprol 400 mg I/mL, Iomeron, Bracco) through an ear vein. The following scan parameters were used: effective tube current, 900 mAs at kV 120; feed per rotation, 3.84 mm; scan direction, craniocaudal. The estimated radiation dose if used for a human protocol would have been 15 mSv for men and 21 mSv for women. Delayed enhancement MDCT data sets were reconstructed at –300, –350, and –400 milliseconds before the next R wave (end-diastolic phase of the cardiac cycle). From

the data set with optimal image quality, images with a slice thickness of 1 mm and an increment of 0.5 mm were reconstructed in the short-axis view with a dedicated software platform with multiplanar capabilities (Leonardo, Siemens).

Data Analysis

One day after MDCT, all pigs were sacrificed and the hearts excised. The myocardium of the left ventricle was cut in 8-mm consecutive slices in the short-axis view with a commercially available meat slicer. For viability staining, the slices were embedded in a solution of 1% triphenyltetrazolium chloride (TTC) and 0.2 mol/L Sørensen's buffer (pH, 7.4) at 37°C for 15 minutes and then fixed in 4% formalin. The slices were photographed with a digital camera. The digitalized TTC-stained slices were loaded in a separate workstation with a commercially available analysis package (SigmaScan Pro 5.0, Systat). TTC-negative borders and endocardial and epicardial borders of the left ventricle were traced manually in all consecutive slices. Infarct size was defined as TTC-negative area as a percentage of total left ventricular slice area.

Reconstructed MDCT images were exported and transferred to a separate workstation with dedicated software (Cine Tool, GE Healthcare). The region with delayed enhancement was selected manually on these images. Infarct size per slice was calculated by dividing the delayed enhanced area by the total slice area. CT attenuation values were measured by drawing three 10-mm² regions of interest in delayed enhanced myocardium, remote myocardium, and the left ventricular cavity in a short-axis slice located at the center of the infarction of each pig³.

Statistical Analysis

Data were presented as mean \pm SD. Univariate linear regression analysis and Bland-Altman analysis were used to evaluate the relation between infarct size measured with MDCT and infarct size measured with postmortem histochemical analysis. One-way analysis of variance with repeated measures was used for the comparison of CT attenuation values of delayed enhanced myocardium, remote myocardium, and the left ventricular cavity. Posthoc Bonferroni correction was applied to adjust for multiple comparisons. Significance was accepted at $p \leq 0.05$ (two-tailed).

Results

All MDCT data sets were of good image quality. Delayed enhancement observed in the lateral wall of the left ventricle corresponded to the perfusion territory of the circumflex coronary artery (Figs. 1 and 2). No delayed enhancement was seen in remote myocardium. Four of the 42 available histochemical slices had to be excluded because postmortem shrinkage made measurement of infarct area and slice area impossible. TTC- negative areas (infarcted myocardium) were found in the lateral wall of the left ventricle but not in remote myocardium (Figs. 1 and 2).

Mean infarct size was 28% \pm 13% on MDCT images and 26% \pm 12% on histochemical images. Infarct size measured with MDCT correlated well with infarct size measured on histochemical images ($R^2=0.92$; $p < 0.001$) (Fig. 3). The mean MDCT value of delayed enhanced myocardium (141 \pm 10 H) was significantly different from that of remote myocardium (71 \pm 8 H; $p < 0.001$) and from that of the left ventricular cavity

(115 ± 8 H; $p < 0.001$). The relative difference in MDCT value between infarcted and uninfarcted myocardium was $206\% \pm 14\%$.

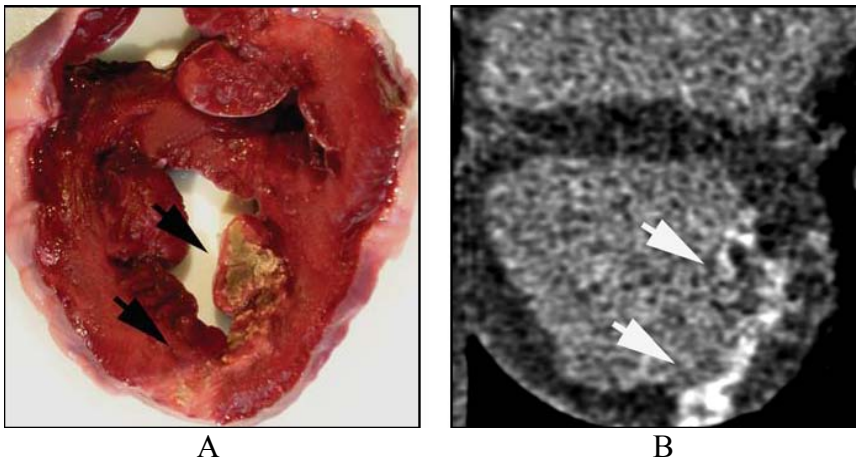


Fig. 1 Pig with subendocardial myocardial infarction. **A**, Photograph of postmortem histochemical specimen in midventricular short-axis view shows infarct (*arrows*). **B**, Delayed enhancement MDCT scan in midventricular short-axis view shows infarct (*arrows*).

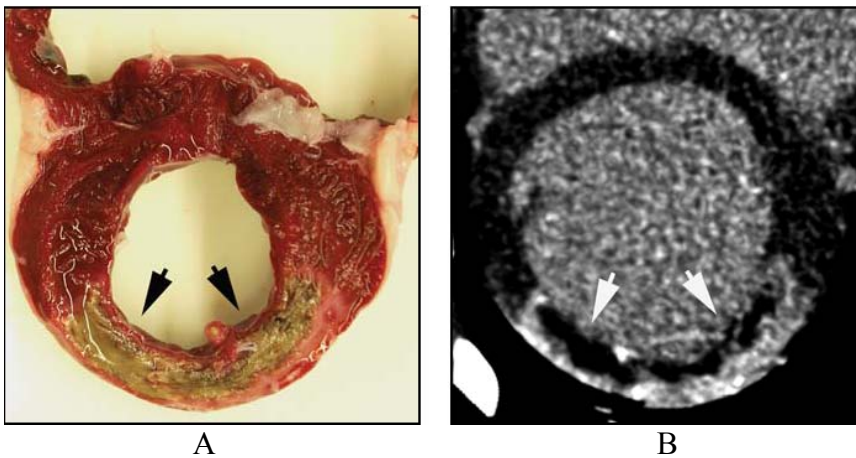
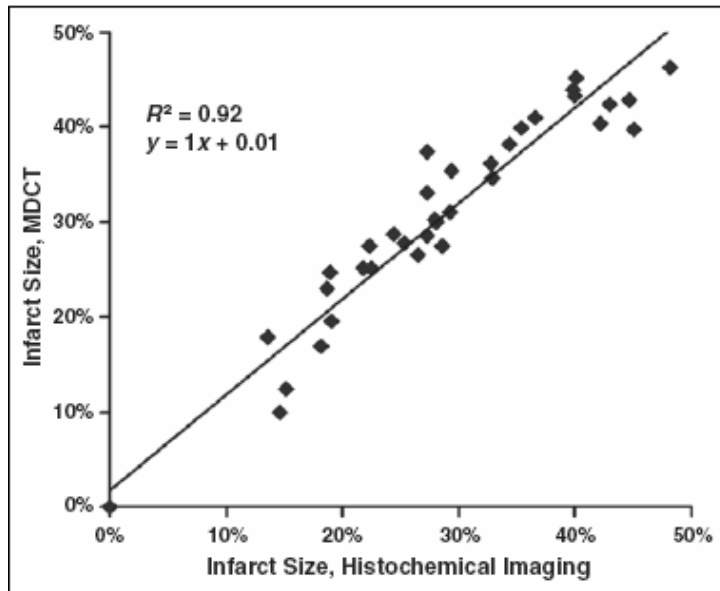


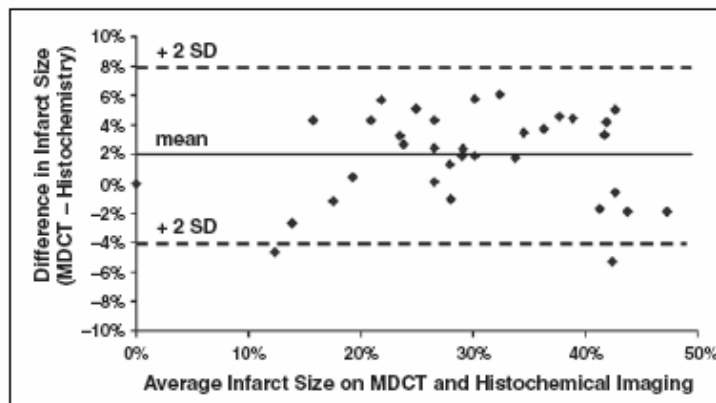
Fig. 2 Pig with transmural myocardial infarction. **A**, Photograph of histochemical specimen in short-axis view shows infarct (*arrows*). **B**, Delayed enhancement MDCT scan of specimen shows infarct (*arrows*).

Discussion

MDCT technology has developed rapidly with a marked increase in temporal and spatial resolution. Noninvasive evaluation of coronary artery disease is feasible, and several studies have shown good diagnostic accuracy in the detection of coronary artery stenosis. Evaluation of myocardial viability in the subacute phase of acute myocardial infarction has been studied with MDCT, but limited data are available. For example, Hoffmann et al.³ performed MDCT coronary angiography within 5 hours



A



B

Fig. 3—Reliability of MDCT versus histochemical analysis in assessment of acute reperfused myocardial infarct size per slice. **A**, Graph shows results of linear regression analysis. **B**, Graph shows results of Bland-Altman analysis.

of acute nonreperfused myocardial infarction in swine and found good correlation between the size of perfusion defects and the size of infarcts estimated at postmortem histochemical analysis. Mahnken et al.⁶ performed 16-MDCT coronary angiography followed by delayed enhancement CT and MRI in patients within 14 days of reperfused acute myocardial infarction. Infarct size measured on delayed enhancement CT and delayed enhancement MRI was comparable, but infarct size measured on perfusion images remained underestimated.

In this study, we used an experimental model of reperfused acute myocardial infarction because early aggressive reperfusion is currently the preferred treatment in the clinical setting of acute myocardial infarction. Delayed enhancement imaging was

performed because the contrast agents used for MDCT (iodinated contrast material) and MRI (gadolinium derivatives) accumulate in infarcted myocardium 10–30 minutes after IV administration while they are being washed out of remote myocardium^{7,8}. We did not perform perfusion imaging because MRI studies of reperfused myocardial infarction have shown that total infarct size remains underestimated with perfusion imaging. During the first pass of a contrast agent, infarcted myocardium with an intact microvasculature becomes normally enhanced while infarcted myocardium with microvascular obstruction appears as a perfusion defect⁹. We found that infarct size can be assessed accurately with delayed enhancement 64-MDCT if imaging is performed 5 days after reperfused myocardial infarction.

A well-known concern about MDCT is the use of iodinated contrast agents and radiation exposure to the patient. Our results encourage further research into optimization of protocols that involve use of less radiation and less iodinated contrast material and into optimal timing of delayed enhancement imaging after contrast administration. Furthermore, image quality is heart rate dependent, and images may be impaired at heart rates greater than 70 BPM¹⁰.

Measurement of infarct size in patients with acute myocardial infarction is clinically relevant because infarct size is predictive of left of myocardial viability in reperfused acute myocarventricular function and geometric configuration and, hence, long-term clinical outcome^{11,12}. Information on infarct size obtained with MDCT would enhance the diagnostic armamentarium of physicians who lack access to RM. Myocardial magnetic resonance imaging cardiac MRI or encounter patients who have contraindications to MRI.

Acknowledgement

We thank Wendy Kerver for her help in the logistics of this study.

References

1. Nieman K, Cademartiri F, Lemos PA, Raaijmakers R, Pattynama PM, de Feyter PJ. Reliable noninvasive coronary angiography with fast submillimeter multislice spiral computed tomography. *Circulation* 2002; 106:2051–2054
2. Leschka S, Alkadhi H, Plass A, et al. Accuracy of MSCT coronary angiography with 64-slice technology: first experience. *Eur Heart J* 2005; 26:1482–1487
3. Hoffmann U, Millea R, Enzweiler C, et al. Acute myocardial infarction: contrast-enhanced multi-detector row CT in a porcine model. *Radiology* 2004; 231:697–701
4. Gosalia A, Haramati LB, Sheth MP, Spindola-Franco H. CT detection of acute myocardial infarction. *AJR* 2004; 182:1563–1566
5. Weinmann HJ, Brasch RC, Press WR, Wesbey GE. Characteristics of gadolinium-DTPA complex: a potential NMR contrast agent. *AJR* 1984; 142:619–624
6. Mahnken AH, Koos R, Katoh M, et al. Assessment of myocardial viability in reperfused acute myocardial infarction using 16-slice computed tomography in comparison to magnetic resonance imaging. *J Am Coll Cardiol* 2005; 45:2042–2047
7. Rehwald WG, Fieno DS, Chen EL, Kim RJ, Judd M. Myocardial magnetic resonance imaging contrast agent concentrations after reversible and irreversible ischemic injury. *Circulation* 2002; 105:224–229
8. Higgins CB, Sovak M, Schmidt W, Siemers PT. Differential accumulation of radiopaque contrast material in acute myocardial infarction. *Am J Cardiol* 1979; 43:47–51

9. Gerber BL, Rochitte CE, Melin JA, et al. Microvascular obstruction and left ventricular remodeling early after acute myocardial infarction. *Circulation* 2000; 101:2734–2741
10. Raff GL, Gallagher MJ, O'Neill WW, Goldstein JA. Diagnostic accuracy of noninvasive coronary angiography using 64-slice spiral computed tomography. *J Am Coll Cardiol* 2005; 46:552–557
11. Miller TD, Christian TF, Hopfenspirger MR, Hodge DO, Gersh BJ, Gibbons RJ. Infarct size after acute myocardial infarction measured by quantitative tomographic 99mTc sestamibi imaging predicts subsequent mortality. *Circulation* 1995; 92:334–341
12. Baks T, van Geuns RJ, Biagini E, et al. Recovery of left ventricular function after primary angioplasty for acute myocardial infarction. *Eur Heart J* 2005; 26:1070–1077

Chapter 3

Multislice Computed Tomography and Magnetic Resonance Imaging for the Assessment of Reperfused Acute Myocardial Infarction

Timo Baks, MD,^{*†} Filippo Cademartiri, MD, PhD,^{*†} Amber D. Moelker, MSc,^{*} Annick C. Weustink, MD,[†] Robert-Jan van Geuns, MD, PhD,^{*†} Nico R. Mollet, MD, PhD,^{*†} Gabriel P. Krestin, MD, PhD,[†] Dirk J. Duncker, MD, PhD,^{*} Pim J. de Feyter, MD, PhD, FACC^{*†}

From the ^{*}Department of Cardiology, Thoraxcenter, and the [†]Department of Radiology, Erasmus University Medical Center, Rotterdam, the Netherlands

Abstract

Objectives We evaluated the accuracy of in vivo delayed-enhancement multislice computed tomography (DE-MSCT) and delayed-enhancement magnetic resonance imaging (DE-MRI) for the assessment of myocardial infarct size using postmortem triphenyltetrazolium chloride (TTC) pathology as standard of reference.

Background The diagnostic value of DE-MSCT for the assessment of acute reperfused myocardial infarction is currently unclear.

Methods In 10 domestic pigs (25 to 30 kg), the circumflex coronary artery was balloon-occluded for 2 h followed by reperfusion. After 5 days (3 to 7 days), DE-MRI (1.5-T) was performed 15 min after administration of 0.2 mmol/kg gadolinium-DTPA using an inversion recovery gradient echo technique. On the same day, DE-MSCT (64-slice) was performed 15 min after administration of 1 gI/kg of iodinated contrast material. One day after imaging, hearts were excised, sectioned in 8 mm short-axis slices, and stained with TTC. Infarct size was defined as the hyperenhanced area on DE-MSCT and DE-MRI images and the TTC-negative area on TTC pathology slices. Infarct size was expressed as percentage of total slice area.

Results Infarct size determined by DE-MSCT and DE-MRI showed a good correlation with infarct size assessed with TTC pathology ($R^2=0.96$ [$p=0.001$] and $R^2=0.93$ [$p=0.001$], respectively). The correlation between DE-MSCT and DE-MRI was also good ($R^2=0.96$; $p=0.001$). The relative difference in CT attenuation value of infarcted myocardium compared to remote myocardium was $191\pm 18\%$. The relative MR signal intensity between infarcted myocardium and remote myocardium was $554\pm 156\%$.

Conclusions We demonstrated that DE-MSCT can assess acute reperfused myocardial infarction in good agreement with in vivo DE-MRI and TTC pathology.

Abbreviations and Acronyms

CT =	computerized tomography
DE-MRI =	delayed-enhancement magnetic resonance imaging
DE-MSCT =	delayed-enhancement multislice computed tomography
HU =	Hounsfield units
TTC =	triphenyltetrazolium chloride

Introduction

Acute myocardial infarct size is a predictor of long-term left ventricular function and geometry and clinical outcome in patients who have suffered acute myocardial infarction^{1,2}. Delayed-enhancement magnetic resonance imaging (DEMRI) is a well established noninvasive imaging modality that allows assessment of myocardial infarct size³⁻⁵. In recent years, multislice computed tomography (MSCT) technology has made great strides, and noninvasive assessment of coronary artery stenosis is now feasible with high diagnostic accuracy using a 64-slice scanner^{6,7}. Delayed-enhancement multislice computed tomography (DEMSCT) has been proposed as an alternative noninvasive imaging modality for the detection of myocardial infarction. However, different imaging protocols have been proposed at different time points after myocardial infarction, and the diagnostic accuracy is currently unclear⁸⁻¹¹. We performed DE-MSCT and DE-MRI in a porcine model of reperfused acute myocardial infarction at a mean of five days after infarction. We evaluated the accuracy of in vivo DE-MSCT and DE-MRI for the assessment of acute reperfused myocardial infarct size and used postmortem viability staining with triphenyltetrazolium chloride (TTC) as standard of reference.

Methods

Animal model

Fourteen Yorkshire-landrace pigs (2 to 3 months old, 25 to 30 kg) were sedated (ketamine 20 mg/kg intramuscular and midazolam 1 mg/kg intramuscular), anesthetized (thiopental, 12 mg/kg intravenously), intubated, and mechanically ventilated (mixture of oxygen and nitrogen 1:2). Anesthesia was maintained with fentanyl (12.5 µg/kg/h). All pigs then received a sheath in a carotid artery to allow coronary X-ray angiography. Under fluoroscopy guidance, balloon occlusion of the left circumflex coronary artery was performed. In 2 pigs, the balloon was deflated after 15 min of occlusion to produce severely ischemic but reversible injured (stunned) myocardium. In 12 pigs, the balloon was deflated after 2 h of occlusion to allow reperfusion of the infarcted area. Reperfusion was proven by coronary angiography. Of the animals who underwent 2 h of occlusion, one pig died after 1 day and one pig died after 3 days after balloon occlusion. The study complied with the regulations of the animal care committee of our hospital and the National Institutes of Health publication "Guide for the Care and Use of Laboratory Animals" (1996).

All pigs were anesthetized as described above before imaging. First, DE-MRI was performed, and 93±23 min later DE-MSCT imaging. The two pigs that underwent 15 min of balloon occlusion underwent imaging at 3 and 4 days, respectively, after induction of ischemia. Of the 10 remaining pigs that underwent the 2-h occlusion protocol, 2 pigs were imaged at 3 days, 6 at 5 days, and 2 at 7 days after reperfusion. One day after the DE-MSCT and DE-MRI imaging session, all animals were euthanized and their hearts excised. The ex vivo hearts were stiffened using alginate impression material (Cavex Holland, Haarlem, the Netherlands). The myocardium of the left ventricle was then sectioned in 8 mm consecutive slices in short-axis view perpendicular to the long axis of the left ventricle using a commercially available

meatslicer. To obtain a viability staining, the slices were embedded in a solution of 1% triphenyltetrazolium chloride (TTC) and 0.2 mol/l Sorensen's buffer (pH 7.4) at 37°C for 15 min, followed by fixation in 4% formalin. Slices that showed a TTC-negative area were photographed digitally after 24 h of exposure to formalin. Exposure to formalin allows delineation between necrotic but hemorrhagic myocardium (which has a red appearance due to the presence of blood) and viable tissue (which stains red owing to the conversion of TTC to the bright red formazan stain). By exposing the TTC-stained tissue to formalin, the hemorrhagic necrotic areas acquire a dark brown color, whereas the red formazan precipitate remains bright red (Fig. 1). Unfortunately, a limitation of this approach was the asymmetric shrinkage (causing the slices to bend) in 9 out of a total of 67 slices (in 10 animals), hampering the accurate assessment of infarct size in these slices, which were excluded from analysis for this reason.

DE-MSCT

A 64-slice clinical CT scanner was used for imaging (Sensation 64; Siemens, Forchheim, Germany) with the following characteristics: number of detector rows 32x2 (oversampling in the z-axis obtained with flying focal spot¹²); individual detector width 0.6 mm; gantry rotation time 330 ms; effective temporal resolution 165 ms. The delayed-enhancement protocol was performed 15 min after administration of 1 gI/kg of iodinated contrast agent through an ear vein at an injection speed of 1.5 ml/s (400 mgI/ml Iomeprol; Iomeron, Bracco, Italy). The following scan parameters were used: tube voltage 120 kV; tube current 900 mA; table feed per rotation 3.84 mm; scan direction craniocaudal and retrospective electrocardiographic gating. Voxel size at acquisition was 0.3x0.3x0.4 mm. The estimated radiation dose if applied in humans was calculated with dedicated software as 15/21 mSv for male/ female (WinDose; Institute of Medical Physics, Erlangen, Germany). Mean heart rate decreased to 51±9 beats/min after administration of zatebradine (10 mg/kg intravenously). An instrumented breath hold was applied to minimize the influence of respiratory motion on data collection. The DE-MSCT datasets were reconstructed at 300 ms, 350 ms, and 400 ms before the next R-wave (enddiastolic phase of the cardiac cycle). From the dataset with optimal image quality, axial slices with a slice thickness of 1 mm and an increment of 0.5 mm were reconstructed using a field of view of 150x50 mm, a 512 mm² reconstruction matrix, and a medium smooth convolution filter (B3of). The MSCT short-axis slices with a slice thickness of 1 mm were then reconstructed perpendicular to the long axis of a double-oblique true four-chamber view using a dedicated software platform with multiplanar capabilities (Leonardo; Siemens).

DE-MRI

A clinical 1.5-T MRI scanner with a dedicated cardiac four-element phased-array receiver coil was used for imaging (Signa CV/i; GE Medical Systems, Milwaukee, Wisconsin). Repeated instrumented breath-holds and gating to the electrocardiogram were applied to minimize the influence of cardiac and respiratory motion on data collection. No medication was administered to control heart rate. Cine-MRI was performed with a steady-state free-precession technique (Fiesta; Medical Systems) with the following imaging parameters: 24 temporal phases per slice, voxel size 1.8x1.5x8 mm; repetition time 3.4 ms; time to echo 1.4 ms; flip angle 45° bandwidth

83 kHz; number of averages 0.75. To cover the entire left ventricle, six to eight consecutive slices of 8 mm were planned in short-axis view perpendicular to the long axis of a double-oblique true four-chamber view.

Myocardial distribution of delayed enhancement was studied 15 min after administration of Gadolinium-DTPA (0.2 mmol/kg; Magnevist, Schering, Germany). A two-dimensional T₁-weighted inversion-recovery segmented fast gradient-echo sequence with the following imaging parameters was used: voxel size 1.1x1.5x8mm; repetition time 7.3 ms; time to echo 1.6 ms; flip angle 20°; inversion pulse 180°; number of averages 1; bandwidth 17.9 kHz; inversion time 180 to 300 ms; data acquisition every second R-R interval. The trigger delay was adjusted per pig to acquire data in mid-to end-diastole, and the inversion time was adjusted per pig to null the signal of remote myocardium. Slice locations for delayed-enhancement imaging were copied from slice locations of short-axis cine-imaging.

Data analysis

The DE-MSCT, DE-MRI, and TTC pathology images were coregistered using anatomical landmarks like the insertion of the right ventricle to the septum and the presence of papillary muscles. Infarct size per slice was calculated by dividing the infarcted area by the total slice area of left ventricular myocardium. The digitalized TTC pathology slices were loaded in a separate workstation with a commercially available analysis package (SigmaScan Pro 5.0). The TTC negative area (including the dark-brown subendocardial area) was considered to be the infarcted area and was segmented manually. Reconstructed DE-MSCT images and DE-MRI images were exported and transferred to a separate workstation with dedicated software (Cine Tool 3.4; GE Medical Systems). Image quality was evaluated on a per-slice basis and classified as good (defined as the absence of any image-degrading artifacts related to motion or miss-triggering), adequate (presence of image-degrading artifacts but evaluation possible), or poor (presence of image-degrading artifacts but evaluation possible with moderate confidence). The region with delayed hyper-enhancement was segmented manually by two different observers (T.B. and A.M.) blinded to the results of the other imaging modality and TTC pathology. Regional wall thickening was assessed on cine-MRI images at the core of the infarction and in remote noninfarcted myocardium of the septum using dedicated software based on the centerline method (CAAS MRV 2.1, Pie Medical Imaging, Maastricht, the Netherlands). CT attenuation values (expressed in Hounsfield Units [HU]) were measured using the scanner software by drawing three 10-mm² regions of interest in delayed enhanced myocardium, remote myocardium and the left ventricular cavity in a short axis slice located at the center of the infarction of each pig¹¹. Noise was considered to be the standard deviation of the CT value in a region of interest of 25 mm² placed in the descending thoracic aorta. The MRI signal intensity values (expressed in arbitrary units [AU]) were measured using the scanner software by drawing 30 mm² regions of interest in delayed enhanced and remote myocardium¹³. Signal intensity of the left ventricular blood pool was measured by drawing a 100 mm² region of interest in the left ventricular cavity. Noise was considered to be the standard deviation of the signal measured in a region of interest 300 mm² placed in the imaged air outside of the pig.

Statistical analysis

All data are presented as mean±standard deviation. The relation between infarct size assessed with DE-MSCT, DE-MRI, and TTC pathology was evaluated with univariate linear regression analysis. Agreement between DE-MSCT, DE-MRI, and TTC pathology for the assessment of infarct size and intra-and interobserver variability was determined with Bland-Altman analysis. Differences in regional wall thickening were tested with an unpaired *t*test. Differences in CT attenuation values and MR signal intensity values between infarcted myocardium, remote myocardium, and left ventricular blood pool were tested with one-way analysis of variance followed by post hoc Bonferroni correction to adjust for multiple comparisons.

Results

The two pigs that underwent 15 min of balloon occlusion of the circumflex coronary artery showed hypokinesia of the lateral wall on echocardiography performed 20 min after reperfusion, indicating the presence of stunned myocardium. The DE-MSCT and DE-MRI imaging demonstrated no regions with delayed enhancement. The TTC staining confirmed that there was no infarcted myocardium. In 10 pigs that underwent 2-h balloon occlusion of the circumflex coronary artery, acute reperused myocardial infarction was accurately detected by both DE-MSCT and DE-MRI (Figs. 1 and 2). The DE-MSCT image quality was classified as good in 83% (48 of 58), moderate in 10% (6 of 58), and poor in 7% (4 of 58) of slices. The DE-MR image quality was classified as good in 75% (43 of 58), moderate in 17% (10 of 58), and poor in 8% (5 of 58) of slices. No delayed enhancement was seen in myocardium outside the perfusion territory of the circumflex coronary artery. Mean infarct size was 21±15% on DE-MSCT images, 22±16% on DE-MR images, and 20±15% on TTC pathology images. Infarct size assessed with DEMSCT correlated well with infarct size measured on TTC pathology slices ($R^2=0.96$; $p=0.001$). Also, infarct size assessed with DE-MRI correlated well with infarct size measured on TTC pathology slices ($R^2=0.93$; $p=0.001$). Accordingly, infarct size assessed with DE-MSCT correlated well with infarct size assessed with DE-MRI ($R^2=0.96$; $p=0.001$) (Fig. 3A). Bland-Altman analyses demonstrated a good agreement for the assessment of infarct size between DE-MSCT, DE-MRI, and TTC pathology (Fig. 3B). The intraobserver variability for the assessment of infarct size was 1.0±3.9% for DE-MSCT and 0.5±4.6% for DE-MRI. The interobserver variability for the assessment of infarct size was 2.1±5.6% for DE-MSCT and 3.0±5.9% for DE-MRI. Regional wall thickening was significantly decreased in infarcted myocardium of the lateral wall compared with remote noninfarcted myocardium of the septum (0±14% vs. 50±14%; $p=0.001$) (Fig. 4).

Mean CT attenuation value of delayed-enhanced myocardium was significantly different from CT attenuation value of remote myocardium (126±20 HU vs. 66±6HU; $p=0.001$; three pair-wise comparisons) (Fig. 5). The relative difference in CT attenuation value between delayed-enhanced and remote myocardium was 191±18%. Noise measured in the descending aorta was 17±3 HU. Mean MR signal intensity value of delayed-enhanced myocardium was significantly higher than MR signal intensity of remote myocardium (154±37 AU vs. 28±6 AU; $p=0.001$; three pairwise comparisons)

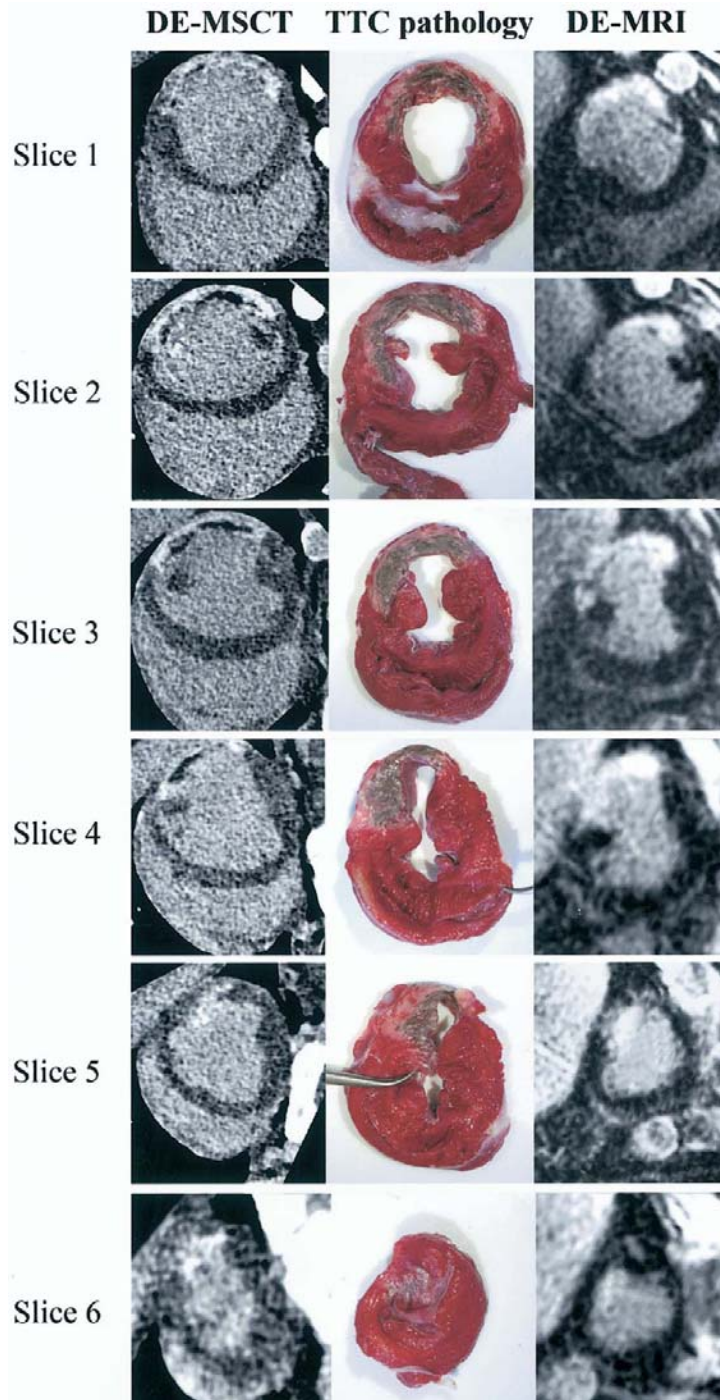


Figure 1 Acute reperfused myocardial infarction can be assessed accurately with delayed-enhancement multislice computed tomography (DE-MSCT) and delayed-enhancement magnetic resonance imaging (DE-MRI) compared with postmortem triphenyltetrazolium chloride (TTC) pathology. The left ventricle is shown from base (Slice 1) to apex (Slice 6). The MSCT images represent 1-mm slices compared with the photographed TTC pathology slices and the MRI slices of 8 mm.

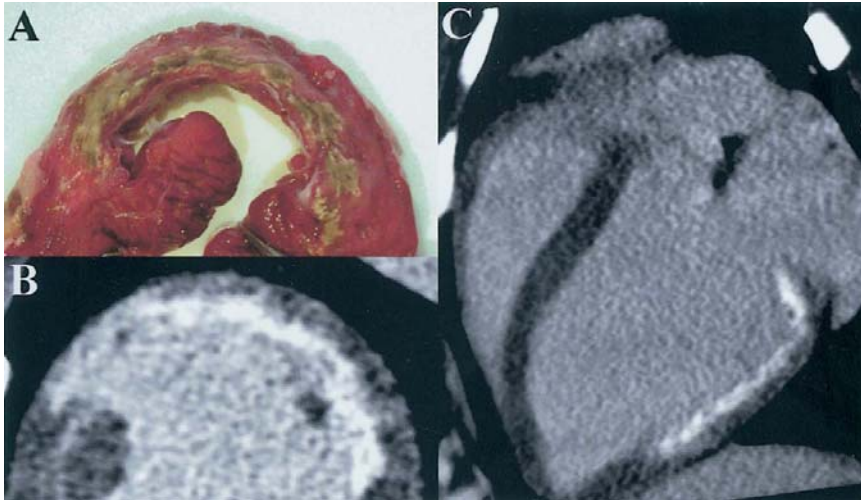


Figure 2 In this pig with subendocardial infarction, the transmural differentiation of viable and nonviable myocardium is demonstrated with DE-MSCT in short-axis view (**B**) and long-axis view (**C**) with TTC pathology as standard of reference (**A**).

(Fig. 5). Relative MR signal intensity value of delayed-enhanced myocardium compared with remote myocardium was $554 \pm 156\%$. Noise measured in the air outside the pig was 6 ± 1 AU.

Discussion

Our results demonstrate that DE-MSCT can assess acute reperfused myocardial infarction in good agreement with in vivo DE-MRI and postmortem TTC pathology.

Delayed-enhancement imaging

Delayed-enhancement imaging is feasible with MSCT and MRI because both iodinated contrast agents and gadolinium chelates passively diffuse into the increased extracellular matrix of infarcted myocardium¹⁴. Higgins et al.¹⁵ demonstrated elevated concentrations of iodinated contrast material in infarcted tissue compared with uninfarcted tissue if assessed more than 5 min after administration of these contrast materials. Rehwald et al.¹⁶ showed significantly higher concentrations of gadolinium chelates in infarcted myocardium compared with remote myocardium after a delay of 10 min. Because accumulation of contrast agents in necrotic myocardium is a passive process, the timing between administration of contrast agents and imaging may be crucial to accurately assess infarct size. Amado et al.¹⁷ performed DE-MRI between 6 and 30 min after administration of gadolinium chelates and observed no difference in measured infarct size. The optimal time delay for performing DEMSCT after administration of iodinated contrast agents remains to be determined, because no data are available for DE-MSCT in infarctions more than 2 days old. The pharmacokinetic behavior of gadolinium chelates and iodinated contrast agents is relatively similar, but differences in molecule size may influence the rate of diffusion

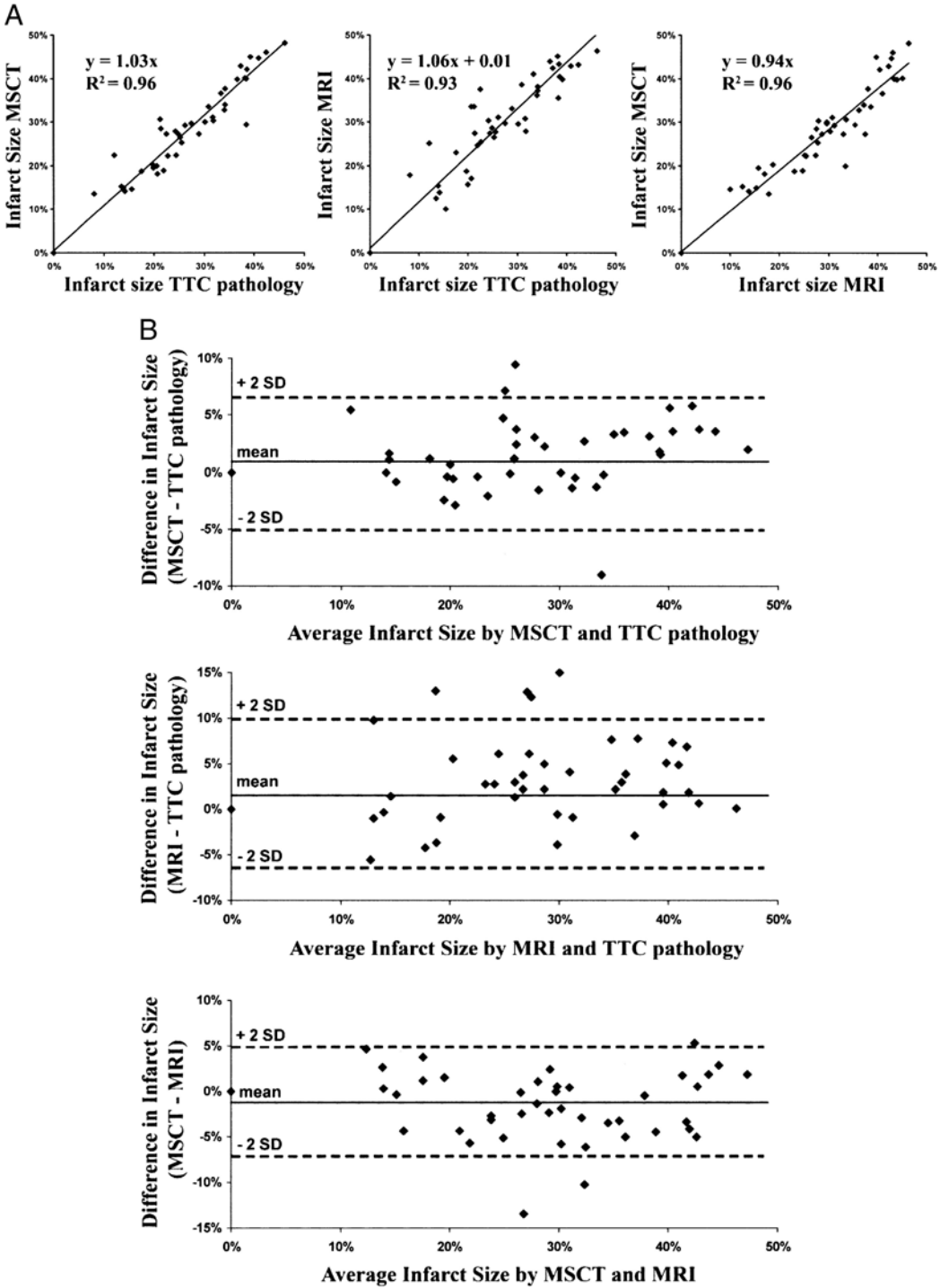


Figure 3 (A) The relation between infarct size assessed with DE-MSCT, DE-MRI, and postmortem TTC pathology. **(B)** Bland-Altman analyses show the excellent agreement between infarct size assessed with DE-MSCT, DE-MRI, and postmortem TTC pathology. Abbreviations as in Fig. 1.

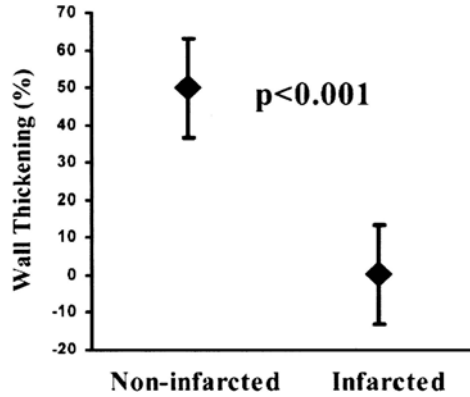


Figure 4 Regional wall thickening was significantly reduced in infarcted compared with noninfarcted myocardium.

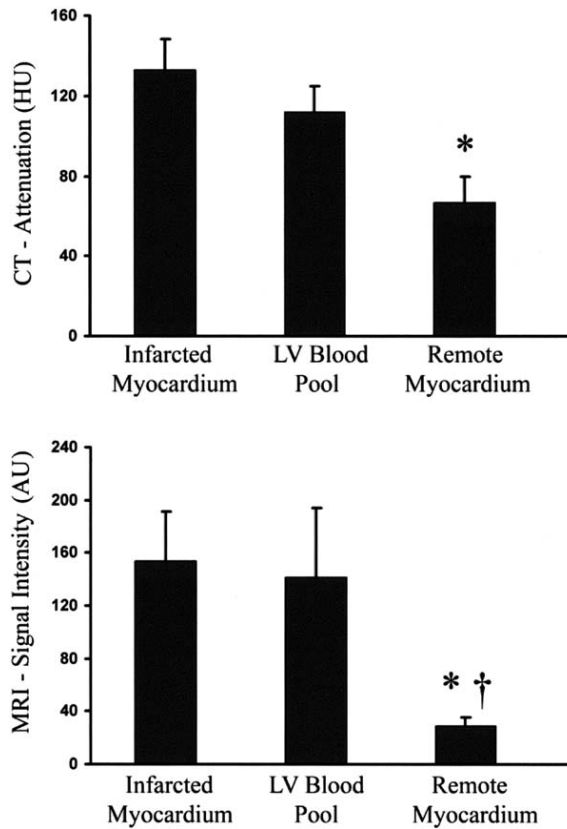


Figure 5 Mean computerized tomography (CT) attenuation value for infarcted myocardium is significantly higher compared with noninfarcted myocardium. Mean magnetic resonance (MR) signal intensity value of infarcted myocardium is significantly higher compared with noninfarcted myocardium. * $p=0.001$ compared with infarcted myocardium. † $p=0.001$ compared with left ventricular (LV) blood pool.

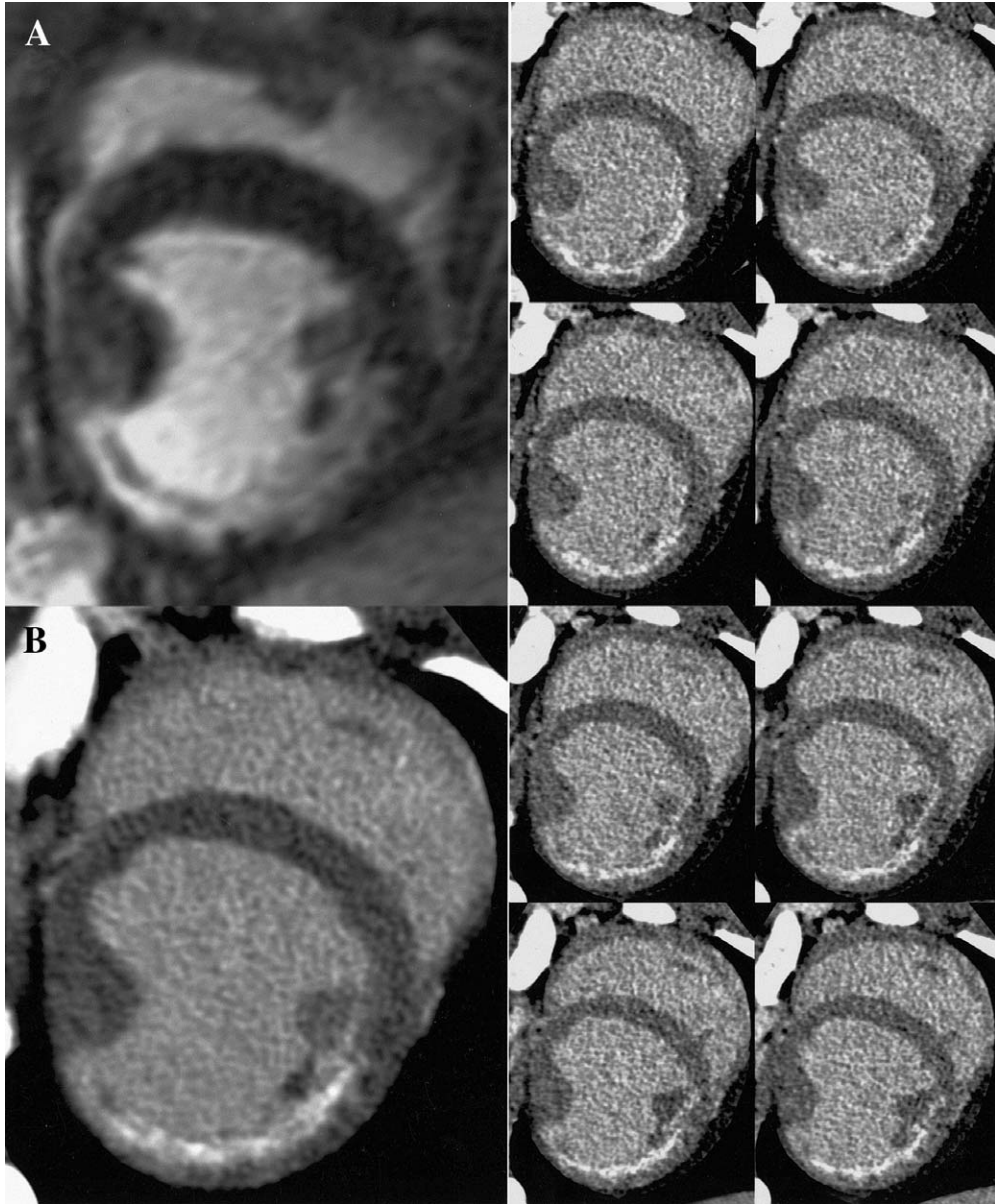


Figure 6 DE-MSCT provides higher spatial resolution than DE-MRI. Image **A** represents an 8-mm-thick DE-MRI image, and image **B** represents the similar slice reconstructed from eight different 1-mm-thick DE-MSCT images. Images on the right represent the eight reconstructed 1-mm-thick slices that together form image B. Abbreviations as in Fig. 1.

in infarcted myocardium¹⁸.

DE-MSCT

Delayed-enhancement CT for the assessment of myocardial infarction was performed as early as the late 1970s, and these initial results were encouraging¹⁹. However, practical use of this technique was hampered by insufficient image quality mainly

caused by cardiac motion. Computerized tomography technology has developed rapidly during the last decade, and with the introduction of spiral and later multislice spiral CT a marked increase in temporal and spatial resolution was obtained. Three recent experimental studies demonstrated the excellent diagnostic accuracy of 4-, 16-, and 32-slice CT for the assessment of nonreperfused and reperfused myocardial infarction if performed within 5 h after induction of infarction^{10,11,20}. However, infarct morphology may change after myocardial infarction with early infarct expansion (~2 days) and late infarct shrinkage (~10 days)^{5,21}, and the ability of DE-MSCT to assess infarctions more than 5 h old is currently unknown. To assess infarct size between 2 and 7 days after infarction is clinically relevant, because infarct size predicts long-term left ventricular remodeling and clinical outcome^{4,22-24}. In the current study, we demonstrated that DE 64-slice CT can assess infarct size between 3 and 7 days after infarction and can differentiate between necrotic myocardium and stunned myocardium with good correlation with in vivo DE-MRI and ex vivo TTC pathology. More studies are needed to demonstrate if DE-MSCT can also show myocardial infarction or scar at a longer time of follow-up after myocardial infarction.

An advantage of MSCT is that it offers high spatial resolution, allowing reconstruction of thin slices and thereby reducing possible partial volume artifacts. High-resolution DE-MSCT imaging also allowed the transmural differentiation of viable and nonviable myocardium. A major disadvantage of MSCT is the limited soft tissue contrast that is obtained. Tissue contrast is related to the radiation dose that is applied and the amount of iodinated contrast material administered. For DE-MSCT imaging, we used the radiation dose that is used for MSCT coronary angiography (15/21 mSv for men/women). We administered 1 gI/kg iodine contrast to the pigs, equivalent to approximately 200 ml iodine contrast to a patient of 70 kg, which is considered a normal dose of contrast during a conventional angiography procedure²⁵. Technical developments are desirable that reduce radiation exposure and limit the amount of iodinated contrast material needed. Recent developments include tube-current modulation which reduces radiation exposure by nearly one-half by applying radiation only in the mid-to end-diastolic phase of the cardiac cycle²⁶.

An advantage of MSCT is that it offers high spatial resolution, allowing reconstruction of thin slices and thereby reducing possible partial volume artifacts. High-resolution DE-MSCT imaging also allowed the transmural differentiation of viable and nonviable myocardium. A major disadvantage of MSCT is the limited soft tissue contrast that is obtained. Tissue contrast is related to the radiation dose that is applied and the amount of iodinated contrast material administered. For DE-MSCT imaging, we used the radiation dose that is used for MSCT coronary angiography (15/21 mSv for men/women). We administered 1 gI/kg iodine contrast to the pigs, equivalent to approximately 200 ml iodine contrast to a patient of 70 kg, which is considered a normal dose of contrast during a conventional angiography procedure (25). Technical developments are desirable that reduce radiation exposure and limit the amount of iodinated contrast material needed. Recent developments include tube-current modulation which reduces radiation exposure by nearly one-half by applying radiation only in the mid-to end-diastolic phase of the cardiac cycle²⁶.

DE-MRI

Delayed-enhancement MRI is an established noninvasive imaging modality that can assess reperfused and nonreperfused myocardial infarction⁴. It is safe and patient friendly and can be repeated multiple times to evaluate therapy without causing harm to the patient. No heart rate control is necessary. Excellent soft tissue contrast is obtained with gadolinium chelates that have T1 shortening characteristics. Further improvement in tissue contrast is obtained by applying a nonselective inversion pulse before data acquisition, allowing suppression of signal of remote myocardium²⁷. We observed a relative signal intensity between hyperenhanced and remote myocardium of $554 \pm 156\%$. A disadvantage of MRI is the limited through-plane resolution, resulting in a slice thickness of 4 to 8 mm (Fig. 6). In the present study, differences in infarct size between postmortem TTC pathology, DE-MSCT, and DE-MRI may have been caused by dissimilarity in slice thickness offered by these different modalities. The DE-MSCT allowed reconstruction of a slice thickness of 1 mm, whereas DE-MRI was performed with a slice thickness of 8 mm, and TTC pathology, the standard of reference, was analyzed on a two-dimensional digital photograph. The accuracy and reproducibility of infarct size measurements with DE-MSCT and DE-MRI may further improve by using a semiautomated quantification software¹⁷.

Conclusions

Delayed-enhancement MRI is a well established noninvasive imaging modality that allows assessment of myocardial infarct size and has been shown to provide prognostic information in patients who have suffered acute myocardial infarction. We demonstrated that DE-MSCT can assess acute reperfused myocardial infarction in good agreement with in vivo DE-MRI and postmortem TTC pathology. Ongoing technical improvements of the CT scanner have resulted in high diagnostic performance to detect significant coronary stenosis in selected groups of patients without arrhythmia and a heart rate below 70 beats/min^{6,7}. Together with the assessment of infarct size, this new CT technology may emerge as a clinically valuable tool to comprehensively evaluate post-infarction patients.

Acknowledgments

The authors thank Wendy Kerver for her help in the logistics of this study.

References

1. Baks T, van Geuns RJ, Biagini E, et al. Recovery of left ventricular function after primary angioplasty for acute myocardial infarction. *Eur Heart J* 2005;26:1070–7.
2. Miller TD, Christian TF, Hopfenspirger MR, Hodge DO, Gersh BJ, Gibbons RJ. Infarct size after acute myocardial infarction measured by quantitative tomographic 99mTc sestamibi imaging predicts subsequent mortality. *Circulation* 1995;92:334–41.
3. Judd RM, Lugo-Olivieri CH, Arai M, et al. Physiological basis of myocardial contrast enhancement in fast magnetic resonance images of 2-day-old reperfused canine infarcts. *Circulation* 1995;92:1902–10.
4. Kim RJ, Fieno DS, Parrish TB, et al. Relationship of MRI delayed contrast enhancement to irreversible injury, infarct age, and contractile function. *Circulation* 1999;100:1992–2002.
5. Gerber BL, Rochitte CE, Melin JA, et al. Microvascular obstruction and left ventricular remodeling

- early after acute myocardial infarction. *Circulation* 2000;101:2734–41.
6. Raff GL, Gallagher MJ, O'Neill WW, Goldstein JA. Diagnostic accuracy of noninvasive coronary angiography using 64-slice spiral computed tomography. *J Am Coll Cardiol* 2005;46:552–7.
 7. Mollet NR, Cademartiri F, van Mieghem CA, et al. High-resolution spiral computed tomography coronary angiography in patients referred for diagnostic conventional coronary angiography. *Circulation* 2005; 112:2318–23.
 8. Mahnken AH, Koos R, Katoh M, et al. Assessment of myocardial viability in reperfused acute myocardial infarction using 16-slice computed tomography in comparison to magnetic resonance imaging. *J Am Coll Cardiol* 2005;45:2042–7.
 9. Gosalia A, Haramati LB, Sheth MP, Spindola-Franco H. CT detection of acute myocardial infarction. *AJR Am J Roentgenol* 2004;182:1563–6.
 10. Buecker A, Katoh M, Krombach GA, et al. A feasibility study of contrast enhancement of acute myocardial infarction in multislice computed tomography: comparison with magnetic resonance imaging and gross morphology in pigs. *Invest Radiol* 2005;40:700–4.
 11. Hoffmann U, Millea R, Enzweiler C, et al. Acute myocardial infarction: contrast-enhanced multi-detector row CT in a porcine model. *Radiology* 2004;231:697–701.
 12. Flohr T, Stierstorfer K, Raupach R, Ulzheimer S, Bruder H. Performance evaluation of a 64-slice CT system with z-flying focal spot. *Rofo Fortschr Geb Rontgenstr Neuen Bildgeb Verfahr* 2004;176:1803–10.
 13. Gupta A, Lee VS, Chung YC, Babb JS, Simonetti OP. Myocardial infarction: optimization of inversion times at delayed contrast-enhanced MR imaging. *Radiology* 2004;233:921–6.
 14. Mahrholdt H, Wagner A, Judd RM, Sechtem U. Assessment of myocardial viability by cardiovascular magnetic resonance imaging. *Eur Heart J* 2002;23:602–19.
 15. Higgins CB, Siemers PT, Newell JD, Schmidt W. Role of iodinated contrast material in the evaluation of myocardial infarction by computerized transmission tomography. *Invest Radiol* 1980;15:S176–82.
 16. Rehwald WG, Fieno DS, Chen EL, Kim RJ, Judd RM. Myocardial magnetic resonance imaging contrast agent concentrations after reversible and irreversible ischemic injury. *Circulation* 2002;105: 224–9.
 17. Amado LC, Gerber BL, Gupta SN, et al. Accurate and objective infarct sizing by contrast-enhanced magnetic resonance imaging in a canine myocardial infarction model. *J Am Coll Cardiol* 2004;44:2383–9.
 18. Weinmann HJ, Brasch RC, Press WR, Wesbey GE. Characteristics of gadolinium-DTPA complex: a potential NMR contrast agent. *AJR Am J Roentgenol* 1984;142:619–24.
 19. Gray WR, Buja LM, Hagler HK, Parkey RW, Willerson JT. Computed tomography for localization and sizing of experimental acute myocardial infarcts. *Circulation* 1978;58:497–504.
 20. Lardo AC, Cordeiro MA, Silva C, et al. Contrast-enhanced multidetector computed tomography viability imaging after myocardial infarction: characterization of myocyte death, microvascular obstruction, and chronic scar. *Circulation* 2006;113:394–404.
 21. Baks T, van Geuns RJ, Biagini E, et al. Effects of primary angioplasty for acute myocardial infarction on early and late infarct size and left ventricular wall characteristics. *J Am Coll Cardiol* 2006;47:40–4.
 22. Gerber BL, Garot J, Bluemke DA, Wu KC, Lima JA. Accuracy of contrast-enhanced magnetic resonance imaging in predicting improvement of regional myocardial function in patients after acute myocardial infarction. *Circulation* 2002;106:1083–9.
 23. Beek AM, Kuhl HP, Bondarenko O, et al. Delayed contrast-enhanced magnetic resonance imaging for the prediction of regional functional improvement after acute myocardial infarction. *J Am Coll Cardiol* 2003;42:895–901.
 24. Hombach V, Grebe O, Merkle N, et al. Sequelae of acute myocardial infarction regarding cardiac structure and function and their prognostic significance as assessed by magnetic resonance imaging. *Eur Heart J* 2005;26:549–57.
 25. Dawson P. Administration of contrast media. In: Dawson P, Claus W, editors. *Contrast Media in Practice*. Heidelberg, Germany: Springer-Verlag, 1999:132.
 26. Jakobs TF, Becker CR, Ohnesorge B, et al. Multislice helical CT of the heart with retrospective ECG gating: reduction of radiation exposure by ECG-controlled tube current modulation. *Eur Radiol* 2002;12:1081–6.
 27. Simonetti OP, Kim RJ, Fieno DS, et al. An improved MR imaging technique for the visualization of myocardial infarction. *Radiology* 2001;218:215–23.

Chapter 4

Umbilical cord blood derived stem cells

Amber D. Moelker¹ MSc, Kim M.A.M. Wever¹ MSc, Jan J. Cornelissen² PhD, Dirk J. Duncker¹ MD, PhD, Wim J. van der Giessen^{1,3} MD, PhD

¹Department of Cardiology, Thoraxcenter, Erasmus MC, Rotterdam, The Netherlands

²Department of Hematology, Erasmus MC, Rotterdam, The Netherlands

³Interuniversity Cardiology Institute of the Netherlands (ICIN), Utrecht, The Netherlands

Abstract

Umbilical cord blood (UCB) cells may offer a promising, of the shelf, therapy for the treatment of myocardial infarction. In this review the current use of UCB as an alternative to bone marrow to obtain cells for transplantation purposes is described. In addition, preclinical studies using umbilical cord blood derived cells for cardiac regeneration are discussed including our own experience in a porcine model of reperfused myocardial infarction.

Introduction

Myocardial infarction (MI) is a major cause of heart failure and thus forms one of the main targets for cardiac regeneration by cell transplantation. The treatment of MI with stem cell therapy seems promising; however the cellular source with the highest potential for cardiac regeneration remains unclear. To optimally treat MI patients with stem cell therapy, a widely available source of stem cells would be of much use¹. Many candidates have been proposed in clinical and experimental cell transplantation e.g. bone marrow mononuclear cells, mesenchymal adult progenitor cells, cardiac progenitor cells and skeletal myoblasts¹. Umbilical cord blood (UCB) derived cells have the advantage of being easy to obtain in large numbers, which is especially important for the sick and elderly population because they may have impaired stem cell numbers and their cells may have a decreased capacity for proliferation and differentiation². Together with their presumed hypoimmunogenic properties, UCB holds great potential to facilitate cardiac regeneration after myocardial infarction.

UCB in routine clinical use

Allogeneic hematopoietic stem cell transplantation has been firmly established as an important treatment modality for advanced hematological diseases. However, allogeneic transplantation has been limited by the availability of suitable related and unrelated donors. Hematopoietic progenitor cells can be harvested from the donor bone marrow, from mobilized peripheral blood, and such progenitors can also be found in UCB. Although the first transplantation was reported more than a decade ago, UCB is still considered a relatively novel source of hematopoietic progenitor cells. The first clinical application of UCB was reported in 1972 when American scientists transfused fetal cord blood cells into a 16-year old boy with acute lymphoblastic anemia. He received UCB units from 8 different donors from which one unit engrafted successfully and lasted 38 hours³. The first successful transplantation had to wait until 1989 in the treatment of a child with Fanconi's anemia⁴. Since then, regeneration of hematopoiesis by UCB is considered as a valuable alternative source for bone marrow derived stem cells, especially in pediatric patients. The relatively low number of progenitor cells in UCB has long limited the use mainly to pediatric patients, but the development of UCB transplantation in adults with hematological disorders is now rapidly evolving. Recent comparative studies have suggested that outcome after UCB transplantation compares well to outcome after volunteer unrelated donor transplantation^{5,6}. However, major challenges of UCB transplantation in adults still include better approaches to improve engraftment, reduce the incidence of graft versus host disease and improve immune reconstitution⁷. Apart from the presence of hematopoietic progenitor cells, UCB may contain other progenitor cells, including mesenchymal, endothelial stem cells, and neuronal precursor cells. The combination of hematopoietic and mesenchymal stem cells as well as endothelial progenitors and the presumed hypo-immunogenicity of UCB sparks hope for the future of stem cell mediated tissue regeneration. To date clinical trials on the use of UCB in non hematopoietic disorders are scarce, but experimental data hold promises for the future. In neurology, UCB have been identified as candidates for tissue regeneration

in a range of neurodegenerative disorders⁸. In comparison, in the field of cardiology recent evidence for possible tissue regeneration in vitro of several cardiac cell types like heart valves^{9,10}, blood vessels⁹ and cardiomyocytes¹¹ have lead to an increased interest in UCB.

Studies in animal models

In the last three years ten preclinical studies¹²⁻²¹ have been published in which UCB derived cells were studied in the heart (Table 1). All but one¹⁸ evaluated the effect of UCB derived cell injection in a MI model. MI was induced by a permanent occlusion of the left anterior descending coronary artery^{12-17,19-21} or by cryoinfarction²⁰. Cells were administered intramyocardially^{12-15,18-21} or intravenously^{16,17,20}. Table 1 shows that studies used different derived umbilical cord blood cells and injected different numbers of cells at various time points. The variety of experimental models can explain the equivocal effects of cell therapy after MI. In only two studies^{15,17} a baseline measurement of left ventricular (LV) function after MI but before stem cell injection was performed. In previous studies in mice and rats a significant decrease in infarct size was observed in cell treated animals^{12,13,16,19-21}. Furthermore, a significant improvement in ejection fraction^{12,13,19} or fractional shortening^{14,17}, which was measured with echo, was observed in UCB derived cell treatment in rodents in all but two studies^{20,21}. Only one study¹⁴ reported a positive effect of UCB on LV remodeling. In several studies histology showed a higher capillary density^{12,14,16,19,20} in cell treated animals compared to controls, however this finding was not observed by Leor *et al.*¹⁷.

In our laboratory MI was induced in 12 swine by proximal PTCA balloon occlusion of the left circumflex coronary artery for 2 hours followed by reperfusion²². Five additional swine were used as healthy controls to assess normal cardiac growth and function. One week after MI a baseline MRI was performed on all swine to assess LV function and infarct size. The next day, 6 of the MI swine received an intracoronary injection of $\sim 100 \times 10^6$ umbilical cord blood derived cultured unrestricted human somatic stem cells (USSC) in 10 mL unconditioned culture medium. The other 6 MI swine received 10 mL medium intracoronary. Cells or medium were injected slowly (1 mL/min) in the infarct related artery. Four weeks later all animals underwent a second MRI to assess the effect of USSC treatment. The pigs were sacrificed afterwards and the hearts were examined by histology. All swine received 8 mg/Kg/day Cyclosporine A, starting one week after MI.

Four weeks after USSC injection in this porcine model of reperfused MI, we could not detect a beneficial effect of USSC treatment on global or regional LV function. Furthermore, there was no reduction observed in infarct size as measured with delayed enhancement MRI compared to medium only treated animals. Infarct size actually increased slightly after USSC injection. Histology showed a transmural infarct in all MI-swine, containing abundant collagen and fibrous tissue. In USSC treated swine an increased number of calcifications and inflammatory cells (CD3+ and CD45+) were detected. Immunohistochemistry showed that four weeks after injection USSC had not transdifferentiated into a cardiac or vascular phenotype. However, some USSC had become CD45 positive.

Table 1: Effect of cord blood derived cell therapy in experimental myocardial infarction

	n		Cells			Time		Results	
	Treated	Control	Type	Route	#	Cell injection	FU	LV function	Histology
Hu ¹²	rats 15	15	MNC, 24h culture	i.m.	10x10 ⁶	after MI	4 w	EF↑	IS↓ CD↑
Henning ¹³	rats 38	33	Fresh MNC	i.m.	1x10 ⁶	1 h	4 m	EF↑	IS↓
Hirata ¹⁴	rats 7	6	Fresh CD34+	i.m.	0.2x10 ⁶	20 min	4 w	FS↑	CD↑
Kim ¹⁵	swine 8	8	Cultured USSC	i.m.	100x10 ⁶	4 w	4 w	EF↑	IS↓ CD↑
Ma ¹⁶	mice 19	6	Fresh MNC	i.v.	6x10 ⁶	24 h	3 w		IS↓ CD↑
Leor ¹⁷	rats 9	8	Fresh CD133+	i.v.	1.2-2x10 ⁶	7 d	1 m	FS↑	CD=
Min ¹⁸	rats 12	-	Cultured MSC	i.m.	1x10 ⁶	-	8 d		
Chen ¹⁹	mice 5	5	Cultured CD34+	i.m.	1x10 ⁶	after MI	4 w	EF↑	IS↓ CD↑
Ma ²⁰	mice ?	?	Fresh MNC	i.v.	6x10 ⁶	24 h	4 w		IS↓ CD↑
	mice ?	?	Fresh CD133+	i.m.	0.5x10 ⁶	after MI	3 w	FS=	IS=
Moelker	swine 6	6	Cultured USSC	i.c.	100x10 ⁶	1 w	4 w	EF=	IS↑

n= number of animals, FU= follow-up, Cell injection= time of cell injection post MI, LV=left ventricular, MNC= umbilical cord blood derived mononuclear cells, USSC= umbilical cord blood derived unrestricted somatic stem cells, MSC= umbilical cord blood derived mesenchymal stem cells, i.m.= intramyocardial, i.v.= intravenous, i.c.= intracoronary, EF= ejection fraction, FS= fractional shortening, IS= infarct size, CD= capillary density, ↑= increased, =; no change, ↓= decreased

The different results between the preclinical studies predominantly performed in small rodents and in our own laboratory, can be explained by the differences between the experimental models (Table 1). Differences in heart size, heart rate and hemodynamics between large mammals such as the pig and rodents could account for the differences found in cell therapy. Ours was the only study that created an infarct model with reperfusion, which closely matches clinical settings, but creates a very different environment for the injected cells. Furthermore, we injected cells intracoronary instead of intramyocardial or intravenously. The different infarct model and method of cell delivery we used could account for the differences observed after UCB cell therapy.

There are also large differences between the different UCB derived cell types which were injected in the studies; freshly isolated mononuclear cells^{13,16,20}, cryopreserved mononuclear cells²¹, CD34+ cells¹⁴ and CD133+ cells^{17,20} were used but also cultured mononuclear cells¹², mesenchymal stem cells¹⁸, CD34+¹⁹ cells and USSC¹⁵. Furthermore the number of injected cells, the timing of cell injection and the follow-up time differ between the studies. Taken together all these differences in experimental setup could be the reason why our results contradict earlier reports of the effect of UCB on myocardial infarction.

The study by Kim *et al.*¹⁵, which was also performed in swine, showed a beneficial effect on LV function of the same USSC cell line as used in our studies. However, in that study cells were injected intramyocardially, and furthermore, the MI was created by permanent LAD ligation. To get more insight in the contradicting findings between the study of Kim *et al.*¹⁵ and our study we performed some additional experiments. We chose to inject cells into the healthy myocardium in five swine and sacrificed the animals four days later.

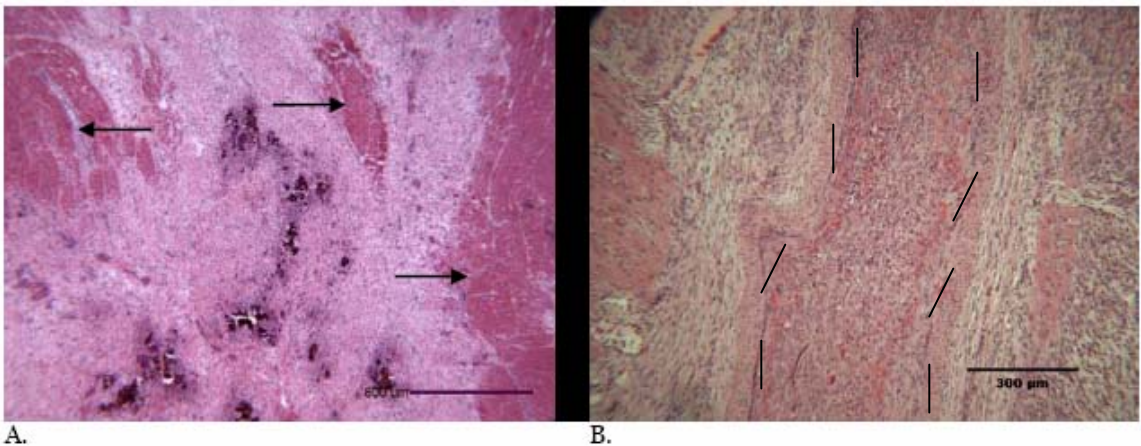


Figure 1: A. Hematoxylin-Eosin staining 4 days after USSC injection in normal myocardium. Note the extensive fibrosis and calcification. Arrows indicate surviving myocytes. B. Hematoxylin-Eosin staining of an occluded vessel (between black lines) 4 days after USSC injection in normal non-ischemic myocardium.

Extensive micro infarctions (Figure 1A) were observed four days after USSC injection in non-ischemic myocardium caused by occluded vessels (Figure 1B). In situ hybridization showed that the cells in the occluded vessel were predominantly of human origin. Micro infarctions were also observed by Vulliet *et al.*²³ after

intracoronary injection of cultured mesenchymal stem cells in dogs. These findings suggest that intracoronary injection of these cultured USSC is not suitable, and intramyocardial injection might be preferable. Further studies are required to investigate whether USSC occlude vessels due to their large cell size (~20 µm). Bone marrow derived mononuclear cells, however, are only ~5-7 µm in size.

In some studies immune suppression was administered to the animals^{14,15,18}. Min *et al.*¹⁸ showed that 7 days after injection, human cells could not be detected anymore in rats that did not receive immune suppression. With immune suppression human UCB derived cells could still be detected 8 days after injection. Three other studies^{16,17,20} have shown that after injection of human cells in rodents, these cells could be detected in the heart of some but not all of the injected animals. Overall, it is still unclear whether UCB cells are really hypo immunogenic. Kim *et al.*¹⁵ even observed a higher number of CD3 positive cells and macrophages in UCB treated swine. But they could also detect human cells that were positive for cardiomyocyte specific markers such as troponin I and myosin heavy chain. Except for the study of Henning *et al.*¹, all other preclinical studies showed that the human UCB derived cells were detected near vessels and cardiomyocytes or myofibroblasts, but the injected cells predominantly kept their hematopoietic phenotype.

Conclusions

Treatment of infarcted myocardium with UCB derived cells is promising but there should be caution when using these cells in patients. The results of our own experiment suggest that intracoronary injection of cultured UCB derived stem cells is not suitable. More studies in large animal models with reperfused MI are needed to investigate the optimal mode of administration for these cells. Furthermore, since the immunogenicity of these cells is not yet determined, this should be tested in appropriate models.

Since an infarct area is a very hostile environment for injected cells due to ischemia and inflammation, it is not surprising that very few cells seems to survive and that thusfar limited evidence exists that injected cells are able to differentiate towards a cardiomyocyte-like phenotype. Potential approaches to overcome these limitations might be the overexpression of survival genes or to direct the differentiation of the UCB cells towards a cardiac lineage before injection.

References

1. Bartunek J, Dimmeler S, Drexler H, Fernandez-Aviles F, Galinanes M, Janssens S, Martin J, Mathur A, Menasche P, Priori S, Strauer B, Tendera M, Wijns W, Zeiher A. The consensus of the task force of the European Society of Cardiology concerning the clinical investigation of the use of autologous adult stem cells for repair of the heart. *Eur Heart J.* 2006;27:1338-40.
2. Vasa M, Fichtlscherer S, Aicher A, Adler K, Urbich C, Martin H, Zeiher AM, Dimmeler S. Number and migratory activity of circulating endothelial progenitor cells inversely correlate with risk factors for coronary artery disease. *Circ Res.* 2001;89:E1-7.
3. Ende M, Ende N. Hematopoietic transplantation by means of fetal (cord) blood. A new method. *Va Med Mon (1918).* 1972;99:276-80.
4. Gluckman E. Bone marrow transplantation for Fanconi's anaemia. *Baillieres Clin Haematol.* 1989;2:153-62.

5. Laughlin MJ, Eapen M, Rubinstein P, Wagner JE, Zhang MJ, Champlin RE, Stevens C, Barker JN, Gale RP, Lazarus HM, Marks DI, van Rood JJ, Scaradavou A, Horowitz MM. Outcomes after transplantation of cord blood or bone marrow from unrelated donors in adults with leukemia. *N Engl J Med.* 2004;351:2265-75.
6. Rocha V, Labopin M, Sanz G, Arcese W, Schwerdtfeger R, Bosi A, Jacobsen N, Ruutu T, de Lima M, Finke J, Frassoni F, Gluckman E. Transplants of umbilical-cord blood or bone marrow from unrelated donors in adults with acute leukemia. *N Engl J Med.* 2004;351:2276-85.
7. Brunstein CG, Wagner JE. Cord blood transplantation for adults. *Vox Sang.* 2006;91:195-205.
8. El-Badri NS, Hakki A, Saporta S, Liang X, Madhusodanan S, Willing AE, Sanberg CD, Sanberg PR. Cord blood mesenchymal stem cells: Potential use in neurological disorders. *Stem Cells Dev.* 2006;15:497-506.
9. Perry TE, Roth SJ. Cardiovascular tissue engineering: constructing living tissue cardiac valves and blood vessels using bone marrow, umbilical cord blood, and peripheral blood cells. *J Cardiovasc Nurs.* 2003;18:30-7.
10. Schmidt D, Hoerstrup S. Tissue engineered heart valves based on human cells. *Swiss Med Wkly.* 2006;136:618-23.
11. Kadirav M, Khatami S, Mortazavi Y, Shokrgozar MA, Taghikhani M, Soleimani M. In vitro cardiomyogenic potential of human umbilical vein-derived mesenchymal stem cells. *Biochem Biophys Res Commun.* 2006;340:639-47.
12. Hu CH, Wu GF, Wang XQ, Yang YH, Du ZM, He XH, Xiang P. Transplanted human umbilical cord blood mononuclear cells improve left ventricular function through angiogenesis in myocardial infarction. *Chin Med J (Engl).* 2006;119:1499-506.
13. Henning RJ, Abu-Ali H, Balis JU, Morgan MB, Willing AE, Sanberg PR. Human umbilical cord blood mononuclear cells for the treatment of acute myocardial infarction. *Cell Transplant.* 2004;13:729-39.
14. Hirata Y, Sata M, Motomura N, Takanashi M, Suematsu Y, Ono M, Takamoto S. Human umbilical cord blood cells improve cardiac function after myocardial infarction. *Biochem Biophys Res Commun.* 2005;327:609-14.
15. Kim BO, Tian H, Prasongsukarn K, Wu J, Angoulvant D, Wnendt S, Muhs A, Spitkovsky D, Li RK. Cell transplantation improves ventricular function after a myocardial infarction: a preclinical study of human unrestricted somatic stem cells in a porcine model. *Circulation.* 2005;112:196-104.
16. Ma N, Stamm C, Kaminski A, Li W, Kleine HD, Muller-Hilke B, Zhang L, Ladilov Y, Egger D, Steinhoff G. Human cord blood cells induce angiogenesis following myocardial infarction in NOD/scid-mice. *Cardiovasc Res.* 2005;66:45-54.
17. Leor J, Guetta E, Feinberg MS, Galski H, Bar I, Holbova R, Miller L, Zarin P, Castel D, Barbash IM, Nagler A. Human umbilical cord blood-derived CD133+ cells enhance function and repair of the infarcted myocardium. *Stem Cells.* 2006;24:772-80.
18. Min JJ, Ahn Y, Moon S, Kim YS, Park JE, Kim SM, Le UN, Wu JC, Joo SY, Hong MH, Yang DH, Jeong MH, Song CH, Jeong YH, Yoo KY, Kang KS, Bom HS. In vivo bioluminescence imaging of cord blood derived mesenchymal stem cell transplantation into rat myocardium. *Ann Nucl Med.* 2006;20:165-70.
19. Chen HK, Hung HF, Shyu KG, Wang BW, Sheu JR, Liang YJ, Chang CC, Kuan P. Combined cord blood stem cells and gene therapy enhances angiogenesis and improves cardiac performance in mouse after acute myocardial infarction. *Eur J Clin Invest.* 2005;35:677-86.
20. Ma N, Ladilov Y, Kaminski A, Piechaczek C, Choi YH, Li W, Steinhoff G, Stamm C. Umbilical cord blood cell transplantation for myocardial regeneration. *Transplant Proc.* 2006;38:771-3.
21. Henning RJ, Burgos JD, Ondrovic L, Sanberg P, Balis J, Morgan MB. Human umbilical cord blood progenitor cells are attracted to infarcted myocardium and significantly reduce myocardial infarction size. *Cell Transplant.* 2006;15:647-58.
22. Moelker AD, Baks T, van den Bos EJ, van Geuns RJ, de Feyter PJ, Duncker DJ, van der Giessen WJ. Reduction in infarct size, but no functional improvement after bone marrow cell administration in a porcine model of reperfused myocardial infarction. *Eur Heart J.* 2006;27:3057-64.
23. Vulliet PR, Greeley M, Halloran SM, MacDonald KA, Kittleson MD. Intra-coronary arterial injection of mesenchymal stromal cells and microinfarction in dogs. *Lancet.* 2004;363:783-4.

Chapter 5

Intracoronary Delivery of Umbilical Cord Blood Derived Unrestricted Somatic Stem Cells is Not Suitable to Improve LV Function after Myocardial Infarction in Swine

Amber D. Moelker¹ MSc, Timo Baks^{1,2} MD, Kim M.A.M. Wever¹ MSc, Dimitry Spitskovsky³ PhD, Piotr A. Wielopolski² PhD, Heleen M.M. van Beusekom¹ PhD, Robert-Jan van Geuns^{1,2} MD, PhD, Stephan Wnendt⁴ PhD, Dirk J. Duncker¹ MD, PhD, Wim J. van der Giessen^{1,5} MD, PhD

¹Cardiology, Thoraxcenter, Erasmus MC Rotterdam, The Netherlands

²Radiology, Erasmus MC Rotterdam, The Netherlands

³Kourion Therapeutics AG, Langenfeld, Germany**

⁴Viacell, Cambridge, MA, USA**

⁵Interuniversity Cardiology Institute of the Netherlands

Abstract

Objective Regeneration of infarcted myocardium by injecting stem cells has been proposed to prevent heart failure. We studied the i.c. administration of human umbilical cord blood stem cells (USSC) in a porcine model of myocardial infarction (MI) and reperfusion.

Methods In 15 swine, MI was induced by balloon-occlusion of the circumflex coronary artery (LCX) for two hours followed by reperfusion. Five swine served as healthy controls. One week later, magnetic resonance imaging (MRI) was performed to assess left ventricular (LV) function and infarct size. Then, under immune suppression, 6 of the 12 surviving MI swine received intracoronary injection of $\sim 10^8$ human USSC in the LCX while the other MI-swine received medium. Four weeks later all swine underwent follow-up MRI, and were sacrificed for histology.

Results One week after MI, end-diastolic volume (92 ± 3 mL) and LV mass (75 ± 2 g) were larger, while ejection fraction (42 ± 2 %) was smaller than in healthy control (68 ± 3 mL, 66 ± 3 g and 55 ± 3 %, $P < 0.05$). Regional wall thickening (-7 ± 2 %) in the LCX area became akinetic. No difference in global and regional LV function at five weeks was observed between MI animals receiving USSC or medium. Infarct size after USSC treatment was significantly larger (8 ± 2 g vs. 20 ± 3 g, $P < 0.05$). USSC survived only in the infarct border zone at 5 weeks and did not express markers of cardiomyocyte or endothelial phenotype. Histology showed that intracoronary injection of USSC caused micro infarctions by obstructing blood vessels.

Conclusion In swine with a one week old MI, injection of USSC via the intracoronary route doesn't improve LV function four weeks later.

Introduction

Tissue regeneration after myocardial infarction (MI) via stem cell transplantation has shown potential as a novel therapy to prevent left ventricular (LV) remodeling and heart failure.¹⁻⁴ For example, direct injection of autologous skeletal muscle progenitor cells into the infarcted myocardium, resulted in improved LV function after MI in experimental studies⁵ as well as in patients with an old MI and chronic heart failure.⁶ Beneficial effects on LV function have also been reported for bone marrow derived stem cells⁷. Thus, in a large number of studies performed in small animal models of MI produced by permanent coronary artery ligation, injection of cells within hours after ligation (either intravenously or directly into the infarcted area) attenuated LV remodeling and dysfunction.^{1,2} Clinical studies also showed similarly favorable, albeit smaller, effects of autologous bone marrow derived stem cells (injected into the coronary artery supplying the infarcted but reperfused myocardial region) on LV function after MI,⁷⁻¹¹ although more recent evidence suggests that the beneficial effects at 6 months were no longer significantly different from controls at 18 months.¹¹

Although transplantation of autologous cells has the obvious advantage of lack of rejection, therapy with autologous cells has also potential disadvantages. First, autologous cells are harvested from MI patients, who are likely to have risk factors that are associated with decreased precursor cell functionality.¹² In addition, the number of stem cells obtained during harvesting may be variable, resulting in non-standardized re-injections¹² or necessitating subsequent culture steps, particularly in the case of skeletal myoblasts.^{5,6,13}

Human umbilical cord blood is a rich source of stem cells for hematopoietic reconstitution and other potential applications in regenerative medicine, especially with respect to the recently described Unrestricted Somatic Stem Cells (USSC) from human cord blood.¹⁴ Recent evidence suggests that human umbilical cord blood derived cells may have a beneficial effect on LV remodeling and function after MI.¹⁵⁻¹⁹ Importantly, all five studies produced MI by permanent coronary artery ligation, i.e. without reperfusion, which clearly differs from the clinical setting. Furthermore, cells were injected either intravenously^{17,18} or directly into the infarcted territory,^{15,16,19} whereas the intracoronary injection of bone marrow derived mononuclear cells are typically used in more recent clinical post-myocardial infarction studies.¹¹ Consequently, the present xenotransplantation study was designed to assess in a porcine model of reperfused acute MI the effects of intracoronary (i.c.) injection of human umbilical cord blood derived cultured USSC¹⁹ on regional and global LV function, LV geometry as well as infarct size, using magnetic resonance imaging (MRI).²⁰ For this study USSC cultured by Kourion Therapeutics were used, this cell line was *ex vivo* described by Kögler et al.¹⁴ and exactly the same cell line was used for direct intramyocardial injection by Kim et al.¹⁹

Material and methods

Experiments were performed in 2-3 month old Yorkshire-landrace pigs, in compliance with the "Guide for the Care and Use of Laboratory Animals" (NIH publication 1996) and written approval of the Animal Care Committee of Erasmus MC.

Umbilical Cord Blood Derived Cells

USSC were established from human umbilical cord blood as described by Kögler et al.,¹⁴ and were negative for CD14, CD33, CD34, CD45, and express CD13, CD29, CD44, CD49e and HLA-I.

Cell culture and preparation for transplantation was performed by Kourion Therapeutics AG (Langenfeld, Germany) according to proprietary methods.^{14,19}

Experimental Protocols

Protocol I: Cell Injection and Survival

We first investigated the survival of human USSC in infarcted porcine myocardium in a pilot group of 4 swine. For this purpose, animals were sedated (ketamine 20 mg/kg intramuscular (i.m.), and midazolam 1 mg/kg i.m.), anesthetised (thiopental, 12 mg/kg intravenously (i.v.)), intubated and mechanically ventilated with a mixture of oxygen and nitrogen (1:2 vol/vol). Anesthesia was maintained with fentanyl (12.5 µg/kg/h, i.v.) and isoflurane (0.6-0.8% started after onset of occlusion). Subsequently, animals received antibiotic prophylaxis (200 mg procainebenzylpenicillin and 250 mg dihydrostreptomycinesulfate i.m.) and underwent coronary catheterization through the carotid artery approach, followed by balloon occlusion of the proximal left circumflex coronary artery (LCX) for 2 hr followed by reperfusion. Heparin was administered every hour (5000 Units).

One week after MI, swine were anesthetized and heparinized as described above and received an i.c. injection of ~ fifty million DAPI-labelled USSC (Sigma-Aldrich, Schnellendorf, Germany) suspended in 10 mL Dulbecco's Modified Eagle's Medium (DMEM) in the infarct related artery. USSC were filtered (100 µm pore size) and injected slowly (1 mL/min) into the coronary artery perfusing the MI area using a delivery catheter (Multifunctional Probing, Boston Scientific Co, Boston, MA). The site of injection was identical to the position of the occlusion balloon during MI induction.

To prevent hyper-acute rejection, two out of the four swine received 600 mg mycophenolic acid mofetil (Novartis, The Netherlands) 6 hours prior to cell injection followed by 600 mg b.i.d. starting 24 hours after injection, and cyclosporine A (CsA, Novartis, The Netherlands) 4 mg/kg b.i.d. starting 24 hours after cell injection. The other two animals did not receive immune suppression. Four days after cell injection animals were sacrificed for histological and immunocytochemical analyses.

Protocol II: Effect of USSC on LV Remodeling, Global and Regional Function and Infarct Size

Experiments were performed in 21 swine. Six swine served as healthy controls for normal cardiac growth and function. Fifteen swine underwent MI as described above; 3 swine died within 24 h post-MI due to arrhythmias. One week after MI, swine were again anesthetized as described above and underwent magnetic resonance imaging (MRI) to assess LV geometry and global and regional function, and infarct size. One control animal did not recover from anesthesia. Subsequently, MI swine were randomized to receive an intracoronary injection of ~ 100 million USSC suspended in 10 mL DMEM (n=6), or 10 mL DMEM (n=6). All swine (including that receiving medium and the controls) received 300 mg prednisone 24 hours before cell or

medium injection followed by 300 mg daily for 2 days. In addition, swine received CsA 4 mg/kg b.i.d. starting 24 h after cell or medium injection until sacrifice. Four weeks later all 17 swine underwent follow-up MRI, after which animals were sacrificed for histological and immunocytochemical analyses of the LCX perfused infarct area and remote areas of the LV.

Magnetic Resonance Imaging

Data Acquisition

A clinical 1.5-Tesla MRI with a dedicated cardiac four element phased-array receiver coil was used for imaging (Signa CV/i, GE Medical systems, Milwaukee, WI, USA). Repeated breath-holds and gating to the ECG were applied to minimize the influence of cardiac and respiratory motion on data collection. Baseline and follow-up contrast enhanced (ce) MRI protocol consisted of cine-MRI and Delayed Enhancement (DE) imaging. Cine-MRI was performed using steady-state free-precession technique (imaging parameters: 24 temporal phases per slice, FOV26-30, rect. FOV 75%, TR 3.4, TE 1.4, flip angle 45°, matrix 160x128, bandwidth 83 kHz, 0.75 NEX). To cover the entire left ventricle, six to eight consecutive slices of 8 mm were planned in the short axis view, perpendicular to the long axis four-chamber view of the left ventricle (gap=0). DE imaging was performed to assess total myocardial infarct mass 10-20 minutes after administration of gadolinium-DTPA (0.5 mmol/kg, Magnevist®, Schering) with a 2-dimensional T1-weighted inversion-recovery gradient-echo sequence (imaging parameters: slice thickness 8 mm, FOV26-30, rect FOV 75%, TR 7.3, TE 1.6, flip angle 20 degrees, TI 180-275 ms, matrix 256x192, 1 NEX, bandwidth 17.9 kHz). The inversion time was adjusted per animal to null the signal of remote myocardium. Locations were copied from the cine-images.

Image Analysis

The MR images were analyzed with dedicated cardiac software (Cine display application 3.0, General Electric medical systems, USA). End-diastolic volume (EDV), end-systolic volume (ESV) and left ventricular weight (LVW) were measured by manually drawing the endocardial and epicardial borders in the end-diastolic and end-systolic image of each slice. Stroke volume ($SV = EDV - ESV$), ejection fraction ($EF = [SV/EDV] \times 100\%$) and cardiac output ($CO = SV \times HR$) were computed. End-diastolic wall thickness (EDT) and end systolic wall thickness (EST) was measured and expressed in millimeter in 36 sections per slice. Regional systolic wall thickening (SWT) was calculated as $[EST - EDT]/EDT \times 100\%$. Baseline and endpoint scans were matched for location using anatomical landmarks like insertion of the right ventricle to the septum and the papillary muscles.²⁰ The volume of DE was quantified by manually selecting the enhanced regions from the consecutive 2D slices encompassing the left ventricle. DE volume was multiplied by 1.05 g/ml to obtain myocardial infarct mass (1 millilitre corresponds to 1.05 gram as measured in our own laboratory). The anterior and posterior sections immediately adjacent to the akinetic infarct region were defined as border zone.

Histology and Immunohistochemistry

The hearts were excised and cut in 6-8 transverse slices similar to the MRI short axis slices. From the basal plane the first ring, and all other odd rings, were fixed in 4% buffered formaldehyde and embedded in paraffin. The second ring, and all other even rings, were embedded in tissue tec OCT and frozen in liquid nitrogen. Sections (5 µm) were stained with hematoxylin eosin (HE), resorcin-fuchsin (RF, collagen), von Kossa (calcium). Immunohistochemistry was also performed for identification of porcine leukocytes (CD45, Serotec, Kidlington, UK), porcine T-cells (CD3, Abcam, Cambridge, UK), human leukocytes (CD45, Chemicon, Hampshire, UK), human endothelial cells (vWF, Sigma, Missouri, USA), human cardiomyocytes (Troponin T, Abcam, Cambridge, UK), human mitochondria (MAB1273, Chemicon, Hampshire, UK) and USSC (in situ hybridization for human chromosome one with PUC1.77 staining²¹).

Sections were semi-quantitatively assessed as negative (-) or extent of positivity (+, ++ or +++) for the amount of collagen, calcium deposition, CD45⁺ cells and vascularization.

Statistical Analysis

Data were analyzed with SPSS 11.0. All data were analyzed using two-way analysis of variance (ANOVA), followed by one-way ANOVA and post-hoc analysis using unpaired t-testing with Bonferoni correction to test for significant intergroup differences at corresponding time points. Intragroup differences between baseline and endpoint were determined using paired t-testing with Bonferoni correction. Effect of USSC therapy was tested using analysis of co-variance (ANCOVA) with baseline values as covariate. Statistical significance was accepted when $P \leq 0.05$ (two-tailed). All data are presented as mean \pm SEM.

Results

Cell Injection and Survival

DAPI labeled cells could be detected 4 days after injection into infarcted area both in the presence (Figure 1A) or absence (Figure 1B) of immune suppression. Mononucleated USSC were also detected with PUC 1.77 staining (Figure 1C) thereby excluding cell fusion. Histological analysis using HE, RF, and CD45 staining, showed similar numbers of fibroblasts, collagen deposition and inflammatory cell infiltration at 4 days after USSC injection in swine that did not, as compared to animals that did, receive immune suppression.

Effect of USSC on LV Remodeling, Global and Regional Function and Infarct Size

Twenty-one animals entered the study. Four animals died prematurely, three of which died within 24 hours after induction of MI. One control animal did not recover from anesthesia after the baseline MRI, therefore five control swine completed the protocol. In all surviving MI animals (n=12), USSC or medium infusion was successful.

LV Remodeling and Global Function

One week after MI, significant LV remodeling as demonstrated by a higher end-diastolic volume (97 ± 5 mL vs. 68 ± 4 mL in control swine), end-systolic volume (54 ± 3 mL vs. 32 ± 3 mL) and LV weight (75 ± 2 g vs. 66 ± 3 g) in MI swine compared to control swine (all $P\leq 0.05$; Table 1 and Figure 2) had already occurred. LV remodeling was accompanied by LV dysfunction resulting in a lower ejection fraction (42 ± 2 % vs. 55 ± 4 %, $P\leq 0.05$), but not in overt heart failure, as stroke volume (38 ± 2 vs. 37 ± 3 mL) was maintained (Table 1). LV-volumes increased between 1 and 5 weeks, but that was likely due to growth of the animals, since also the volumes in the control group increased (Figure 2). Importantly, the increases in LV weight and volumes over the 4 week follow-up period were not significantly different between medium- and USSC-treated MI swine. Furthermore, ejection fraction remained constant over the 4 week period in both medium- and USSC-treated animals (Table 1 and Figure 2).

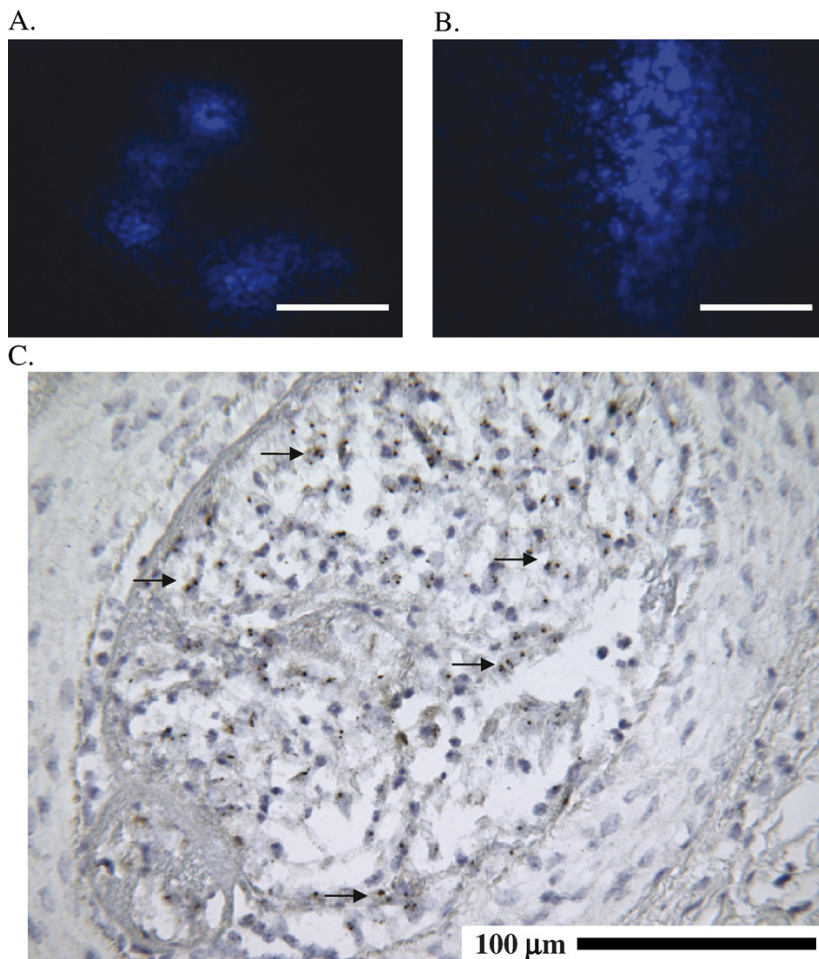


Figure 1 DAPI labeled USSC detected 4 days after injection into infarcted LCX region either with (photomicrograph A) or without (photomicrograph B) immunosuppression. Photomicrograph C shows the presence of USSC as being positive for PUC1.77 (black dots indicated by black arrows) in an animal not receiving immunosuppression. Each bar represents 100 μm .

Table 1: Hemodynamic and anatomical data

		Control Swine (n=5)	MI Swine	
			Medium (n=6)	USSC (n=6)
BW (Kg)	Baseline	23 ± 1	24 ± 1	26 ± 0.4 [†]
	Endpoint	35 ± 1*	38 ± 1*	39 ± 1* [†]
HR (bpm)	Baseline	108 ± 4	91 ± 5 [†]	84 ± 5 [†]
	Endpoint	83 ± 5*	93 ± 10	76 ± 5
SV (mL)	Baseline	37 ± 3	39 ± 2	38 ± 2
	Endpoint	58 ± 5	57 ± 6	59 ± 5
LVW (g)	Baseline	66 ± 3	76 ± 3 [†]	74 ± 2 [†]
	Endpoint	99 ± 6*	104 ± 5*	119 ± 5* [§]
Infarct size (g)	Baseline	-	9 ± 3	14 ± 3
	Endpoint	-	8 ± 2	20 ± 3* [§]
Infarct size (% of the LV)	Baseline	-	12 ± 3	19 ± 3
	Endpoint	-	7 ± 2**	17 ± 2* [§]

BW = body weight; HR = heart rate; SV = stroke volume; LVW = left ventricular weight; Baseline = 1 wk post-MI; Endpoint = 5 wk post-MI. * $P < 0.05$, ** $P = 0.08$ endpoint vs. baseline, [†] $P < 0.05$ vs. corresponding Control, [‡] $P < 0.05$ USSC vs. corresponding medium-treated MI animals, [§] $P < 0.05$ change from baseline USSC- vs. medium-treated MI animals.

Regional LV Function

Analysis of regional LV function at 1 week post-MI showed akinesis of the infarcted lateral wall resulting in complete loss of systolic wall thickening in the central infarct zone ($-7 \pm 2\%$) and partial loss of systolic wall thickening in the border zones ($25 \pm 3\%$) as compared to systolic wall thickening of the lateral wall in control swine ($62 \pm 7\%$; Figure 3). The abnormalities in regional function remained virtually unchanged during the next 4 weeks of the follow-up period. Furthermore, no differences were observed between medium- as well as USSC-treated animals in end-diastolic wall thickness or absolute or percent systolic wall thickening, either at baseline or 4 weeks after treatment (Figure 3).

Infarct Size

DE-MRI showed that at 1 week post-MI, the infarcted region encompassed $16 \pm 3\%$ of LV weight (Table 1). During the 4 week follow-up period, the absolute weight of the infarcted region remained constant in the medium-treated swine, and considering the increase in total LV weight the relative infarct size thereby tended to decrease (from $12 \pm 3\%$ to $7 \pm 2\%$; $P = 0.08$). In contrast, in the USSC-treated swine absolute infarct size actually increased slightly and relative infarct size did not decrease. This change in infarct size over the four week period between the groups was statistically different ($P < 0.05$).

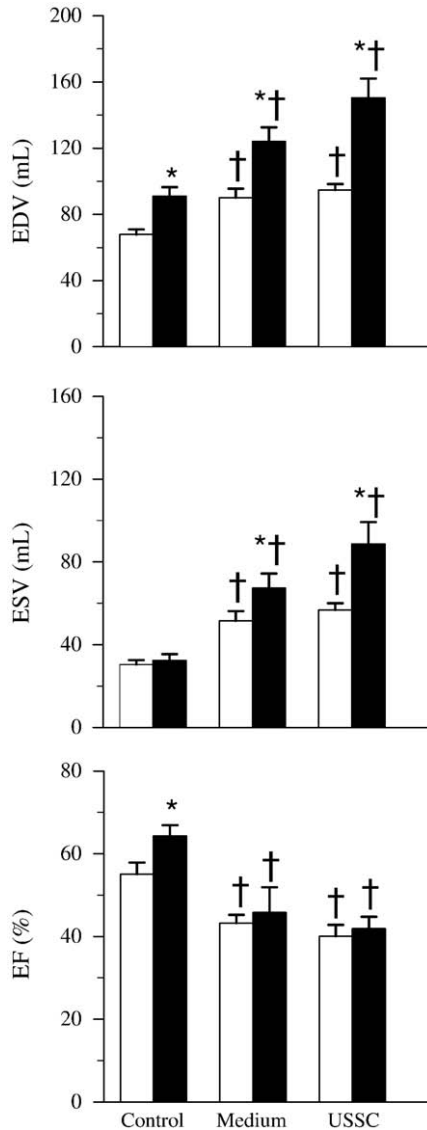


Figure 2 LVend-diastolic volume (EDV), LVend-systolic volume (ESV), and LV ejection fraction (EF) at baseline (open bars) and at endpoint (solid bars) in Control swine, and MI swine receiving either medium or USSC. *P<0.05 endpoint vs. baseline, †P<0.05 vs. corresponding control. There were no differences between USSC- and medium-treated MI animals either at baseline or endpoint, or in the response over the 4 week follow-up period.

Histology

Histology confirmed the presence of transmural infarcts in the LCX region with a nearly complete loss of viable tissue in all MI animals (Figure 4A and 4B), matching the DE scans performed at 5 weeks after MI. The medium- and USSC-treated swine both showed abundant collagen (Figure 4C and 4D) and fibrous tissue (Figure 4E and 4F) in the center of the infarct. The amount of calcification (4A, B) and inflammatory cell infiltration (4G, H) appeared larger in USSC-treated compared to medium-treated

swine. There were no discernible differences in histological appearance within the border zones between USSC- and medium-treated swine.

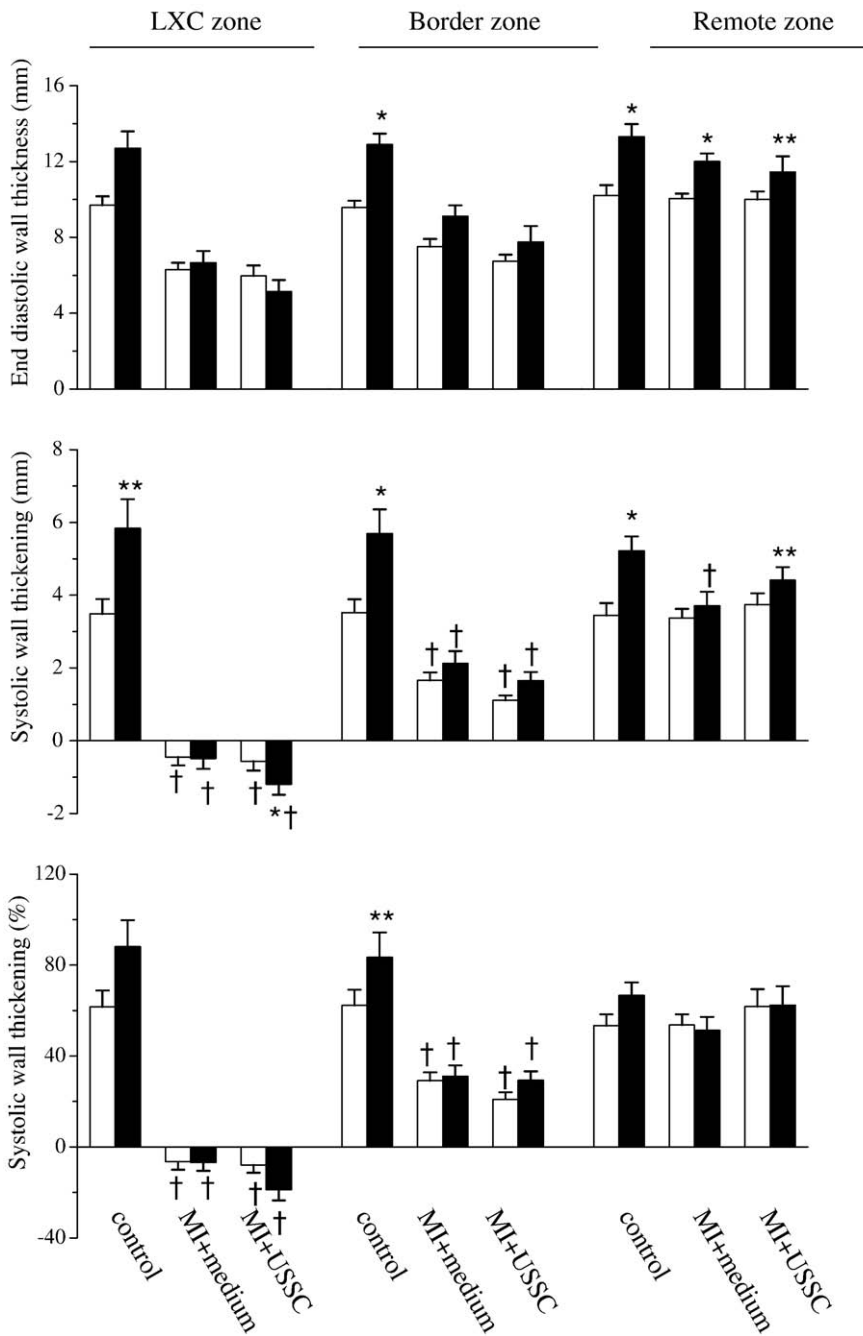


Figure 3 End-diastolic wall thickness (EDT, upper panel), absolute SWT (middle panel) and percent SWT (lower panel) at baseline (open bars) and at endpoint (solidbars) in Control swine, and MI swine receiving either medium or USSC. *P<0.05, **P<0.1 endpoint vs. baseline, †P<0.05 vs. corresponding control. There were no differences between USSC and medium treated MI animals.

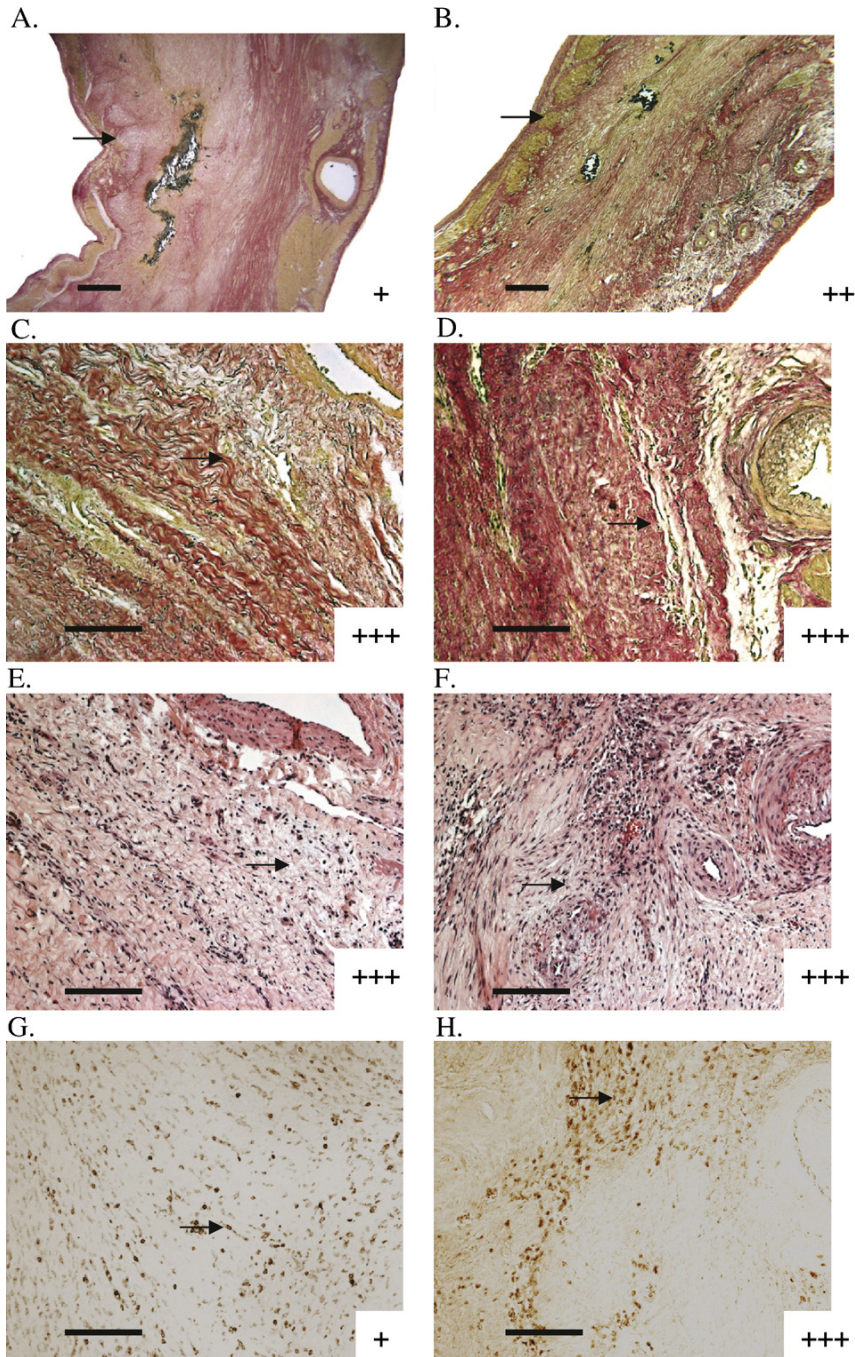


Figure 4 Infarct area of medium-treated (A, C, E, G) compared with USSC-treated (B, D, F, H) swine, showing transmural infarction (photomicrographs A, B; von Kossa staining; arrows point indicate endocardium), and abundant collagen (arrows in C, D; RF staining) and fibroblasts (arrows in E, F; HE staining), and inflammatory cells (arrows in G, H; panleucocyte marker CD45). The + symbols denote the degree of calcification (A, B), collagen (C, D), vascularization (E, F) and CD45+ cells (G, H). Bars denote 1 mm (A, B) and 300 μ m (C–H).

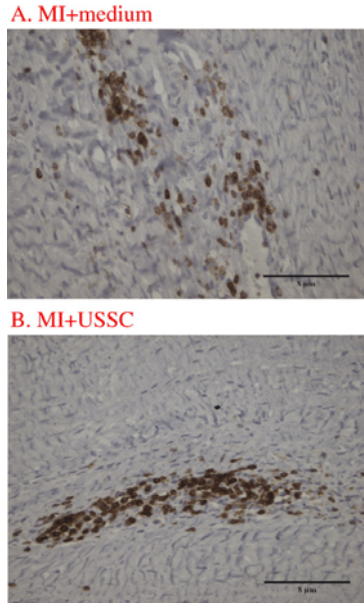


Figure 5 CD3 positive cells (brown) in the infarct area of medium treated swine (A) and USSC treated swine (B).

CD3 staining showed that more CD3 positive cells were detected in animals which were treated with USSC compared to the medium treated animals (Figure 5).

Immunohistochemistry double labeling with human anti-mitochondria antibody showed that USSC were negative for von willebrand factor (Figure 6A) and for cardiac troponin T (Figure 6C). Some USSC however were positive for CD45 (Figure 6B).

Using PUC1.77 staining we could not demonstrate the presence of USSC in the central infarct zone. However, a few USSC (2.0 ± 0.6 cells/cm²) could be detected in the border zone (Figure 7), which corresponds with 0.026% of the injected cells.

Discussion

The present study investigated the effects of intracoronary injection of USSC in a porcine model of reperfused MI. USSC were injected 1 week after reperfusion and swine were studied 4 weeks later. The main finding is that intracoronary injection of USSC does not attenuate MI-induced LV remodeling or ameliorate global and regional LV dysfunction. In addition, USSC resulted in a larger infarct size at 4 weeks follow-up, which was accompanied by increases in inflammatory cells and calcifications in the infarct zone compared to medium-treated swine. The implications of these findings will be discussed in detail.

Previous studies

To date a few studies have investigated the effects of cord blood derived cells on post-MI LV remodeling and dysfunction and infarct size. In rats direct injection of CD34+, CD133+ or mononuclear cells from cord blood into viable myocardium, bordering the

ischemic region, within 1 hour after permanent coronary artery ligation resulted in significantly better LV function at 4 weeks^{16,17} or 4 months.¹⁵ Intravenous injection of mononuclear cells from cord blood one day after permanent coronary artery ligation in mice was reported to reduce infarct size and enhance angiogenesis in the infarct border zone.¹⁸ Recently, Kim *et al.*¹⁹ reported in a porcine model of permanent ligation induced MI, that USSC directly injected into the border zone of the infarct area 4 weeks post-MI, resulted in significant reduction in end-diastolic volume and improvement of ejection fraction compared to medium-treated swine at 8 weeks post-MI. In addition, these authors observed a decrease in relative infarct size (as measured *ex-vivo* with planimetry). In contrast to the beneficial effects observed in studies that used direct intramyocardial injection in models of non-reperfused MI¹⁹, the present study fails to reveal a beneficial effect of intracoronary injection of USSC on LV remodeling, function and infarct size in a model of reperfused MI, although the identical cell line was used. Several reasons could be forwarded to explain the negative results in the present study, including timing of USSC administration after MI, insufficient duration of follow-up in order to detect beneficial effects, insufficient cell survival, and/or route of administration.

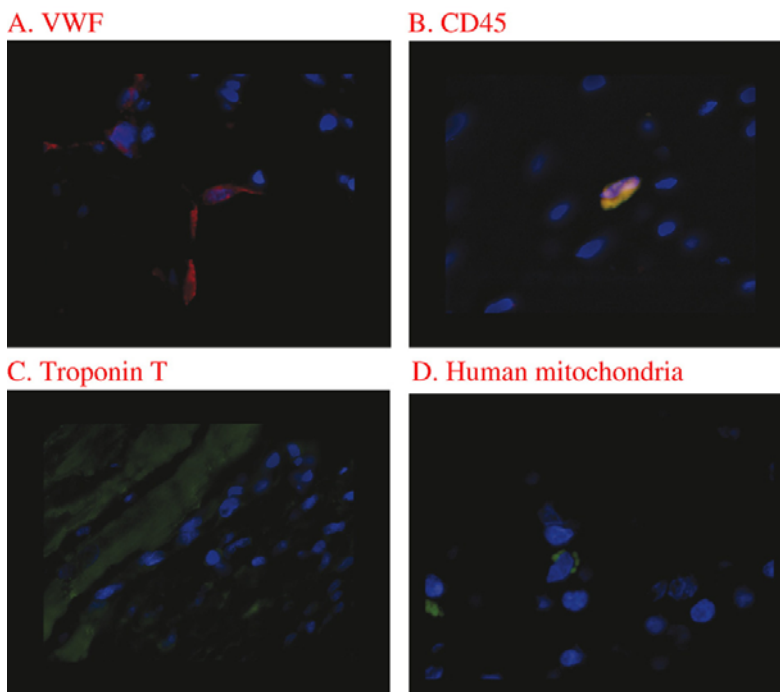


Figure 6 Picture (A) shows vWF positive cells in red, human mitochondria in green (which are not present in this slice) and DAPI in blue. (B) shows a CD45 positive cell in red, human mitochondria in green and DAPI in blue. The yellow stain indicates double labeling for CD45 and human mitochondria, (C) shows troponin T positive cells in green and DAPI in blue, (D) shows human mitochondria in green and DAPI in blue.

Timing of cell administration

The optimal timing of progenitor cell administration after MI is still incompletely understood. Hence, it could be argued that USSC injection 7 days after MI was too

early to be effective. However, this is unlikely as previous studies showed favorable effects of cord blood cell injection as early as 20-min,¹⁶ 60-min,¹⁵ or 1 day¹⁸ after coronary ligation. We decided to inject USSC 7 days post- MI, as this approximates the time-point of injection that is often used in clinical trials.⁷⁻⁹ Alternatively, one might forward that injection of USSC 7 days post-MI was too late to be effective. However, this is unlikely as Kim *et al.*¹⁹ showed favorable effects of USSC injection as late as 4 weeks after ligation. Furthermore, the REPAIR-AMI trial¹¹ suggests that optimal results are obtained when cells are injected at least 5 days after MI. Hence the timing of administration of USSC cannot explain the observed lack of benefit of USSC on LV remodeling, function or infarct size in the present study.

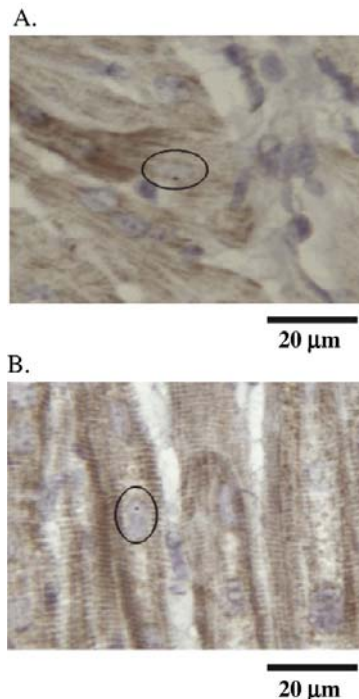


Figure 7 PUC 1.77 positive cell (encircled) in the border zone of the MI area in 2 USSC-treated swine.

Follow-up time

Another reason for the lack of benefit observed in our study could be that the 4 week follow-up period was insufficient to allow detection of an effect of USSC transplantation. However, previous studies reported positive effects on LV remodeling, function, and infarct size as early as three¹⁸ or four^{16,17,19} weeks after MI in rats,^{16,17} mice¹⁸ and swine,¹⁹ indicating that 4 weeks should be sufficient.

Cell survival

An obvious concern when administrating human USSC to swine is low cell survival due to transplant rejection. USSC are purportedly hypo-immunogenic.²² Furthermore, we detected DAPI-labeled USSC in the infarct zone 4 days after injection even in swine that did not receive immune-suppression, suggesting the absence of hyper-acute rejection.

Table 2: Available studies with cord blood derived cells in myocardial infarction

Author	Animal	Type of MI	Cell type	Route of injection	Timing of cell injection Post MI	FU	LV function cells vs. control	Infarct size cells vs. control
Henning et al.	Rat	LAD ligation	MNC	i.m.	1 h	4 m	EF 69% vs. 51%	9.2% vs. 40%
Hirata et al.	Rat	LAD ligation	CD34+	i.m.	20 min	4 w	FS 31% vs. 24%	
Leor et al.	Rat	LAD ligation	CD133+	i.v.	1 week	1 m	Δ FS +42% vs. -39%	
Ma et al.	Mice	LAD ligation	MNC	i.v.	1 day	3 w		38.7% vs. 47.8%
Kim et al.	swine	LAD Coil	USSC	i.m.	4 weeks	4 w	Δ EF +4% vs. -4%	8% vs. 11%
Moelker et al.	swine	LCX reperused	USSC	i.a.	1 week	4 w	Δ EF +1.8% vs. 2.6%	17% vs. 7%

FU= follow up, m= months, w= weeks, LAD = left anterior descending coronary artery, LCX = left circumflex coronary artery, MNC+ mononuclear cells, EF = ejection fraction cell treated animals vs. controls, FS = fractional shortening cell treated animals vs. controls, Δ FS = percent change in FS, Δ EF= absolute change in EF

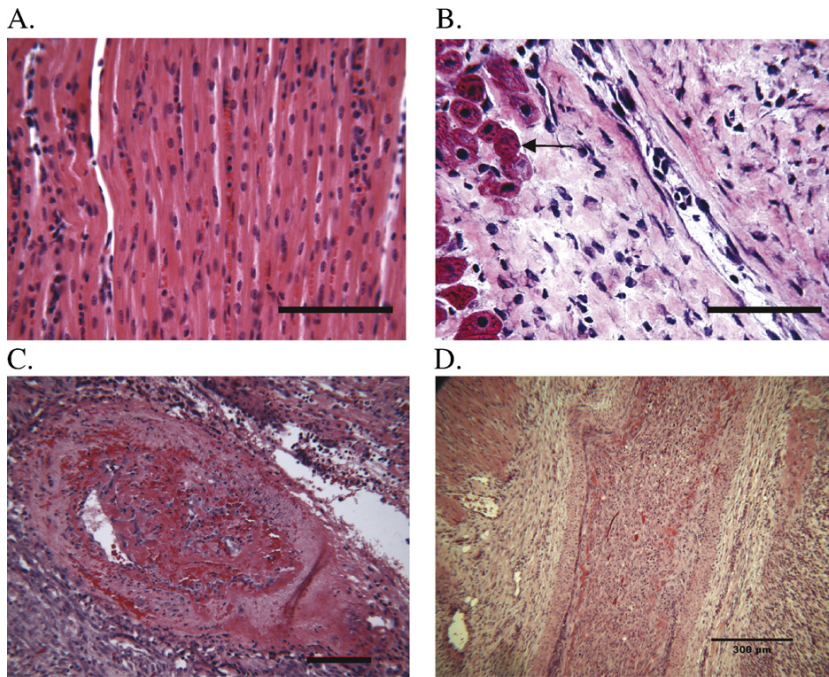


Figure 8 HE staining of normal LAD area showing healthy myocardium (A). HE staining of LAD area 4 days after injection of USSC demonstrating extensive (micro) infarctions (B), caused by occluded vessels (C, transverse cross-section of a vessel, D longitudinal cross-section of a vessel). Arrows indicate surviving myocytes. Bars denote 100 μ m in A-C.

Nevertheless, we decided to use immune-suppression with prednisolone and CsA in our study, because injecting human cells in a pig is by definition a HLA-mismatched xenotransplantation. It is well known that even under immune suppression, cells will be lost by rejection in leukemia patients receiving cell transplants.

Using in-situ hybridization for human chromosome 1 (PUC1.77 staining),²¹ we could not detect any USSC in the central infarct zone. However, surviving USSC were found in the border zone, at the site where the regenerative capacity of progenitor cells is considered most plausible.^{4,11} Kim *et al.*¹⁹, who used the same cell line, observed

survival of a number of USSC in the implanted area, 4 weeks after transplantation in swine, using a dose of CsA of 5 mg/Kg/day. In view of the higher dose of CsA that was administered in the present study (8 mg/Kg/day), the low number of USSC found in the infarct area in the present study was unlikely the result of rejection due to insufficient dosing of CsA. However, immunohistochemistry with CD3 showed that more T-cells were present in USSC treated swine compared to medium treated MI swine, therefore, there were signs of increased rejection after human USSC injection in a porcine MI model even under immune suppression. These findings were also observed by Kim *et al.*¹⁹, which used the same cell line in a different experimental model. Therefore, the immunogenicity of the umbilical cord blood derived USSC is still questionable.

In the present study swine underwent a 2 hour coronary artery balloon occlusion followed by reperfusion to induce MI, which mimics the clinical procedure of percutaneous coronary intervention as closely as possible. Importantly, however, previous studies that reported beneficial effects of cord blood derived cells used an animal model in which MI was induced by permanent coronary ligation.¹⁵⁻¹⁹ It is likely that reperfusion results in more abrupt and pronounced inflammation and hence creates a more hostile environment that is less appropriate for cell survival during the first few days after reperfusion²³. In addition, the transmural, inflammatory infarct region will not stimulate the undifferentiated USSC to develop into a cardiomyocyte or endothelial cell. It is more likely that USSC will develop into an inflammatory cell-type, which can contribute to the higher degree of inflammation and calcification which was observed in our study. This is why we injected USSC 7 days after reperfusion, as it also corresponds with the time of intracoronary injection of progenitor cells in clinical studies that reported beneficial effects.^{8,9}

Fate of the injected cells

Although only a few of the injected cells could be detected four weeks after injection, we studied whether these cells have differentiated into a cardiac, vascular or hematopoietic phenotype. Immunohistochemistry showed that the injected USSC did not transdifferentiate into a cardiomyocyte or endothelial phenotype since they were negative for Troponin and vWF. However some of the injected cells were still CD45 positive meaning that they kept their hematopoietic phenotype, which could mean that they contributed to the increased inflammation observed in cell treated animals.

Mechanism: Route of administration causing micro infarctions

We purposely choose to inject USSC into the coronary artery supplying the infarct area, in view of this being the most common route of administration for stem cell therapy in the setting of AMI,³ One advantage of intracoronary injection is that cells will follow blood flow distribution and reach areas that are well perfused, providing oxygen and nutrients to the transplanted cells which will enhance their survival.⁴ Conversely, intracoronary injection of cells carries the risk of obstruction of the coronary vascular bed. Although this does not appear to be a major issue with purified bone marrow cells in most clinical trials, the risk for embolic complications seems to be more likely when infusing *ex vivo* expanded cells. Intracoronary injections of bone marrow derived mesenchymal stromal stem cells that were twice the size of freshly

harvested bone marrow cells caused micro-infarctions in dogs.²⁴ In the present study, USSC increased inflammatory cells and calcification 4 weeks after injection into the infarct zone. To further explore the issue of micro-embolization in greater detail we injected $\sim 50 \times 10^6$ USSC into the LAD of normal hearts in four swine. Four days after injection of USSC (which are $\sim 20 \mu\text{m}$ in size) in normal healthy myocardium, extensive micro infarctions were observed in the injected area (Figure 8). USSC could be detected in the myocardium obstructing blood vessels. This induction of micro infarction may be the mechanism behind the increased infarct size in our USSC-group. These results show a potential complication of injection of USSC into the coronary circulation. In addition there is evidence that cells expanded in culture show increased expression of adhesion molecules compared to freshly isolated cells,²⁵ so that adhesion to the endothelium throughout the coronary vascular tree resulted in vascular obstruction. Hence, it cannot be excluded that a possible positive effect of USSC injection on LV function after MI was thus obscured by the induction of micro-infarctions caused by the intracoronary injection procedure. In conjunction with the positive results obtained with direct intramyocardial injection of the same USSC-cell line,¹⁹ the present study indicates that intracoronary injection is not the preferred route of administration for cultured USSC. Future studies are needed to assess whether transendomyocardial injections (rather than intracoronary injections) could provide an alternative catheter-based approach to treatment with USSC in reperfused MI.

Acknowledgements

Dr. H. Eussen (Department of Clinical Genetics) is gratefully acknowledged for providing the PUC 1.77 probe, Wendy Kerver is acknowledged for her assistance with the animal procedures and the histology and Prof. J. Cornelissen (Department of Hematology) is acknowledged for carefully reading the manuscript.

References

1. Taylor DA, Atkins BZ, Hungspreugs P, Jones TR, Reedy MC, Hutcheson KA, Glower DD, Kraus WE. Regenerating functional myocardium: improved performance after skeletal myoblast transplantation. *Nat Med* 1998;4(8):929-33.
2. Murry EM, Field LJ, Menasche P. Cell-based cardiac repair: reflections at the 10-year point. *Circulation* 2005;112:3174-83.
3. Histrov M, Weber C. The therapeutic potential of progenitor cells in ischemic heart disease: Past present and future. *Basic Res Cardiol* 2005;100:1-7.
4. Dimmeler S, Zeiher AM, Schneider MD. Unchain my heart: the scientific foundations for cardiac repair. *J Clin Invest* 2005;115:572-83.
5. Van den Bos EJ, Thomson RB, Wagner A, Mahrholdt H, Morimoto Y, Thomson LEJ, Wang LH, Duncker DJ, Judd RM, Tayler DA. Functional assessment of myoblast transplantation for cardiac repair with magnetic resonance imaging. *Eur J Heart Fail* 2005;7(4):435-43.
6. Menasche P, Hagege AA, Vilquin JT, Desnos M, Bergel EA, Pouzet B, Bel A, Sarateanu S, Scorsin M, Schwartz K, Bruneval P, Benbunan M, Marolleau JP. Autologous skeletal myoblast transplantation for severe post infarction left ventricular dysfunction. *Am Coll Cardiol* 2003;41:1078-1083.
7. Bartunek J, Van der Heyden M, Vanderkerckhove B, Mansour S, De Bruyne B, de Bondt P, Van Haute I, Lootens N, Heyndrickx G, Wijns W. Intracoronary injection of CD133-positive enriched bone marrow progenitor cells promotes cardiac recovery after recent myocardial infarction: feasibility and safety. *Circulation* 2005;112(30, 9 Suppl):I178-83.

8. Wollert KC, Meyer GP, Lotz J, Ringes-Lichtenberg S, Lippolt P, Breidenbach C, Fichtner S, Korte T, Horning B, Messinger D, Arseniev L, Hertenstein B, Ganser A, Drexler H. Intracoronary autologous bone-marrow cell transfer after myocardial infarction: the BOOST randomized controlled clinical trial. *Lancet* 2004;364(9429): 141-8.
9. Strauer BE, Brehm M, Zeus T, Kostering M, Hernandez A, Sorg RV, Kogler G, Wernet P. Repair of infarcted myocardium by autologous intracoronary mononuclear bone marrow cell transplantation in humans. *Circulation* 2002;106:1913-1918.
10. Schachinger V, Assmus B, Britten MB, Honold J, Lehmann R, Teupe C, Abolmaali ND, Vogl TJ, Hofmann WK, Martin H, Dimmeler S, Zeiher AM. Transplantation of progenitor cells and regeneration enhancement in acute myocardial infarction: final one-year results of the TOPCARE-AMI Trial. *J Am Coll Cardiol* 2004;44:1690-1699.
11. Cleland JGF, Freemantle N, Coletta AP, Clark AL. Clinical trials update from the American Heart Association: REPAIR-AMI, ASTAMI, JELIS, MEGA, REVIVE-II, SURVIVE, and PROACTIVE. *Eur J Heart Fail* 2006;8:105-110.
12. Vasa M, Fichtlscherer S, Aicher A, Adler K, Urbich C, Martin H, Zeiher AM, Dimmeler S. Number and migratory activity of circulating endothelial progenitor cells inversely correlate with risk factors for coronary artery disease. *Circ Res* 2001;89(1):E1-7.
13. Smits PC, van Geuns RJ, Poldermans D, Bountiokos M, onderwater EE, Lee CH, Maat AP, Serruys PW. Catheter-based intramyocardial injection of autologous skeletal myoblasts as a primary treatment of ischemic heart failure: clinical experience with six-month follow-up. *J Am Coll Cardiol* 2003;42:2063-2069.
14. Kögler G, Senksen S, Airey js, Trapp T, Muschen M, Feldhahn N, Liedtke S, Sorg RV, Fischer J, Rosenbaum C, Greschat S, Knipper A, Bender J, Degistirici O, Gao J, Caplan AI, Colleti EJ, Almeida-Porada G, Muller HW, Zanjani E, Werner P. A new human somatic stem cell from placental cord blood with intrinsic pluripotent differentiation potential. *J Exp Med* 2004;2:123-135.
15. Henning RJ, Abu-Ali H, Balis JU, Morgan MB, Willing AE, Sanberg PR. Human umbilical cord blood ononuclear cells for the treatment of acute myocardial infarction. *Cell Transplant* 2004;13(7-8):729-39.
16. Hirata Y, Sata M, Motomura N, Takanashi M, Suematsu Y, Ono M, Takamoto S. Human umbilical cord blood cells improve cardiac function after myocardial infarction. *BBRC* 2005;327: 609-614.
17. Leor J, Gyetta E, Feinberg MS, Galksi H, Bar I, Holbova R, Miller L, Zarin P, Castel D, Barbash IM, Nagler A. Human umbilical cord blood derived CD133+ cells enhance function and repair of the infarcted myocardium. *Stem Cells Express Epub ahead of print october 2005*.
18. Ma N, Stamm C, Kaminski A, Li W, Kleine HD, Muller-Hilke B, Zhang L, Ladilov Y, Egger D, Steinhoff G. Human cord blood cells induce angiogenesis following myocardial infarction in NOD/scid-mice. *Cardiovasc Res* 2005;66(1):45-54.
19. Kim BO, Tian H, Prasongsukarn K, Wu J, Angoulvant D, Wnendt S, Muhs A, SpitkovskyD, Li RK. Cell transplantation improves ventricular function after a myocardial infarction: a preclinical study of human unrestricted somatic stem cells in a porcine model. *Circulation* 2005;112(9 Suppl):I96-104.
20. Baks T, van Geuns RJ, Biagini E, Wielopolski P, Mollet NR, Cademartiri F, Boersma E, van der Giessen WJ, Krestin GP, Ducnker DJ, Serruys PW, de Feyter PJ. Recovery of left ventricular function after primary angioplasty for acute myocardial infarction. *Eur Heart J* 2005;26(11):1070-7.
21. Verdoodt B, Charlette I, Maillet B, Kisch-Volders M. Numerical aberrations of chromosomes 1 and 17 in tumor cell lines of the exocrine pancreas as determined by fluorescence In Situ Hybridization. *Cancer Genet Cytogenet* 1997;94:125-30.
22. Rocha V, Gluckman E. Clinical use of umbilical cord blood hematopoietic stem cells. *Biol Blood Marrow Transplant* 2006;12:34-41.
23. Bartunek J, Wijns W, Heyndrickx GR, Vanderheyden M. Timing of intracoronary bone-marrow-derived stem cell transplantation after ST-elevation myocardial infarction. *Nat Clin Pract Cardiovasc Med* 2006;3(Suppl 1):S52-6.
24. Vulliet PR, Greeley M, Halloran SM, MacDonald KA, Kittleson MD. Intra-coronary arterial injection of mesenchymal stromal cells and microinfarction in dogs. *Lancet* 2004;363(9411): 783-4.
25. Liu B, Buckley SM, Lewis ID, Goldman AI, Wagner JE, van der Loo JCM. Homing defect of cultured human hematopoietic cells in the NOD/SCID mouse is mediated by Fas/CD95. *Experimental Hematology* 2003;31:824-832.

Chapter 6

Reduction in infarct size, but no functional improvement after bone marrow cell administration in a porcine model of reperfused myocardial infarction

Amber D. Moelker¹, MSc; T. Baks^{1,2}, MD; E.J. van den Bos¹, MD, RJ van Geuns^{1,2}, MD, PhD, P. J. de Feyter^{1,2}, MD, PhD, D.J. Duncker¹, MD, PhD; W.J. van der Giessen^{1,3}, MD, PhD

¹ Cardiology, Thoraxcenter, Erasmus MC Rotterdam, The Netherlands

² Radiology, Erasmus MC Rotterdam, The Netherlands

³ Interuniversity Cardiology Institute of the Netherlands

Abstract

Aims Stem cell therapy after myocardial infarction (MI) has been studied in models of permanent coronary occlusion. We studied the effect of intracoronary administration of unselected bone marrow (BM) and mononuclear cells (MNC) in a porcine model of reperfused MI.

Methods and Results In 34 swine, the left circumflex coronary artery was balloon-occluded for two hours followed by reperfusion. Ten swine without MI served as controls. All swine underwent magnetic resonance imaging (MRI) 1 week post-MI. The next day, 10 of the 30 surviving MI-swine received BM, 10 other MI-swine received MNC and the remaining MI-swine received medium intracoronary. Four weeks later all swine underwent a follow-up MRI.

One week after MI, end-diastolic volume (92 ± 16 mL) and left ventricular (LV) weight (78 ± 12 g) were greater, while ejection fraction (40 ± 8 %) was lower than in controls (69 ± 11 mL, 62 ± 13 g and 53 ± 6 %). Injection of BM or MNC had no effect on the MI-induced changes in global or regional LV-function. However, there was a significant reduction in infarct size four weeks after MNC injection (-6 ± 3 %), compared to medium (-3 ± 5 %).

Conclusions Intracoronary injection of BM or MNC in swine does not improve regional or global LV-function 4 weeks after injection. However, a reduction in infarct-size was noted after MNC injection.

Key words: Myocardial infarction; Bone marrow stem cells; Left ventricular function; Magnetic resonance imaging; Infarct size; Swine.

Introduction

Regeneration of infarcted myocardium by transplanting bone marrow (BM) derived stem cells into the infarct region has been proposed to prevent heart failure by angiogenesis and/or myogenesis.^{1,2} Early experimental studies in animals with a myocardial infarction (MI) reported improvements in left ventricular (LV) function following cell therapy with bone marrow derived mononuclear cells (MNC),³ or a cell sub-population selected from MNC.¹ These highly promising initial observations sparked a large number of non-randomized clinical trials, reporting beneficial effects of MNC therapy on global LV function and myocardial viability.⁴⁻⁸ However, out of four recent randomized trials (BOOST-update⁹, Leuven trial¹⁰, REPAIR-AMI¹¹, ASTAMI¹²), three failed to show an improvement in global LV function^{9,10,12}, although one reported a reduction in infarct size.¹⁰

In contrast to the discordant results obtained in clinical trials, to date the majority of experimental studies reported positive effects of MNC therapy on global LV function,^{3,13-15} although one study reported no effect.¹⁶ However, the beneficial effects of MNC on infarct size, which have been observed clinically,^{4,6,10} have not been investigated in these studies. Furthermore, all studies used a permanent coronary artery ligation, while all but one¹⁵ (which injected the MNC cells in a coronary venous vessel) injected the MNC directly in the peri-infarct area. Hence, these experimental studies have a markedly different design compared to the clinical trials. Furthermore, most animal studies used more selected, enriched populations, such as the CD34+, c-kit_{pos} or lin- bone marrow derived cells or bone marrow derived mesenchymal stem cells.

Consequently, we designed an experimental study that matches the clinical trial protocols more closely, using a porcine reperfused MI model and intracoronary cell injections. For this purpose, we first established cell survival and efficacy of the method of cell delivery in several pilot experiments. Subsequently, we studied the effect of bone marrow derived cell injection on LV geometry, function and infarct size. Myocardial infarction was induced by PTCA-balloon inflation followed by reperfusion. LV remodeling as well as global and regional LV function was assessed using cine-magnetic resonance imaging (cine-MRI). Contrast enhanced MR Imaging (Ce-MRI) was used to assess infarct size and infarct remodeling over time.

Although the clinical trials suggest that intracoronary BM derived cell delivery appears safe, recently Yoon et al.¹⁷ reported increased calcifications after unselected BM cell injection. Therefore we compared the effects of MNC to those of unselected BM.

Methods

Experiments were performed in 2-3 month old Yorkshire-Landrace pigs of either sex (n=49), in compliance with the "Guide for the Care and Use of Laboratory Animals" (NIH publication 1996) and after approval of the Animal Care Committee of the Erasmus MC.

Myocardial infarction

Animals were sedated (ketamine 20 mg/kg IM, and midazolam 1 mg/kg IM), anaesthetised (thiopental, 12 mg/kg IV), intubated and mechanically ventilated with a mixture of oxygen and nitrogen (1:2 vol/vol). Anaesthesia was maintained with fentanyl (12.5 µg/kg/h) and isoflurane (0.6-0.8% started after onset of occlusion). Subsequently, animals received antibiotic prophylaxis (200 mg procainebenzylpenicillin and 250 mg dihydrostreptomycinesulfate IM) and underwent coronary catheterization through a carotid artery guided by fluoroscopy, followed by balloon occlusion of the proximal left circumflex coronary artery (LCX), for 2 hr followed by reperfusion. Heparin was administered every hour (5000 Units).

Bone marrow aspiration and preparation

One week after MI, animals were anaesthetised as described above and anaesthesia was maintained with 1-1.5% isoflurane. Approximately 40 mL of BM was aspirated from the iliac crest, using the same bone marrow aspiration/biopsy needles (Kendall monoject, Tyco Healthcare, Gosport, UK) which are routinely used for clinical purposes in our hospital. MNC were isolated by Ficoll Paque-plus (Amersham Biosciences Europe GmbH, Freiburg, Germany) density gradient separation (25 min at 400g) and suspended in 10 mL Modified Eagle's Medium (MEM). Crude BM (40 mL) was prepared for injection by filtering through a 100 micron filter. MNC were counted using a cell counter (Sysmex CDA 500, Malvern Instruments Ltd, Malvern, UK). In view of the identical volume of BM that was aspirated, the amount of MNC administered in either group was considered to be similar. BM and MNC were injected within one hour after aspiration.

Efficacy of cell delivery

To investigate the efficacy of cell delivery we tested injection with a selective, non flow-limiting injection catheter (Multifunctional probing, Boston Scientific Co., Boston, MA, USA). One week after MI, bone marrow was aspirated and five swine received an intracoronary injection of $\sim 50 \cdot 10^6$ PKH-labelled MNC (PKH 26, Sigma-Aldrich, Schnellendorf, Germany) suspended in 10 mL saline; 5 mL was injected into the LCX (infarct area). The other 5 mL was injected into the left anterior descending coronary artery (LAD; non-infarct area) to investigate if cell injections cause micro infarctions¹⁸. MNC were injected slowly (1 mL/min) into the coronary artery perfusing the MI area using a probing catheter. The site of injection was identical to the position of the occlusion balloon during MI induction. Four days after cell injection animals were sacrificed for histological and immunocytochemical analyses.

Functional assessment

Thirty-four swine underwent MI as described above and 10 swine without MI served as controls for normal cardiac growth and function.

One week after induction of MI, all swine were anaesthetized as described above and underwent magnetic resonance imaging (MRI) to assess global and regional LV function. Then, 20 of the 30 surviving MI swine were randomized to undergo a BM aspiration after which 10 MI swine received an intracoronary injection of ~ 40 mL unselected autologous BM and 10 swine received an intracoronary suspension of MNC, a total of $\sim 5 \cdot 10^8$ cells in 10 mL MEM. The remaining 10 MI-swine received an

intracoronary injection of 10 mL of MEM. The site of injection was identical to the position of the occlusion balloon one week before, and cells were slowly injected into the coronary artery (1 mL/min). Investigators were not blinded to treatment.

Four weeks later, animals underwent follow-up MRI for assessment of LV function and infarct size, after which animals were sacrificed for histological analysis of the LCX perfused area and remote area of the left ventricle.

Magnetic Resonance Imaging

Data Acquisition

A clinical 1.5-Tesla MRI with a dedicated cardiac four element phased-array receiver coil was used for imaging (Signa CV/i, GE Medical systems, Milwaukee, WI, USA).¹⁹ Repeated breath-holds and gating to the ECG were applied to minimize the influence of cardiac and respiratory motion on data collection. To cover the entire left ventricle, six to eight consecutive slices of 8 mm were planned in the short axis view, perpendicular to the long axis four-chamber view of the left ventricle (gap=0). DE imaging was performed to assess total myocardial infarct mass 10-20 minutes after administration of gadolinium-DTPA (0.5 mmol/kg, Magnevist®, Schering).¹⁹ We have previously shown an excellent correlation between histological (TTC staining) and MRI (delayed enhancement) assessment of infarct size.¹⁹

Image Analysis

The MR images were analyzed with dedicated cardiac software (Cine display application 3.0, General Electric medical systems, USA).¹⁹ End-diastolic volume (EDV), end-systolic volume (ESV) and left ventricular weight (LVW) were measured and stroke volume (SV= EDV-ESV), ejection fraction (EF= [SV/EDV]x100%) and cardiac output (CO= SVxHR) were computed. End-diastolic wall thickness (EDT) and end systolic wall thickness (EST) was measured in 18 sections per slice, and regional systolic wall thickening (SWT) was calculated as [EST-EDT]/EDTx100%. Baseline and endpoint scans were matched for location using anatomical landmarks like insertion of the right ventricle to the septum and the papillary muscles.¹⁹

Histology and Immunohistochemistry

The hearts were excised and cut in 6-8 transverse slices similar to the MRI short axis slices. From the basal plane the first, third, fifth and seventh slice were fixed in 4% buffered formaldehyde and embedded in paraffin. The second, fourth, sixth and eighth slice, were embedded in tissue tec OCT and frozen in liquid nitrogen. Sections (5 µm) were stained with hematoxylin eosin (HE) and resorcin-fuchsin (RF, collagen). Immunohistochemistry was performed in the infarct sections to determine the expression of the pan-leukocyte marker CD45 (MCA1447, Setotec, Oxford, UK), macrophage surface marker (MAC378, Setotec, Oxford, UK), vimentin (Clone DE-R-11, DakoCytomation, California, USA) and desmin (Clone V9, DakoCytomation, California, USA). Desmin is expressed by myocytes and smooth muscle cells; vimentin is expressed by fibroblasts and endothelial cells.

Sections were semi-quantitatively assessed as negative (0) or the degree (from 1 to 5) of calcium deposition, collagen deposition and vascularization. The infarct sections were scored for surface area covered with collagen, calcifications or

vascularization. In each animal, 1 section was scored per LV slice (corresponding with each of the 5-6 MRI LV short-axis slices). For each section the total infarct area was scored (power field 10x).

Statistical Analysis

Data were analyzed with SPSS 11.0. All data were analyzed using a one-way ANOVA and post-hoc analysis using unpaired t-testing with Bonferoni correction to test for significant intergroup differences at corresponding time points. Effect of BM and MNC therapy at the follow-up MRI was tested using analysis of co-variance (ANCOVA) with baseline values as covariate. Statistical significance was accepted when $P < 0.05$ (two-tailed). All data are presented as mean \pm STDEV.

Results

Efficacy of cell delivery

In three additional *in vitro* experiments, trypan blue exclusion staining showed that 99.7% of the cells were viable after the aspiration procedure. Furthermore, following subsequent injection through the probing catheter 99.5% of the aspirated cells were viable. These results indicate negligible cell loss due to the bone marrow cell aspiration and handling.

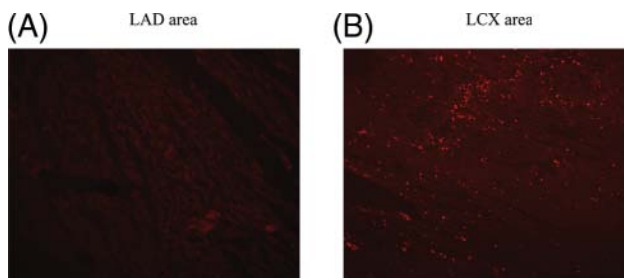


Figure 1 PKH-labeled cells do not home to healthy myocardium (A), but PKH positive cells (in red) home in infarcted myocardium after injection with a probing catheter (B).

PKH labeled cells could be detected in the infarcted LV lateral wall of 5 swine, 4 days after injection into the LCX, whereas only a few cells (< 1 cell/cm²) could be detected in the healthy non-infarcted LV anterior wall following injection into the LAD (Figure 1). Systematic histological analysis did not reveal any myocardial damage in the normal LAD-perfused myocardium. Quantitative analysis showed that an average of 248 ± 136 PKH positive cells/cm² could be detected in the infarct zone, 4 days after injection with a probing catheter, corresponding to $\sim 6.5\%$ of the injected cells.

Functional assessment of cell therapy

Infarct related mortality

A total of 44 swine entered the study. Out of 34 MI swine, three animals encountered ventricular fibrillation during the 2 h occlusion, for which they were treated successfully by DC shock. Four animals died prematurely, of which three died within

24 hours after induction of MI, while one animal died shortly after the baseline MRI (i.e. prior to any therapeutic intervention). Consequently, forty surviving animals completed the protocol.

Magnetic resonance imaging

MI swine had a transmural myocardial infarction of the lateral left ventricular wall encompassing $14.7 \pm 5\%$ of the left ventricle. There were no differences in body weight (BW), stroke volume (SV) or cardiac output (CO) between controls and MI-animals at baseline (Table 1). Due to normal growth, BW, SV and CO increased in all four groups over the four week follow-up period. Consequently, there were no significant differences in BW or systemic hemodynamics during the endpoint scan (Table 1).

One week after MI, LVW, EDV and ESV were greater, while EF was lower, in MI compared to control swine (Figure 2). Changes in LV volumes and mass from baseline to four weeks after cell injection did not differ significantly between medium, BM and MNC treated MI-animals (Figure 2).

Table 1: Systemic hemodynamics and infarct size measured by delayed enhancement

		Baseline	Endpoint	<i>p</i> -values
BW (Kg)	Control	23±5	40±7	
	MI+medium	26±3	43±6	
	MI+BM	26±1	43±4	0.669
	MI+MNC	24±1	39±3	0.185
HR (bpm)	Control	107±15	83±14	
	MI+medium	87±16	84±19	
	MI+BM	103±23	83±15	0.702
	MI+MNC	85±21	86±17	0.733
SV (mL)	Control	37±6	51±8	
	MI+medium	38±10	60±11	
	MI+BM	36±7	56±9	0.466
	MI+MNC	27±9	50±11	0.041
CO (mL/min)	Control	3.9±0.9	4.2±1.0	
	MI+medium	3.3±1.0	5.0±1.2	
	MI+BM	3.8±1.2	4.6±1.0	0.324
	MI+MNC	3.2±1.2	4.2±1.0	0.099
Infarct size (g)	Control	NA	NA	
	MI+medium	11.1±5.0	12.3±3.9	
	MI+BM	12.0±3.3	11.6±5.6	0.340
	MI+MNC	10.8±5.5	8.7±4.2	0.045
Infarct size (%LV)	Control	NA	NA	
	MI+medium	14.3±5.6	11.0±4.2	
	MI+BM	14.3±3.6	10.0±4.2	0.236
	MI+MNC	14.3±6.5	8.2±4.2	0.024

BW= body weight; HR= heart rate; SV= stroke volume; CO= cardiac output; Baseline = 1 wk post-MI; Endpoint = 5 wk post-MI, %LV = is as a percentage of the left ventricle, *P*-values= change from baseline in BM or MNC vs. medium-treated MI animals, NA= not applicable. Data are mean ± STDEV. 10 animals per group, except for infarct size (medium n=8, BM n=8 and MNC n=10)

One week after MI, there were no significant differences in diastolic wall thickness between the different groups (Figure 3). Systolic wall thickening in the LCX area was abolished in the MI animals compared to control, which was not affected by BM or MNC treatment. Infarct size measured with delayed enhancement revealed that MNC treatment resulted in a significant decrease in infarct mass from 10.8 ± 5.5 g to 8.7 ± 4.2 g, compared to medium treatment (11.1 ± 5.0 g and 12.3 ± 3.9 ; $P=0.045$ change baseline MNC vs. medium), while BM treatment had no significant effect (Table 1). Similarly, there was a greater decrease in infarct size expressed as a percent of the LV in the MNC, but not in the BM treated animals, compared to the medium treated swine (Table 1, Figure 4).

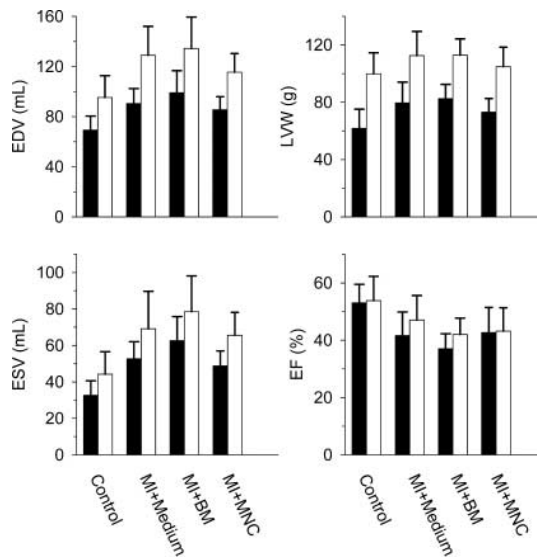


Figure 2 LV end-diastolic volume (EDV), LV weight (LVW), LV ejection fraction (EF) and end-systolic volume (ESV) at baseline (solid bars) and at endpoint (open bars) in Control swine, and MI swine receiving either medium, BM or MNC. There were no significant differences (all variables $P>0.20$) between BM, MNC and medium-treated MI animals in the response over the 4 wk follow-up period.

Histology

Histology confirmed that all MI animals had a transmural infarct in the LCX region with total loss of viable myocardium, which matched the delayed enhancement scans performed at 1 and 5 weeks after MI. All treatments resulted in extensive collagen deposition in the center of the infarct (Figure 5). Semi-quantitative analysis showed that there were no significant differences in the degree of calcium or collagen deposition, or of vascularization (Table 2). Immunohistochemistry showed that most of the cells in the infarct area were desmin negative, vimentin positive, CD45 positive and occasionally positive for macrophage surface marker (Figure 6), suggesting that the majority of cells were fibroblasts (vimentin), inflammatory cells (CD45 and macrophage surface marker) and endothelial cells (vimentin).

Discussion

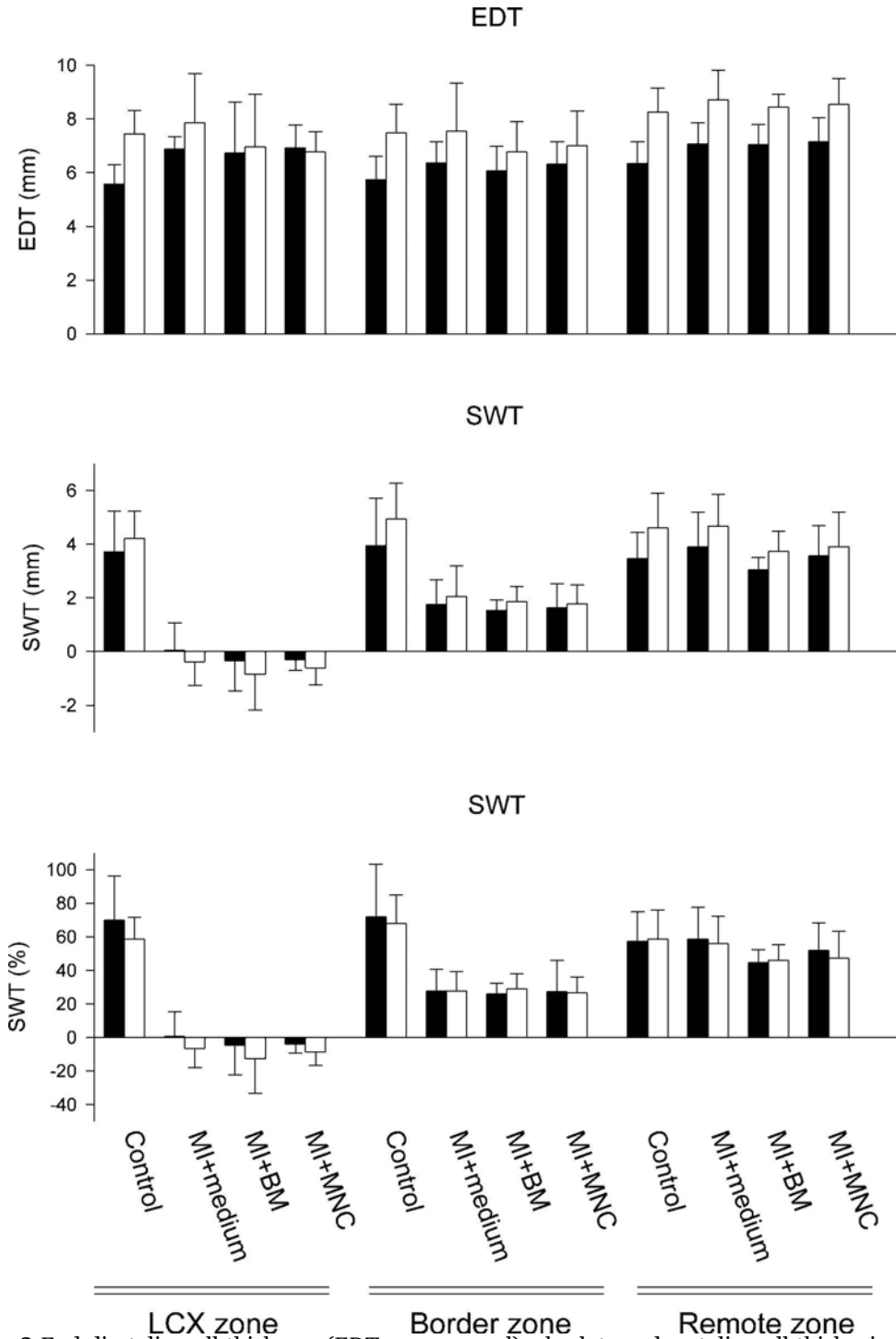


Figure 3 End diastolic wall thickness (EDT, upper panel), absolute end systolic wall thickening (SWT, middle panel) and percent Systolic wall thickening (SWT, lower panel) at baseline (solid bars) and at endpoint (open bars) in Control swine, and MI swine receiving either medium, BM or MNC. There were no significant (all variables $P > 0.10$) differences between BM, MNC and medium treated MI animals.

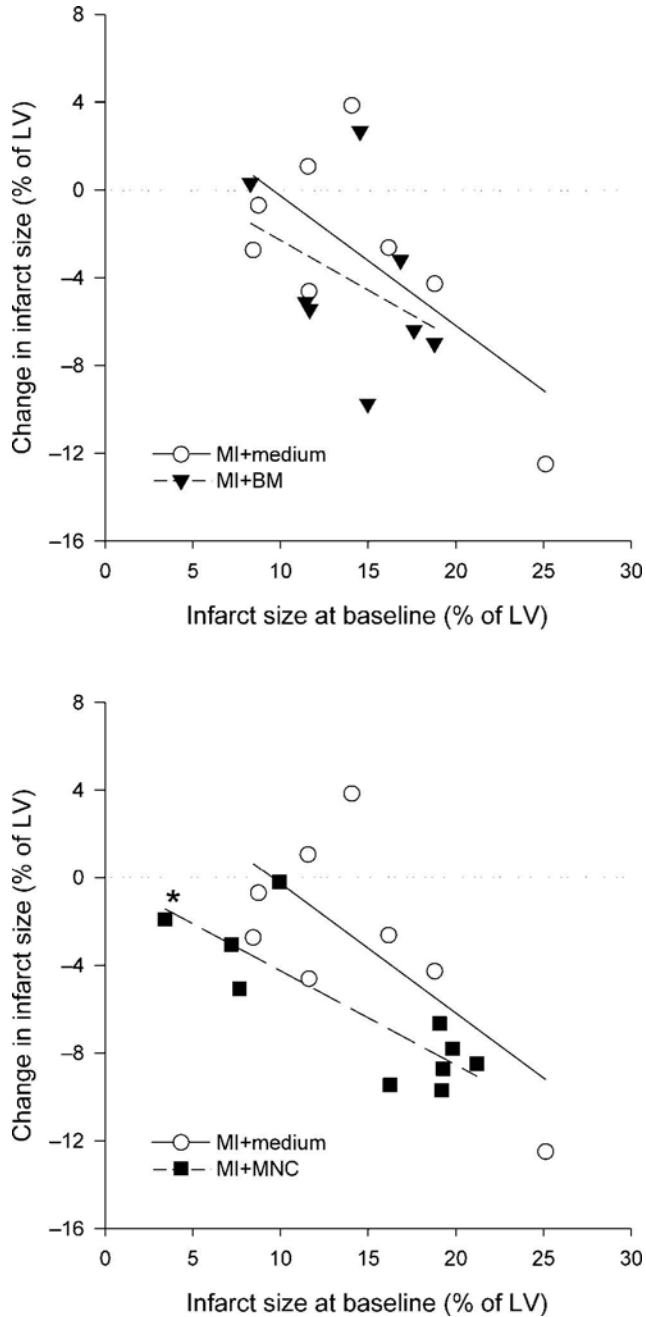


Figure 4 Change in infarct size from baseline in percentage of the LV. Regression lines; * $P < 0.05$ vs. medium treated MI swine.

The present study investigated the effect of intracoronary injection of MNC or BM on left ventricular function and histology at four weeks in a porcine model of acute myocardial infarction followed by reperfusion. Our study shows that in swine an intracoronary injection of both MNC and unselected BM one week after MI does not

improve global or regional indices of LV function four weeks later. In addition, BM derived MNC or unselected BM treatment did not reverse the remodeling of the left ventricle induced by the MI. However, MNC reduced infarct size four weeks after injection, a finding also reported in the clinical study by Janssens et al.¹⁰

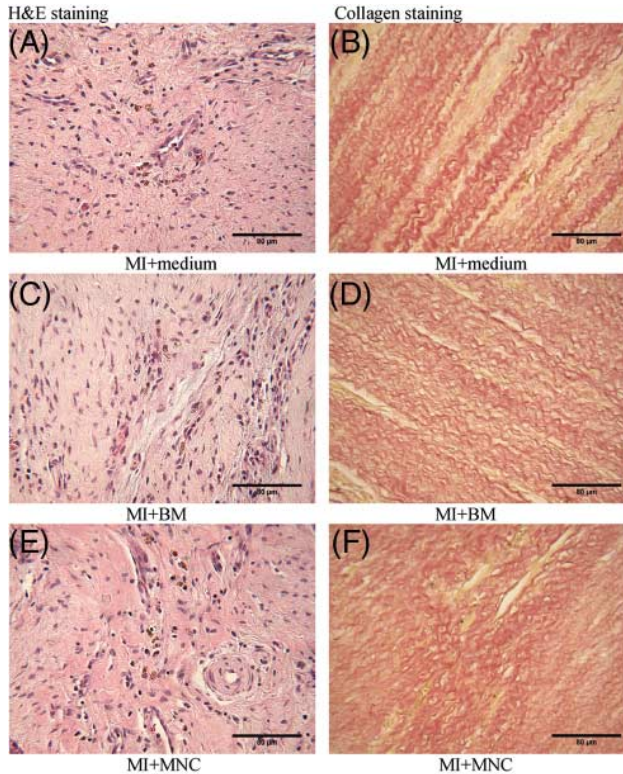


Figure 5 Infarct area of medium treated (A,B) compared with crude BM (C,D) and MNC (E,F) treated swine. HE staining (A,C,E) showed many fibroblasts. RF staining showed a lot of collagen (B,D,F).

Table 2: Semi-quantative histology score

	MI+medium (n=8)	MI+BM (n=8)	MI+MNC (n=10)
Calcium deposits	0.60±1.31	1.37±1.69	1.04±1.64
Collagen	3.95±1.10	4.11±0.89	4.36±0.99
Vascularization	4.05±1.36	3.78±1.22	3.54±1.32

Data are mean ± STDEV. There are no significant differences between groups.

Infarct size reduction

From the present study we cannot determine the underlying mechanism for the infarct size reduction by MNC treatment. Although, it has been shown that BM derived cells can differentiate into cardiomyocytes *in vitro*, it remains unclear whether BM derived stem cells are capable of differentiating into cardiomyocytes *in vivo*,²⁰⁻²² especially in large mammals. Conversely, it has been shown that stem cells engraft in the myocardium and induce angiogenesis,²³ which could result in improved perfusion,

particularly in the border zone. It could be speculated that this might aid in preventing further ischemic damage, thereby rescuing viable tissue in the border zone; alternatively, the MNC-induced angiogenesis may enhance infarct healing.²⁴

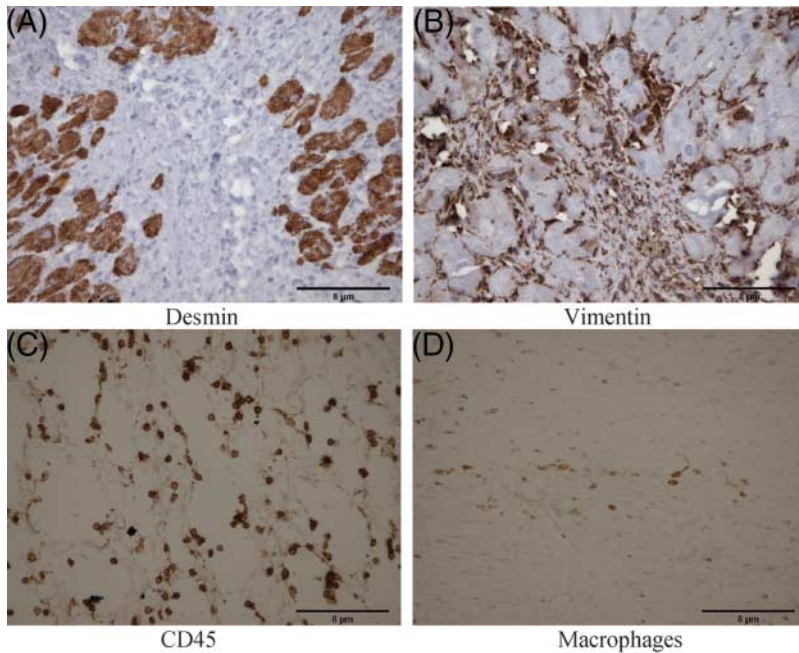


Figure 6 Immunohistochemistry showed that cells (brown) in the infarct are desmin negative (A; infarct border zone), but vimentin positive (B, infarct border zone in a consecutive section), CD45 positive (C; central infarct zone), and that macrophages are present (D; central infarct zone).

Table 3: Overview of preclinical studies on the effects of MNC on global left ventricular function after MI

Species	MI-model	Method of Injection	Time of injection post MI	Follow-up	# of cells	Effect MNC vs. control	
Zhang ¹³	Rat	LAD ligation	i.m.	After MI	2 m	5x10 ⁶	FS +18% vs. -1%
Ott ¹⁴	Rat	LAD ligation	i.m.	1 week	8 weeks	1x10 ⁷	EF +1% vs. -15%
Bel ¹⁶	Sheep	LCX ligation	i.m.	3 weeks	2 ms	422x10 ⁶	EF -9% vs. -8%
Kamihata ³	Swine	LAD ligation	i.m.	60 minutes	3 weeks	1x10 ⁸	EF +15% vs. +1%
Yokoyama ¹⁵	Swine	LAD coil	I.c. vein	6 hours/2 weeks	4 weeks	3x10 ⁹	EF +5% vs. -5%
Moelker	Swine	LCX occlusion reperfusion	I.a. LCX	1 week	4 weeks	5x10 ⁸	EF +1% vs. +5%

MI= myocardial infarction; LAD= left anterior descending coronary artery; LCX= left circumflex coronary artery; m= months, FS= fractional shortening; EF= ejection fraction.

Although there was a reduction in infarct size after MNC treatment, this was not associated with an improvement in global or regional LV function. This is in apparent contrast to the majority of preclinical studies that reported significant increases in EF or fractional shortening (Table 3). However, it should be emphasized that the experimental protocols in these studies differed considerably from the present study. For example, all these studies performed intramyocardial or intravenous cell injection in an infarct model of permanent coronary artery occlusion. In contrast, we

employed a model that more closely mimics the clinical setting, by using intracoronary cell injection in a reperfused MI model, making direct comparison to previous preclinical studies difficult.

Several explanations can be forwarded why cardiac function failed to improve after intracoronary injection of MNC or BM in the MI zone.

Timing of cell administration

Inspection of Table 3 suggests that in permanent ligation MI models, the timing of MNC administration does not appear to be critically important. Thus, MNC injections either immediately or up to 2 weeks after MI were reported to improve global LV function. In contrast, the optimal timing of stem cell delivery in reperfused MI remains incompletely understood. However, the REPAIR-AMI trial showed that the optimal timing of cell injection appears to be at least five days after MI.²⁵ Also Bartunek et al.²⁶ suggest that 3 to 10 days post-MI is the optimal timing of cell therapy. We chose to inject cells one week after MI, with the underlying idea that the acute inflammatory response is most pronounced shortly after MI, while the inflammatory response is diminished one week later, thus creating a better environment for injected cells. Therefore, the lack of functional benefit of bone marrow derived cells in this study can not be explained by the timing of cell administration. It is likely that a proximal two hour during LCX occlusion, followed by reperfusion creates a transmural infarct which represents a too hostile environment for injected cells to contribute to LV function recovery.

Route of administration

In contrast to previous experimental studies, which either used intramyocardial or retrograde coronary venous injection (Table 3), clinical trials have invariably used intracoronary arterial injections of MNC. Intracoronary injected cells are thought to disappear from the coronary circulation into liver, lung or kidney within a few hours.²⁷ Therefore, in clinical trials the intracoronary cell delivery typically involves repeated proximal balloon occlusion during cell delivery in order to prevent wash-out of cells and facilitate attachment of the injected cells onto the vascular wall.²⁸ We observed that only ~6.5 % of the injected MNC were present in the infarcted area 4 days after injection, which could be interpreted to suggest that the injection via the probing catheter could have resulted in suboptimal cell delivery. Therefore, in 5 additional MI pigs, MNC were injected intracoronary via an over the wire balloon catheter during repetitive balloon occlusions and pigs were sacrificed 4 days later. These experiments yielded a similar number of PKH positive cells (252 ± 144 cells/cm²) in the infarct area as with the probing catheter. These findings indicate that injection during balloon occlusion does not result in better cell engraftment, and that the low number of MNC present in the infarct area 4 days after injection is not the result of the probing catheter.

The cell delivery study showed that injection of MNC in healthy myocardium did not induce myocardial damage. In contrast, intracoronary injection of BM derived mesenchymal stromal stem cells have been shown to cause microinfarctions¹⁸ in dogs. No PKH positive cells could be detected in the LAD area (in contrast to the MI area). It is important to note that the MNC are smaller in size (5-7 μm as measured with the

Sysmex Cell Counter) than cultured mesenchymal stem cells (~20 μm^{18}), and therefore MNC are less likely to occlude micro vessels after intracoronary injection.

Follow-up time

It could be argued that the lack of effect of MNC on global LV function, despite the reduction in infarct size, was due to the relatively short follow-up period of 4 weeks. However, inspection of Table 3 shows that previous studies in swine did report improvement in cardiac function three^{3,13-15} or four^{3,13-15} weeks after MNC injections, albeit that these were performed in a model of permanent coronary artery occlusion. Furthermore, recent clinical trials such as the ASTAMI-trial,¹² the BOOST-update⁹ and the trial performed in Leuven¹⁰ do not suggest that a longer follow-up will lead to an improvement in LV function. Thus, the BOOST-update showed that 18 months after MNC administration the intergroup comparison between MNC treated group and placebo was no longer significant. The ASTAMI-trial as well as the Leuven trial also did not see a beneficial effect on EF or EDV after MNC injection after 6 and 4 months. The preclinical study by Dai et al.²⁹ showed a similar trend as the BOOST-update, in that the initial positive effect observed at four weeks was lost after six months. Taken together, the weight of available evidence from experimental and clinical studies suggests that a longer follow-up period may not yield a significant improvement in LV function.

Infarct composition

There were no significant differences between the MI group receiving medium, and either BM or MNC with respect to the histology. In all MI swine a transmural infarct was observed with transmural loss of viable myocytes. There were no signs of cardiomyocyte regeneration since immunohistochemistry showed that all cells in the infarct were inflammatory cells, fibroblasts or capillaries. A transmural infarct seems a hostile environment for the undifferentiated stem cells in the mononuclear fraction. It is not unlikely that MNC will differentiate into fibroblasts in such an environment, and therewith contribute to infarct reduction by infarct remodeling i.e. scar contracture, but do not contribute to contractility.

Yoon *et al*⁷ reported that injection of unselected BM aggravated calcifications within the infarct zone. Similarly, we observed a trend towards increased calcifications following BM administration, but this failed to reach statistical significance ($P = 0.084$). Together with the lack of effect of BM on infarct size in the present study, these observations support the concept that MNC should be favored over unselected BM.

Conclusions

In a porcine model of myocardial infarction followed by reperfusion, we could not demonstrate improvements in global or regional LV-function by injection of BM-derived MNC. However, we did observe a reduction in infarct size four weeks after MNC-injection, which is in accordance with recent clinical observations.¹⁰

Acknowledgements

The authors gratefully acknowledge Marcel de Jong from the Cardiology department of the Erasmus MC for isolation of the MNC. Financial support by ESA ESTEC (AO-99-LSS-006) is gratefully acknowledged.

References

1. Orlic D, Kajstura J, Chimenti S, Jakoniuk I, Anderson SM, Li B, Pickel J, McKay R, Nadal-Ginard B, Bodine DM, Leri A, Anversa P. Bone marrow cells regenerate infarcted myocardium. *Nature*. 2001;410:701-5.
2. Murry CE, Reinecke H, Pabon LM. Regeneration gaps: observations on stem cells and cardiac repair. *J Am Coll Cardiol*. 2006;47:1777-85.
3. Kamihata H, Matsubara H, Nishiue T, Fujiyama S, Tsutsumi Y, Ozono R, Masaki H, Mori Y, Iba O, Tateishi E, Kosaki A, Shintani S, Murohara T, Imaizumi T, Iwasaka T. Implantation of bone marrow mononuclear cells into ischemic myocardium enhances collateral perfusion and regional function via side supply of angioblasts, angiogenic ligands, and cytokines. *Circulation*. 2001;104:1046-52.
4. Strauer BE, Brehm M, Zeus T, Kostering M, Hernandez A, Sorg RV, Kogler G, Wernet P. Repair of infarcted myocardium by autologous intracoronary mononuclear bone marrow cell transplantation in humans. *Circulation*. 2002;106:1913-8.
5. Assmus B, Schachinger V, Teupe C, Britten M, Lehmann R, Dobert N, Grunwald F, Aicher A, Urbich C, Martin H, Hoelzer D, Dimmeler S, Zeiher AM. Transplantation of Progenitor Cells and Regeneration Enhancement in Acute Myocardial Infarction (TOPCARE-AMI). *Circulation*. 2002;106:3009-17.
6. Schachinger V, Assmus B, Britten MB, Honold J, Lehmann R, Teupe C, Abolmaali ND, Vogl TJ, Hofmann WK, Martin H, Dimmeler S, Zeiher AM. Transplantation of progenitor cells and regeneration enhancement in acute myocardial infarction: final one-year results of the TOPCARE-AMI Trial. *J Am Coll Cardiol*. 2004;44:1690-9.
7. Dobert N, Britten M, Assmus B, Berner U, Menzel C, Lehmann R, Hamscho N, Schachinger V, Dimmeler S, Zeiher AM, Grunwald F. Transplantation of progenitor cells after reperfused acute myocardial infarction: evaluation of perfusion and myocardial viability with FDG-PET and thallium SPECT. *Eur J Nucl Med Mol Imaging*. 2004;31:1146-51.
8. Mocini D, Staibano M, Mele L, Giannantoni P, MenicHELLa G, Colivicchi F, Sordini P, Salera P, Tubaro M, Santini M. Autologous bone marrow mononuclear cell transplantation in patients undergoing coronary artery bypass grafting. *Am Heart J*. 2006;151:192-7.
9. Meyer GP, Wollert KC, Lotz J, Steffens J, Lippolt P, Fichtner S, Hecker H, Schaefer A, Arseniev L, Hertenstein B, Ganser A, Drexler H. Intracoronary bone marrow cell transfer after myocardial infarction: eighteen months' follow-up data from the randomized, controlled BOOST (BOne marrOw transfer to enhance ST-elevation infarct regeneration) trial. *Circulation*. 2006;113:1287-94.
10. Janssens S, Dubois C, Bogaert J, Theunissen K, Deroose C, Desmet W, Kalantzi M, Herbots L, Sinnaeve P, Dens J, Maertens J, Rademakers F, Dymarkowski S, Gheysens O, Van Cleemput J, Bormans G, Nuyts J, Belmans A, Mortelmans L, Boogaerts M, Van de Werf F. Autologous bone marrow-derived stem-cell transfer in patients with ST-segment elevation myocardial infarction: double-blind, randomised controlled trial. *Lancet*. 2006;367:113-21.
11. Schachinger V, Erbs S, Elsasser A, Haberbosch W, Hambrecht R, Holschermann H, Yu J, Corti R, Mathey DG, Hamm CW, Suselbeck T, Assmus B, Tonn T, Dimmeler S, Zeiher AM. Intracoronary bone marrow-derived progenitor cells in acute myocardial infarction. *N Engl J Med*. 2006;355:1210-21.
12. Lunde K, Solheim S, Aakhus S, Arnesen H, Abdelnoor M, Egeland T, Endresen K, Ilebakk A, Mangschau A, Fjeld JG, Smith HJ, Taraldsrud E, Groggaard HK, Bjornerheim R, Brekke M, Muller C, Hopp E, Ragnarsson A, Brinchmann JE, Forfang K. Intracoronary injection of mononuclear bone marrow cells in acute myocardial infarction. *N Engl J Med*. 2006;355:1199-209.
13. Zhang S, Guo J, Zhang P, Liu Y, Jia Z, Ma K, Li W, Li L, Zhou C. Long-term effects of bone marrow mononuclear cell transplantation on left ventricular function and remodeling in rats. *Life Sci*. 2004;74:2853-64.

14. Ott HC, Bonaros N, Marksteiner R, Wolf D, Margreiter E, Schachner T, Laufer G, Hering S. Combined transplantation of skeletal myoblasts and bone marrow stem cells for myocardial repair in rats. *Eur J Cardiothorac Surg*. 2004;25:627-34.
15. Yokoyama S, Fukuda N, Li Y, Hagikura K, Takayama T, Kunimoto S, Honye J, Saito S, Wada M, Satomi A, Kato M, Mugishima H, Kusumi Y, Mitsumata M, Murohara T. A strategy of retrograde injection of bone marrow mononuclear cells into the myocardium for the treatment of ischemic heart disease. *J Mol Cell Cardiol*. 2006;40:24-34.
16. Bel A, Messas E, Agbulut O, Richard P, Samuel JL, Bruneval P, Hagege AA, Menasche P. Transplantation of autologous fresh bone marrow into infarcted myocardium: a word of caution. *Circulation*. 2003;108 Suppl 1:II247-52.
17. Yoon YS, Park JS, Tkebuchava T, Luedeman C, Losordo DW. Unexpected severe calcification after transplantation of bone marrow cells in acute myocardial infarction. *Circulation*. 2004;109:3154-7.
18. Vulliet PR, Greeley M, Halloran SM, MacDonald KA, Kittleson MD. Intra-coronary arterial injection of mesenchymal stromal cells and microinfarction in dogs. *Lancet*. 2004;363:783-4.
19. Baks T, Cademartiri F, Moelker AD, Weustink AC, van Geuns RJ, Mollet NR, Krestin GP, Duncker DJ, de Feyter PJ. Multislice computed tomography and magnetic resonance imaging for the assessment of reperfused acute myocardial infarction. *J Am Coll Cardiol*. 2006;48:144-52.
20. Balsam LB, Wagers AJ, Christensen JL, Kofidis T, Weissman IL, Robbins RC. Haematopoietic stem cells adopt mature haematopoietic fates in ischaemic myocardium. *Nature*. 2004;428:668-73.
21. Kajstura J, Rota M, Whang B, Cascapera S, Hosoda T, Bearzi C, Nurzynska D, Kasahara H, Zias E, Bonafe M, Nadal-Ginard B, Torella D, Nascimbene A, Quaini F, Urbanek K, Leri A, Anversa P. Bone marrow cells differentiate in cardiac cell lineages after infarction independently of cell fusion. *Circ Res*. 2005;96:127-37.
22. Murry CE, Soonpaa MH, Reinecke H, Nakajima H, Nakajima HO, Rubart M, Pasumarthi KB, Virag JJ, Bartelmez SH, Poppa V, Bradford G, Dowell JD, Williams DA, Field LJ. Haematopoietic stem cells do not transdifferentiate into cardiac myocytes in myocardial infarcts. *Nature*. 2004;428:664-8.
23. Fuchs S, Baffour R, Zhou YF, Shou M, Pierre A, Tio FO, Weissman NJ, Leon MB, Epstein SE, Kornowski R. Transendocardial delivery of autologous bone marrow enhances collateral perfusion and regional function in pigs with chronic experimental myocardial ischemia. *J Am Coll Cardiol*. 2001;37:1726-32.
24. Dimmeler S, Zeiher AM, Schneider MD. Unchain my heart: the scientific foundations of cardiac repair. *J Clin Invest*. 2005;115:572-83.
25. Cleland JG, Freemantle N, Coletta AP, Clark AL. Clinical trials update from the American Heart Association: REPAIR-AMI, ASTAMI, JELIS, MEGA, REVIVE-II, SURVIVE, and PROACTIVE. *Eur J Heart Fail*. 2006;8:105-10.
26. Bartunek J, Wijns W, Heyndrickx GR, Vanderheyden M. Timing of intracoronary bone-marrow-derived stem cell transplantation after ST-elevation myocardial infarction. *Nat Clin Pract Cardiovasc Med*. 2006;3 Suppl 1:S52-6.
27. Chin BB, Nakamoto Y, Bulte JW, Pittenger MF, Wahl R, Kraitchman DL. ¹¹¹In oxine labelled mesenchymal stem cell SPECT after intravenous administration in myocardial infarction. *Nucl Med Commun*. 2003;24:1149-54.
28. Sherman W, Martens TP, Viles-Gonzalez JF, Siminiak T. Catheter-based delivery of cells to the heart. *Nat Clin Pract Cardiovasc Med*. 2006;3 Suppl 1:S57-64.
29. Dai W, Hale SL, Martin BJ, Kuang JQ, Dow JS, Wold LE, Kloner RA. Allogeneic mesenchymal stem cell transplantation in postinfarcted rat myocardium: short- and long-term effects. *Circulation*. 2005;112:214-23.

Chapter 7

Grafting of bone marrow derived mononuclear cells is not enhanced by flow interrupted intracoronary injection in a porcine model of myocardial infarction

A.D. Moelker¹, M. de Jong¹, H.J.F.M.M. Eussen², D.J. Duncker¹, W.J. van der Giessen^{1,3}

¹ Experimental Cardiology, Thoraxcenter, Erasmus MC, Rotterdam, The Netherlands

² Clinical genetics, Erasmus MC, Rotterdam, The Netherlands

³ Interuniversity Cardiology Institute of the Netherlands

Abstract

Background: Repair of infarcted myocardium by injection of bone marrow derived cells has been proposed to prevent heart failure. In most clinical trials, cells were injected during repeated balloon occlusion. To evaluate whether injection during repeated balloon occlusion is the optimal mode of administration, we injected bone marrow derived mononuclear cells (MNC) intracoronary with and without balloon occlusion in a porcine model of a reperfused MI.

Methods: In 14 domestic swine, the proximal left circumflex coronary artery was balloon-occluded for two hours followed by reperfusion. One week after induction of MI, a total of ~100 million MNC labeled with a permanent fluorescent membrane stain (PKH 26) were injected. Seven swine were injected using a selective injection catheter during normal coronary flow, the other seven swine were injected during repetitive balloon occlusion. In all animals, cells were administered in infarcted tissue as well as normal non-ischemic myocardium. Ninety minutes (n=4) and four days (n=10) later swine were sacrificed for histological analysis.

Results: Ninety minutes and four days after injection, no PKH labeled cells were detected in non-ischemic myocardium. However, in infarcted tissue ~6.5% of the injected PKH-labeled cells were demonstrated four days after injection. Similar numbers of PKH-positive cells were found in the infarct area irrespective of whether normal flow or balloon interrupted flow injections were used (249 ± 43 cells/cm² vs. 252 ± 42 cells/cm² $P=NS$).

Conclusion: Bone marrow derived MNC do not home to normal non-ischemic myocardium. Selective injection during uninterrupted flow appears to be as effective as injection during repeated balloon occlusion to deliver MNC to the infarcted myocardium.

Introduction

Improvement of function of infarcted myocardium by injection of bone marrow derived cells into the infarct region to prevent heart failure has been demonstrated in most pre-clinical and clinical studies. Preclinical studies were predominantly performed in models of myocardial infarction (MI) produced by permanent coronary artery occlusion. Furthermore, cells were injected directly into the myocardium¹ or intravenously², mainly because these studies were performed in small rodents, in which intracoronary injection was not feasible. Based on these encouraging initial pre-clinical reports, clinical trials were initiated, which employed intracoronary (i.c.) administration of bone marrow derived cells.³⁻⁵ All these trials invariably used the method of intermittent balloon occlusion during injection of cells through the wire lumen, based on the assumption that this would yield increased adhesion of the injected cells to the vascular wall during the non-flow period, thereby leading to a higher cell engraftment.⁶ While this method of cell delivery via intermittent balloon occlusion appears to be safe and feasible,⁷ its superiority in terms of enhancing cell delivery compared to cell injection during normal coronary arterial flow was never evaluated.

In light of these considerations, we tested the hypothesis that injection during balloon occlusion results in superior grafting of cells as compared to injection during normal arterial flow. For this purpose we performed intracoronary injections of bone marrow derived mononuclear cells (MNC) during intermittent balloon occlusions and during normal coronary blood flow using a selective injection catheter in a porcine model of reperfused MI closely mimicking the clinical settings.

Material and Methods

Experiments were performed in 2-3 month old, 20 Kg Yorkshire-landrace pigs in compliance with the "Guide for the Care and Use of Laboratory Animals" (NIH publication 1996) and after approval of the Animal Care Committee of the Erasmus MC.

MNC isolation and labelling

Approximately 40 mL of BM was aspirated from the iliac crest of the pigs and collected in two tubes containing 15 mL buffered phosphate saline (PBS) with 1250 Units heparin. The BM was washed to remove the PBS and heparin after which MNC were isolated using a Ficoll Paque-plus (Amersham Biosciences Europe GmbH, Freiburg, Germany) gradient separation (20 minutes at 800 G). The isolated MNC were incubated for 5 minutes at 37°C with the permanent fluorescent membrane stain PKH26 (Sigma-Aldrich, Schnelldorf, Germany). After washing and centrifuging steps, MNC were resuspended in 10 ml PBS. The resultant cell suspension showed >99% PKH26 labelling as assessed by fluorescence microscopy.

Viability of cells

In six *in vitro* experiments, trypan blue exclusion (Sigma-Aldrich, Zwijndrecht, The Netherlands) staining was used to check cell viability. This is based on the principle

that live cells possess intact cell membranes that exclude certain dyes, such as trypan blue, whereas dead cells cannot. Cells were incubated with 0.4% trypan blue for 3 minutes at room temperature. Within 5 minutes after incubation cells were counted using a Burker-Turk cell counter chamber under the microscope. Viability was tested immediately after isolation of the MNC as well as after injection with the different injection catheters.

Animal study

The animal model that we used has been described in detail.⁸ For this study fourteen animals were sedated (ketamine 20 mg/kg IM, and midazolam 1 mg/kg IM), anesthetised (thiopental, 12 mg/kg IV), intubated and mechanically ventilated with a mixture of oxygen and nitrogen (1:2 vol/vol). Anesthesia was initially maintained with fentanyl (12.5 µg/kg/h) and continued with isoflurane (0.6-0.8%). Subsequently, animals received antibiotic prophylaxis (200 mg procainebenzylpenicillin and 250 mg dihydrostreptomycinesulfate IM) and underwent coronary catheterization through a carotid artery guided by fluoroscopy, followed by balloon occlusion of the proximal left circumflex coronary artery (LCX), for 2 hr followed by reperfusion. Heparin was administered every hour (5000 Units).

One week after MI, swine were sedated and heparinized as described above. Anesthesia was maintained with 1% isoflurane and seven swine received an intracoronary injection of $\sim 50 \cdot 10^6$ PKH-labelled MNC suspended in 10 mL saline into the LCX (infarct area) and $\sim 50 \cdot 10^6$ into the non-ischemic left anterior descending (LAD) coronary artery. MNC were injected slowly (1 mL/min) into the coronary artery during normal coronary flow using a selective, injection catheter (Multifunctional Probing, Boston Scientific Co, Boston, MA). The site of the LCX injection was identical to the position of the occlusion balloon during MI induction. The seven other MI animals were injected during a flow-limiting balloon occlusion, using an over the wire PTCA-balloon (OTW Maverick, Boston Scientific Co, Boston, MA). Cells were injected into the LAD and LCX in 3-4 short occlusion periods of 3 minutes, followed by 3 minutes of reperfusion. Angiographic flow was normal before cell injection in all experiments.

Two swine from each group were sacrificed 90 minutes after cell injection and five animals per group were sacrificed four days after cell injection with an overdose of pentobarbital for histological and immunocytochemical analyses.

Histology and Immunohistochemistry

Hearts were excised and cut in 6-8 transverse slices of similar thickness. Each slice was divided in infarct zone, border anterior, border posterior and remote LV. Each sample was embedded in tissue tec OCT and frozen in liquid nitrogen. PKH positive cells were counted on sections (5 µm) using fluorescence microscopy. All PKH positive cells per section were counted. For each animal three sections were counted per slice.

Immunohistochemistry was performed for the identification of endothelial cells (mouse anti rat CD31, PECAM-1, BD Biosciences Pharmingen, Alphen aan den Rijn, The Netherlands), leukocytes (mouse anti porcine CD45, Chemicon, Hampshire, UK), fibroblasts (mouse anti human CD90, Thy-1, BD Biosciences Pharmingen, Alphen aan den Rijn, The Netherlands) and macrophages (mouse anti human LN-5,

Sigma, Missouri, U.S.A.). In short, sections were fixed with acetone at 4°C for 10 minutes. Then, sections were rinsed for 5 minutes with phosphate buffered saline (PBS, 0.01M) and blocked with normal goat serum (Serotec, Düsseldorf, Germany, 1:10 PBS) to prevent non-specific binding of the second antibody for 10 minutes. Sections were rinsed again and incubated with the first antibody for 1 hour at 37°C. After three thorough rinsing steps, sections were incubated with the second antibody (Pacific Blue goat anti mouse IgG, Molecular Probes, Eugene, USA) for 1 hour at 37°C. After three thorough rinsing steps, sections were mounted with Vectashield hardset (Brunschwig, Amsterdam, The Netherlands).

Statistical Analysis

Data were analyzed with SPSS 11.0. Data were analyzed using two-way ANOVA. Statistical significance was accepted when $P \leq 0.05$ (two-tailed). All data are presented as mean \pm SEM.

Results

Three trypan blue exclusion staining experiments showed that 99.8% of the MNC were viable after the aspiration procedure. After injection through the probing catheter 99.6% of the cells were viable. The other three *in vitro* experiments demonstrated that 99.2% of the MNC were viable after the aspiration procedure and 99.0% of the MNC were viable after injection during balloon occlusion. PKH labeling did not affect the viability of the cells, since all cells were viable after labeling.

Table 1: average PKH positive MNC

	Probing catheter	Balloon catheter
absolute cell numbers (cells/cm ²)		
1.5 hours (n=2)	314 \pm 74	325 \pm 66
4 days (n=5)	249 \pm 43	252 \pm 42
relative cell numbers (%)		
1.5 hours (n=2)	8.2 \pm 1.9	8.5 \pm 1.7
4 days (n=5)	6.5 \pm 1.1	6.5 \pm 1.1

Data are mean \pm SEM, there are no significant differences between groups

In remote non-ischemic LAD perfused myocardium, no PKH labeled cells were detected either at 90 minutes or 4 days after injection. In contrast, a significant amount of PKH-labeled cells could be demonstrated within post-MI tissue 90 minutes and 4 days after injection (Figure 1). The numbers of PKH-positive cells in the infarct area were similar for both injection methods. Thus, an average of 314 \pm 74 PKH positive cells/cm² could be detected 90 minutes after injection during uninterrupted flow which corresponds to \sim 8.2 \pm 1.9 % of the injected cells (Table 1). After injection during repeated interrupted flow 325 \pm 66 PKH positive cells/cm² could be detected 90 minutes after injection, which corresponds to \sim 8.5 \pm 1.7 % of the injected cells.

Four days after MNC injection, 249 \pm 43 PKH positive cells/cm² could be detected after injection with a probing catheter, corresponding with \sim 6.5 \pm 1.1 % of the

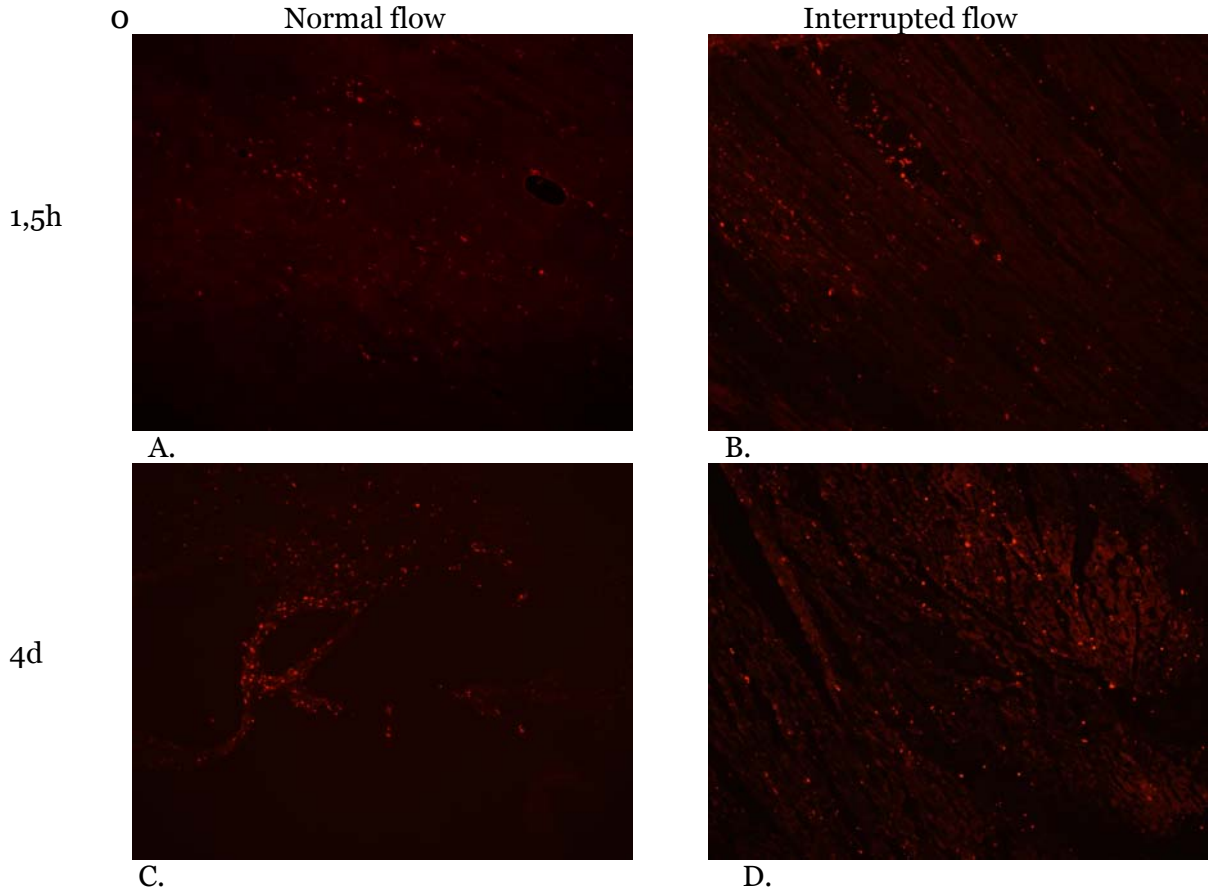


Figure 1: PKH positive cells in the infarct area 1.5 hours (A,B) and 4 days (C,D) after injection using a probing catheter (A,C) or a balloon catheter (B,D). Power field 10x.

injected cells. MNC injection with a balloon catheter resulted in an average of 252 ± 42 PKH positive cells/cm² four days after injection which also corresponds with $\sim 6.5 \pm 1.1$ % of the injected cells.

Immunohistochemistry showed that the injected PKH labeled MNC stained negative for macrophages, however PKH positive cells could be detected near macrophages. Occasionally PKH labeled cells were positive for CD45, CD90 and some PKH labeled MNC could be detected near CD31 positive cells four days after injection (Figure 2).

Discussion

The present study was undertaken to test the hypothesis that flow interrupted injection of MNC results in better engraftment of MNC in a porcine model of reperfused MI. Contrary to this hypothesis, we observed that the method of cell delivery via intermittent balloon occlusion does not lead to higher cell engraftment in our model as compared to injection during normal coronary inflow conditions.

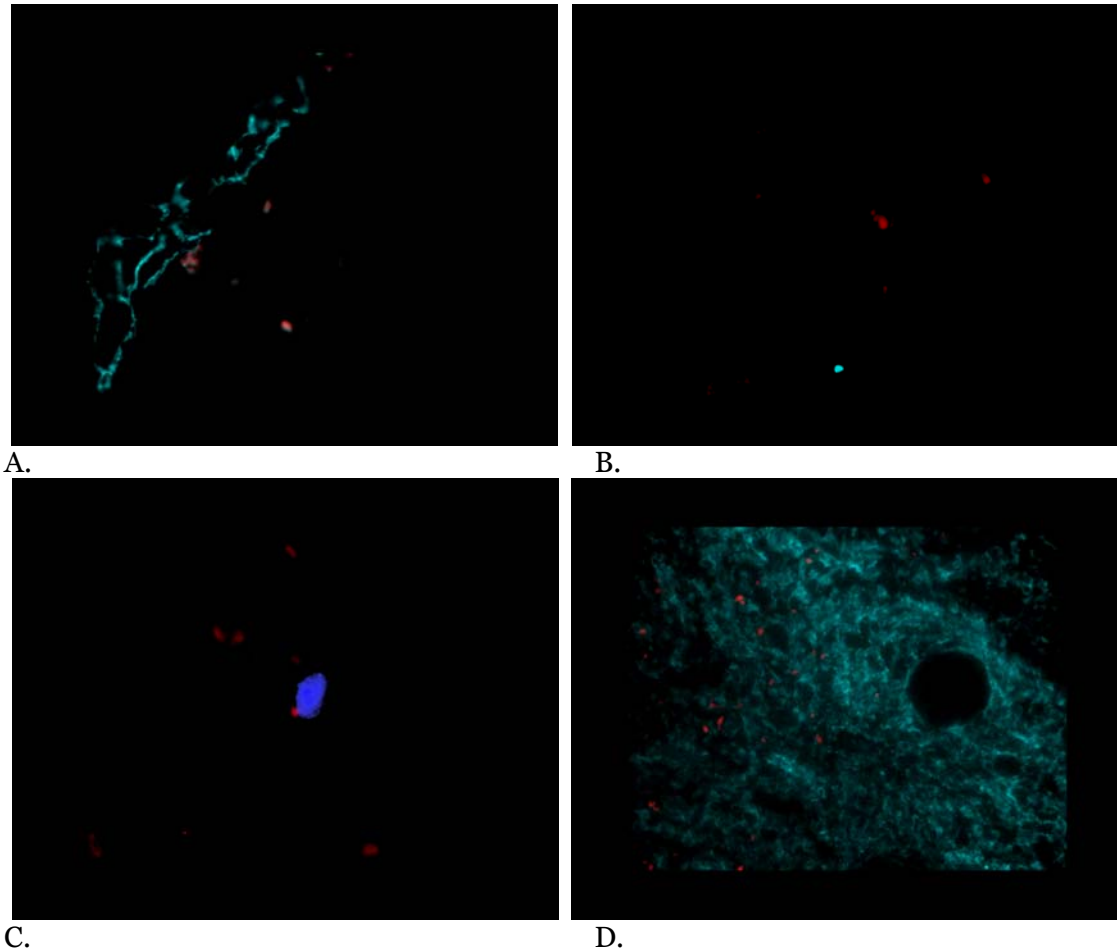


Figure 2: Photomicrograph A shows a CD31+ blood vessel (blue) and PKH positive cells (red) located close to the CD31+ cells. Photomicrograph B shows a CD45+ cell (blue) and PKH positive cells (red). Photomicrograph C shows a macrophage (blue) and PKH positive cells (red). Photomicrograph D shows CD90+ fibroblast (blue) and PKH positive cells (red) located in between the CD90+ cells

Histology showed that four days after injection, some PKH labeled cells expressed leukocyte (CD45) and fibroblast (CD90) markers. The injected cells were not internalized by macrophages and were occasionally located near new blood vessels.

Because the method of intermittent balloon occlusion whereby MNC are typically injected in clinical trials was never validated, we compared this flow-limiting delivery method with cell injection during normal coronary flow in a porcine model of MI. The viability of cells after injection through the different catheters was similar. Our study showed that bone marrow derived MNC do not home in non-ischemic myocardium. This observation is in accordance to the study by Aisher et al.⁹ in rats. However, in the infarct area more cells could be detected 90 minutes after injection, than four days after MNC injection, however, this did not reach levels of statistical significance. Initially, 8 % of the injected cells were detected 90 minutes after injection, and four days later 6.5% remained in the myocardium with either mode of delivery. These findings suggest that the efficacy of intracoronary injection of MNC in

the infarct zone is independent of the method of intracoronary delivery in swine one week after MI.

In one of our previous studies⁸ we used a probing catheter to inject MNC intracoronary. We observed a decrease in infarct size, but no effect on left ventricular function. Taken together the finding of the present study, using a different mode of intracoronary administration of MNC would probably not have had a different effect on left ventricular function or infarct size.

In clinical trials PTCA was thought to thoroughly prevent the backflow of cells and at the same time produced a stop-flow beyond the site of the balloon inflation to facilitate high-pressure infusion of cells into the infarcted zone and thereby prolong contact time for adhesion and potential cellular transmigration of the infused cells through the endothelium.^{10,11}

Although engraftment of injected stem cells was thought to be higher under non-flow conditions,⁶ this was not the case in our study. Apparently a few minutes of balloon occlusion are not enough to increase the number of cells that adhere to the vessel wall and eventually end up in the myocardium. It cannot be excluded that a longer occlusion period, and thus a longer non-flow period might enhance the number of adhered cells. However, extending the occlusion duration may increase the likelihood of arrhythmias and also induce an additional inflammatory response or reperfusion damage.

The limitation of our study is that no absolute flow measurements were performed during and before cell injection.

Clinical relevance

Our study suggests that it would not change outcome for patients in clinical trials if a selective injection catheter would be used instead of a balloon catheter for stem cell injections. This potentially prevents additional damage to the vascular wall and additional ischemia, created by balloon occlusions.^{12,13}

References

1. Orlic D, Kajstura J, Chimenti S, Jakoniuk I, Anderson SM, Li B, Pickel J, McKay R, Nadal-Ginard B, Bodine DM, Leri A, Anversa P. Bone marrow cells regenerate infarcted myocardium. *Nature*. 2001;410:701-5.
2. Kocher AA, Schuster MD, Szabolcs MJ, Takuma S, Burkhoff D, Wang J, Homma S, Edwards NM, Itescu S. Neovascularization of ischemic myocardium by human bone-marrow-derived angioblasts prevents cardiomyocyte apoptosis, reduces remodeling and improves cardiac function. *Nat Med*. 2001;7:430-6.
3. Meyer GP, Wollert KC, Lotz J, Steffens J, Lippolt P, Fichtner S, Hecker H, Schaefer A, Arseniev L, Hertenstein B, Ganser A, Drexler H. Intracoronary bone marrow cell transfer after myocardial infarction: eighteen months' follow-up data from the randomized, controlled BOOST (BOne marrOw transfer to enhance ST-elevation infarct regeneration) trial. *Circulation*. 2006;113:1287-94.
4. Schachinger V, Assmus B, Britten MB, Honold J, Lehmann R, Teupe C, Abolmaali ND, Vogl TJ, Hofmann WK, Martin H, Dimmeler S, Zeiher AM. Transplantation of progenitor cells and regeneration enhancement in acute myocardial infarction: final one-year results of the TOPCARE-AMI Trial. *J Am Coll Cardiol*. 2004;44:1690-9.
5. Janssens S, Dubois C, Bogaert J, Theunissen K, Deroose C, Desmet W, Kalantzi M, Herbots L, Sinnaeve P, Dens J, Maertens J, Rademakers F, Dymarkowski S, Gheysens O, Van Cleemput J, Bormans G, Nuyts J, Belmans A, Mortelmans L, Boogaerts M, Van de Werf F. Autologous bone marrow-derived stem-cell transfer in patients with ST-segment elevation myocardial infarction: double-blind, randomised controlled trial. *Lancet*. 2006;367:113-21.

Chapter 7

6. Sherman W, Martens TP, Viles-Gonzalez JF, Siminiak T. Catheter-based delivery of cells to the heart. *Nat Clin Pract Cardiovasc Med*. 2006;3 Suppl 1:S57-64.
7. Freyman T, Polin G, Osman H, Crary J, Lu M, Cheng L, Palasis M, Wilensky RL. A quantitative, randomized study evaluating three methods of mesenchymal stem cell delivery following myocardial infarction. *Eur Heart J*. 2006.
8. Moelker AD, Baks T, van den Bos EJ, van Geuns RJ, de Feyter PJ, Duncker DJ, van der Giessen WJ. Reduction in infarct size, but no functional improvement after bone marrow cell administration in a porcine model of reperfused myocardial infarction. *Eur Heart J*. 2006;27:3057-64.
9. Aicher A, Brenner W, Zuhayra M, Badorff C, Massoudi S, Assmus B, Eckey T, Henze E, Zeiher AM, Dimmeler S. Assessment of the tissue distribution of transplanted human endothelial progenitor cells by radioactive labeling. *Circulation*. 2003;107:2134-9.
10. Strauer BE, Brehm M, Zeus T, Kosterling M, Hernandez A, Sorg RV, Kogler G, Wernet P. Repair of infarcted myocardium by autologous intracoronary mononuclear bone marrow cell transplantation in humans. *Circulation*. 2002;106:1913-8.
11. Assmus B, Schachinger V, Teupe C, Britten M, Lehmann R, Dobert N, Grunwald F, Aicher A, Urbich C, Martin H, Hoelzer D, Dimmeler S, Zeiher AM. Transplantation of Progenitor Cells and Regeneration Enhancement in Acute Myocardial Infarction (TOPCARE-AMI). *Circulation*. 2002;106:3009-17.
12. Baptista J, Umans VA, di Mario C, Escaned J, de Feyter P, Serruys PW. Mechanisms of luminal enlargement and quantification of vessel wall trauma following balloon coronary angioplasty and directional atherectomy. *Eur Heart J*. 1995;16:1603-12.
13. Balian V, Galli M, Marcassa C, Cecchin G, Child M, Barlocco F, Petrucci E, Filippini G, Michi R, Onofri M. Intracoronary ST-segment shift soon after elective percutaneous coronary intervention accurately predicts periprocedural injury. *Circulation*. 2006;114:1944-54.

Chapter 8

Intracoronary injection of cultured bone marrow cells causes micro infarctions in contrast to freshly isolated cells in a porcine model of myocardial infarction

A D. Moelker¹, M. de Jong¹, H.J.F.M.M. Eussen², D. J. Duncker¹, W. J. van der Giessen^{1,3}.

¹ Experimental Cardiology, Thoraxcenter, Erasmus MC, Rotterdam, The Netherlands

² Clinical Genetics, Erasmus MC, Rotterdam, The Netherlands

³ Interuniversity Cardiology Institute of the Netherlands

Abstract

Background: Regeneration of infarcted myocardium by injection of stem cells into the infarct region has been proposed to prevent heart failure. Intracoronary injection appears safe and feasible. However, there have been previous studies that suggest that intracoronary injection of cultured cells is associated with ECG-changes and a higher in-stent restenosis. We, therefore, compared the effect of intracoronary injection of freshly isolated bone marrow derived mononuclear cells (MNC) and cultured MNC in a porcine model of a reperfused MI.

Methods: In 10 domestic swine, the proximal left circumflex coronary artery was balloon-occluded for two hours followed by reperfusion. One week after induction of MI, five swine received intracoronary autologous cultured MNC, a total of ~100 million cells labeled with the permanent fluorescent membrane stain PKH and five swine received PKH labeled freshly isolated MNC. Half of the cells were administered in post-MI myocardial tissue and the other 50% of the cells were injected in normal non-ischemic myocardium. Four days later all swine were sacrificed for histological analysis.

Results: In the non-ischemic myocardium no freshly isolated MNC could be detected and the tissue appeared normal. However, after injection of cultured MNC micro infarctions were observed in the non-infarcted remote zone. In post-MI tissue a significant number of PKH labeled cultured MNC as well as freshly isolated MNC were present.

Conclusion: Freshly isolated MNC do not home in non-ischemic myocardium. Cultured MNC, which are larger in size (~ 12 μm , vs. 5-7 μm for freshly isolated MNC), obstruct blood vessels in healthy myocardium probably due to their larger size, thereby causing micro infarctions.

Introduction

Myocardial infarction (MI) is still one of the leading causes of morbidity and mortality in western society. Regeneration of infarcted myocardium by injection of stem cells into the infarct region has been proposed to prevent heart failure. Experimental studies in small rodent models showed that stem cell therapy has potential to improve left ventricular function after MI. To date, several clinical trials have been completed and intracoronary injection seems safe and feasible. However, there have been previous pre-clinical studies which suggest that intracoronary injection of cultured cells is associated with ECG-changes¹ and myocardial injury and a higher in-stent restenosis in clinical applications²⁻³. Intracoronary administration of umbilical cord blood derived cells can cause micro infarctions after injection in normal myocardium⁴. Intracoronary delivery of bone marrow derived mesenchymal stem cells was also associated with a higher incidence of decreased coronary blood flow⁵. Bone marrow derived cell injection is even believed to induce severe calcifications after intracoronary injection⁶. It is not surprising that injected cells differentiate into fibroblasts after injection⁷ in the scar tissue of a MI instead of into myocytes.

Most animal studies are performed in a small rodent model with a permanent ligated coronary artery, where cells are injected intramyocardial. These models are not able to predict the possible harmful effects of stem cell therapy in patients since heart rate, heart size and hemodynamics in rodent are very different from large mammals, for example humans. In our study we used a pre-clinical porcine model of myocardial infarction followed by reperfusion and thereby more closely mimicking the clinical settings of MI. In patients with a MI reperfusion is still the recommended therapy according to the guidelines. Therefore, we investigated the effect of intracoronary injection of freshly isolated bone marrow derived mononuclear cells (MNC) and cultured MNC in a porcine model of a reperfused MI and intracoronary injection of the cells into healthy myocardium.

Materials and methods

Experiments were performed in 2-3 month old Yorkshire-landrace pigs, in compliance with the "Guide for the Care and Use of Laboratory Animals" (NIH publication 1996) and after approval of the Animal Care Committee of the Erasmus MC.

Animal study

Two groups of animals were compared (Figure 1).

Five animals were sedated (ketamine 20 mg/kg IM, and midazolam 1 mg/kg IM) and approximately 40 mL of bone marrow (BM) was aspirated from the iliac crest. MNC were isolated by Ficoll Paque-plus (Amersham Biosciences Europe GmbH, Freiburg, Germany) density gradient separation. Cells were plated on flasks and cultured in EGM-2 (Cambrex, Biowhittaker, USA) for three weeks.

Two weeks after the BM aspiration the above five animals and a second group of five swine were sedated (ketamine 20 mg/kg IM, and midazolam 1 mg/kg IM), anaesthetised (thiopental, 12 mg/kg IV), intubated and mechanically ventilated with a mixture of oxygen and nitrogen (1:2 vol/vol) as described before^{4,8}. Anaesthesia was

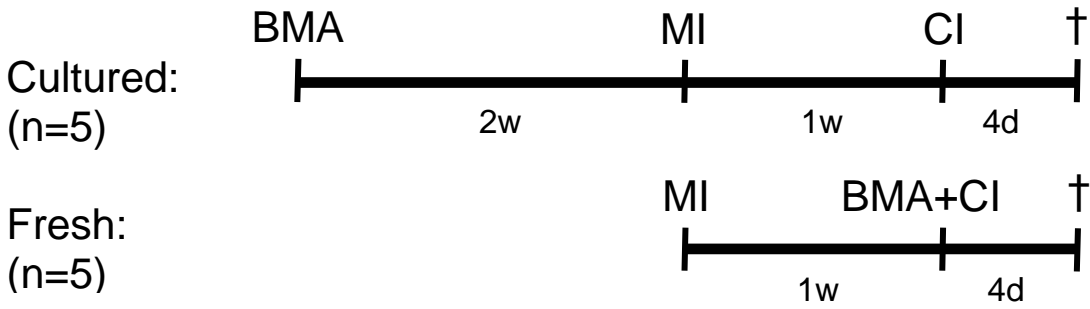


Figure 1: BMA= bone marrow aspiration, MI= myocardial infarction, CI= cell injection, †= sacrifice. Upper timeline demonstrates the model for the group swine that received the cultured MNC. Timeline at the bottom shows the model for the swine that receive fresh MNC.

initially maintained with fentanyl (12.5 µg/kg/h) and continued with isoflurane (0.6-0.8% started only after onset of occlusion to prevent preconditioning). Subsequently, animals received antibiotic prophylaxis (200 mg procainebenzylpenicillin and 250 mg dihydrostreptomycinesulfate IM) and underwent coronary catheterization through a carotid artery guided by fluoroscopy, followed by balloon occlusion of the proximal left circumflex coronary artery (LCX), for 2 hr followed by reperfusion⁸. Heparin was administered every hour (5000 Units).

One week after MI, all 10 swine were sedated and heparinized as described above. Anesthesia was maintained with 1% isoflurane and five swine received an intracoronary injection of ~50·10⁶ PKH-labelled cultured MNC (PKH 26, Sigma-Aldrich, Schnellendorf, Germany) suspended in 10 mL saline into the LCX (infarct area) and into the left anterior descending coronary artery (LAD; non-infarct area). MNC were injected slowly (1 mL/min) into the coronary artery perfusing the MI area using a selective, non flow-limiting probing catheter (Multifunctional Probing, Boston Scientific Co, Boston, MA). The site of injection was identical to the position of the occlusion balloon during MI induction. The five other MI animals first underwent a BM aspiration. MNC were isolated, labeled with PKH, and the same number of cells were injected as described above in the LAD and the LCX.

Four days after cell injection animals were sacrificed with an overdose of pentobarbital for histological and immunohistochemical analyses.

Histology and Immunohistochemistry

The hearts were excised and cut in 6-8 transverse slices. Slices were embedded in tissue tec OCT and frozen in liquid nitrogen. Sections (5 µm) were stained with anti-PCNA (DakoCytomation, California, USA), CD45 (mouse anti porcine CD45, Chemicon, Hampshire, UK), vimentin (Clone DE-R-11, DakoCytomation, California, USA) and desmin (Clone V9, DakoCytomation, California, USA) antibodies. PCNA is a cell proliferation marker, CD45 is a pan-leukocyte marker, desmin is expressed by myocytes and smooth muscle cells and vimentin is expressed by fibroblasts and endothelial cells.

Statistical Analysis

Data were analyzed with SPSS 11.0. All data were analyzed using unpaired t-testing. Statistical significance was accepted when $P \leq 0.05$ (two-tailed). All data are presented as mean \pm SEM.

Results

PKH labeled MNC could be detected 4 days after injection into infarcted area. Quantative analysis showed that an average of 249 ± 43 PKH positive cells/cm² could be detected four days after injection which corresponds to $\sim 6.5\%$ of the injected cells (Table 1).

Table 1: number of PKH positive cells

	# cells/cm ²		% of the injected cells
		LCX	
Freshly isolated MNC	249 \pm 43		6.5 \pm 1.1
Cultured MNC	173 \pm 39		4.5 \pm 1.0
		LAD	
Freshly isolated MNC	<1		<0.03
Cultured MNC	88 \pm 14		2.3 \pm 0.4

Data are mean \pm SEM, There were no significant differences between groups.

After MNC culturing 173 ± 39 PKH positive cells/cm² could be detected four days after injection in the infarcted LCX tissue with a probing catheter which corresponds in $\sim 4.5\%$ of the injected cells (Table 1). This difference between fresh and cultured MNC did not reach levels of significance ($P > 0.05$).

In non-infarcted remote LAD myocardium, only a few (< 1 cell/cm²) PKH labeled freshly isolated MNC could be detected 4 days after injection. Light microscopy showed healthy myocardial tissue without signs of injury.

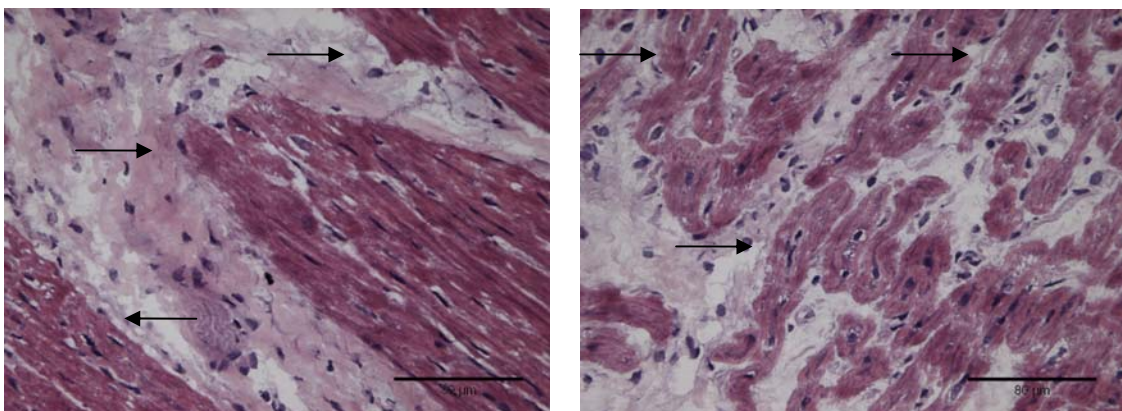


Figure 2: Hemotoxilin-Eosin staining; Photomicrographs A and B shows micro infarctions four days after injection of cultured MNC in normal myocardium. Arrows indicate surviving myocytes, bar indicates 80 μ m.

In contrast, significantly more cultured MNC (88 ± 14 cell/cm²) were detected 4 days after injection in non-infarcted myocardium ($P < 0.05$). In addition, after injection of cultured MNC in swine micro infarctions were observed in the non-infarcted remote zone (Figure 2).

Furthermore, the freshly isolated MNC were spread homogenous in the myocardium perfused by the artery where the cells were injected, however the cultured MNC were detected in cell clusters (Figure 3), especially after injection in the LAD (Figure 3C).

Immunohistochemistry showed that the injected cultured MNC were negative for desmin and occasionally positive for vimentin and CD45 (Figure 4). The PKH labeled cultured MNC were negative for PCNA. There were no differences in histology between the different expression of markers in the different areas (LAD or LCX).

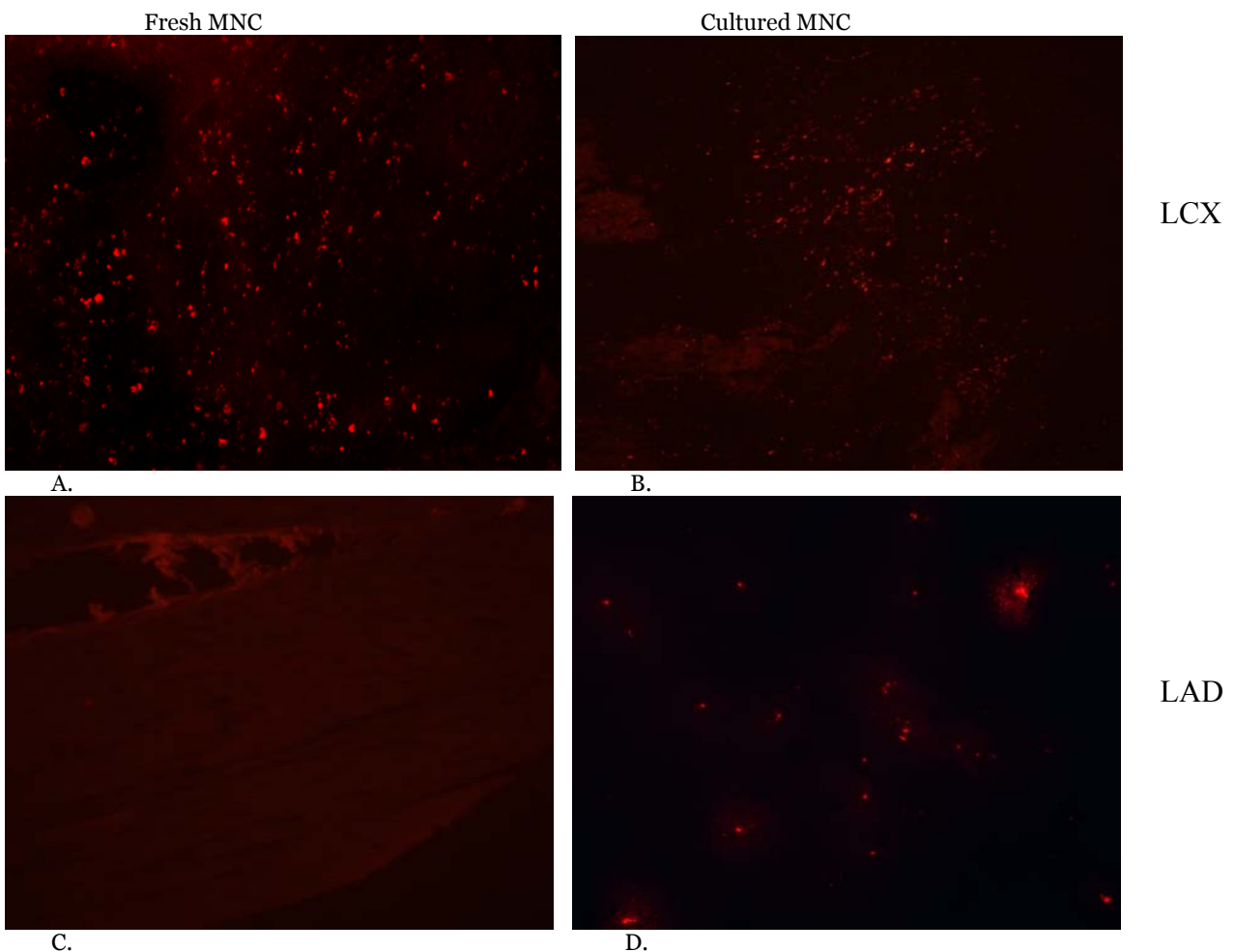


Figure 3: Photomicrograph A and C show PHK labeled cells four days after injection of freshly isolated MNC in the infarcted LCX (A) and the non-infarcted LAD (C). Photomicrograph B and D show PHK labeled cells four days after injection of cultured MNC in the infarcted LCX (B) and the non-infarcted LAD (D). Powerfield 10x

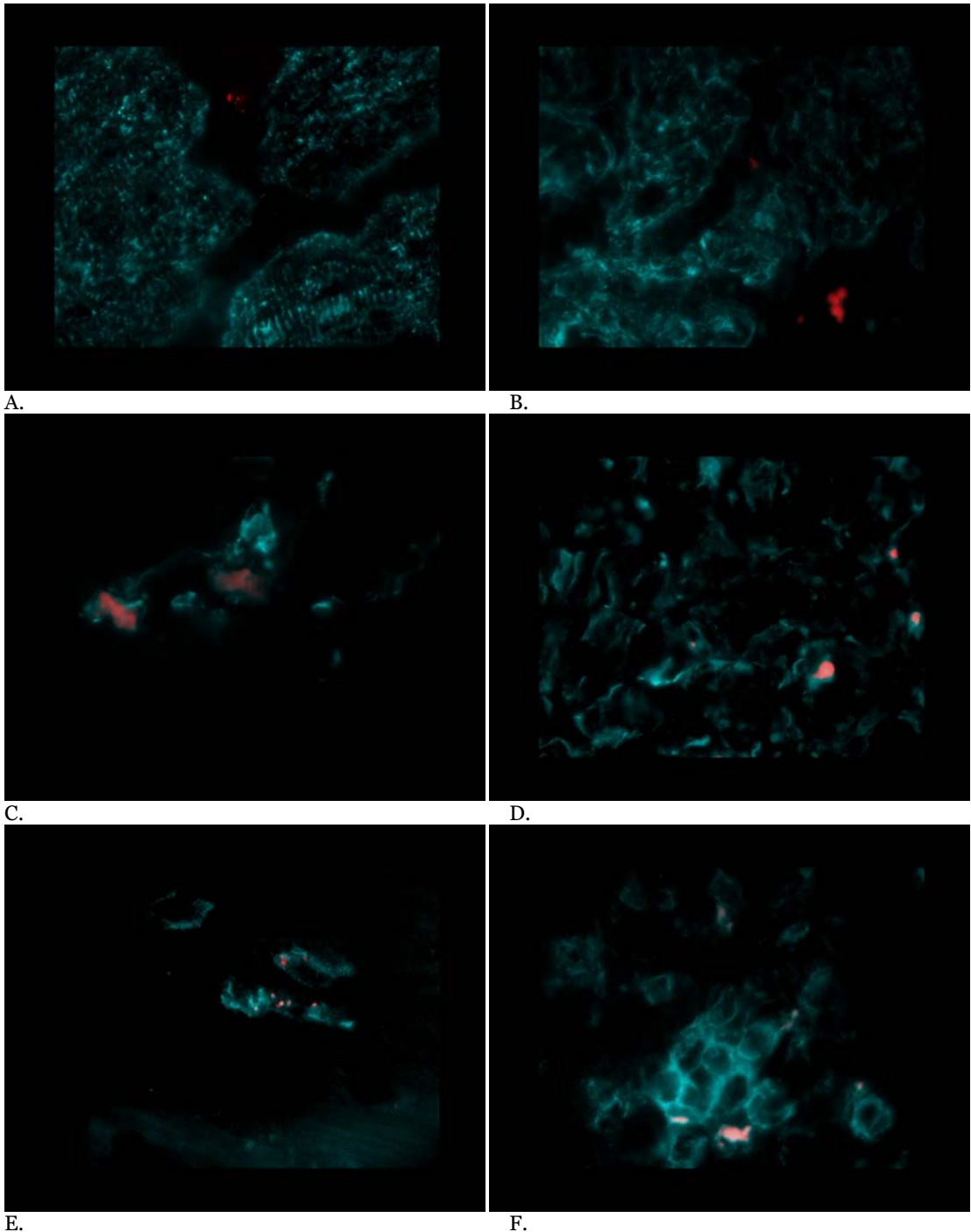


Figure 4: Photomicrograph A and B show desmin positive cells (Blue) and PHK labeled cells (red) 4 days after injection of cultured MNC in the non-schemic LAD (A) and the infarcted LCX (B). C and D show vimentin positive cells (Blue) and PHK+ cells (red) 4 days after injection of cultured MNC in the LAD (C) and the LCX (D). E and F show CD45 positive cells (Blue) and PHK labeled cells (red) 4 days after injection of cultured MNC in the non-ischemic LAD (E) and in the infarcted LCX (F). Powerfield 100x.

Discussion

The aim of this study was to investigate the effect of cultured and freshly isolated BM derived MNC on healthy and infarcted myocardium, since previous studies showed harmful side effects of stem cell injection¹⁻⁷.

Four days after MI, cultured and freshly isolated MNC cells could be detected in the infarct area. Our study showed that freshly isolated MNC do not home in non-ischemic myocardium and there were no changes in the healthy myocardium after injection. However, cultured MNC which are larger in size (~12 µm vs. 5-7 µm), obstruct blood vessels in healthy myocardium probably due to higher expression of adhesion molecules⁹ on the cells and thereby causing micro infarctions. It could be possible that the survival of the cultured cells is lower in the LCX due to additional micro infarctions caused by the cell injection. Or that LAD injected cells in the animals which were injected with freshly isolated MNC, homed to the LCX, and thereby causing higher numbers of cells in the infarcted LCX perfused area.

In one of our previous studies⁴ micro infarctions were also observed after injection of cultured umbilical cord blood derived unrestricted somatic stem cells. These umbilical cord blood derived cells are even larger in cell size (~ 20 µm) than the cultured MNC in this study, and caused more severe micro infarctions with beginning calcifications four days after injection in healthy tissue.

Although clinical trials suggest that intracoronary stem cell injection is safe, cultured stem cells should be used with caution when applied intracoronary. It should be further investigated what the effect of injection of cultured cells is, when applying a different mode of administration, for example intramyocardial cell injection. Furthermore, it is important to know what the long term effect is of the induction of micro infarctions after intracoronary injection.

References

1. Vulliet PR, Greeley M, Halloran SM, MacDonald KA, Kittleson MD. Intra-coronary arterial injection of mesenchymal stromal cells and microinfarction in dogs. *Lancet*. 2004;363:783-4.
2. Mansour S, Vanderheyden M, De Bruyne B, Vandekerckhove B, Delrue L, Van Haute I, Heyndrickx G, Carlier S, Rodriguez-Granillo G, Wijns W, Bartunek J. Intracoronary delivery of hematopoietic bone marrow stem cells and luminal loss of the infarct-related artery in patients with recent myocardial infarction. *J Am Coll Cardiol*. 2006;47:1727-30.
3. Kang HJ, Kim HS, Zhang SY, Park KW, Cho HJ, Koo BK, Kim YJ, Soo Lee D, Sohn DW, Han KS, Oh BH, Lee MM, Park YB. Effects of intracoronary infusion of peripheral blood stem-cells mobilised with granulocyte-colony stimulating factor on left ventricular systolic function and restenosis after coronary stenting in myocardial infarction: the MAGIC cell randomised clinical trial. *Lancet*. 2004;363:751-6.
4. Moelker AD, Baks T, Wever KM, Spitskovsky D, Wielopolski PA, van Beusekom HM, van Geuns RJ, Wnendt S, Duncker DJ, van der Giessen WJ. Intracoronary delivery of umbilical cord blood derived unrestricted somatic stem cells is not suitable to improve LV function after myocardial infarction in swine. *J Mol Cell Cardiol*. 2007.
5. Freyman T, Polin G, Osman H, Crary J, Lu M, Cheng L, Palasis M, Wilensky RL. A quantitative, randomized study evaluating three methods of mesenchymal stem cell delivery following myocardial infarction. *Eur Heart J*. 2006.
6. Yoon YS, Park JS, Tkebuchava T, Luedeman C, Losordo DW. Unexpected severe calcification after transplantation of bone marrow cells in acute myocardial infarction. *Circulation*. 2004;109:3154-7.

Chapter 8

7. Wang JS, Shum-Tim D, Chedrawy E, Chiu RC. The coronary delivery of marrow stromal cells for myocardial regeneration: pathophysiologic and therapeutic implications. *J Thorac Cardiovasc Surg.* 2001;122:699-705.
8. Moelker AD, Baks T, van den Bos EJ, van Geuns RJ, de Feyter PJ, Duncker DJ, van der Giessen WJ. Reduction in infarct size, but no functional improvement after bone marrow cell administration in a porcine model of reperfused myocardial infarction. *Eur Heart J.* 2006;27:3057-64.
9. Liu B, Buckley SM, Lewis ID, Goldman AI, Wagner JE, van der Loo JC. Homing defect of cultured human hematopoietic cells in the NOD/SCID mouse is mediated by Fas/CD95. *Exp Hematol.* 2003;31:824-32.

Chapter 9

Magnetic resonance imaging of haemorrhage
within reperfused myocardial infarcts: possible
interference with iron oxide-labelled cell
tracking?

Ewout J. van den Bos¹, Timo Baks^{1,2}, Amber D. Moelker¹, Wendy Kerver¹, Robert-Jan van Geuns², Willem J. van der Giessen¹, Dirk J. Duncker¹, and Piotr A. Wielopolski^{2*}

¹ Experimental Cardiology, Thoraxcenter, Erasmus MC r, Rotterdam, The Netherlands

² Department of Radiology, Erasmus MC, Rotterdam, The Netherlands

Abstract

Aims Magnetic resonance imaging (MRI) has been proposed as a tool to track iron oxide-labelled cells within myocardial infarction (MI). However, infarct reperfusion aggravates microvascular obstruction (MO) and causes haemorrhage. We hypothesized that haemorrhagic MI causes magnetic susceptibility-induced signal voids that may interfere with iron oxide-labelled cell detection.

Methods and results Pigs (n= 23) underwent 2 h occlusion of the left circumflex artery. Cine, T2*-weighted, perfusion, and delayed enhancement MRI scans were performed at 1 and 5 weeks, followed by ex vivo high-resolution scanning. At 1 week, MO was observed in 17 out of 21 animals. Signal voids were observed on T2*-weighted scans in five out of eight animals, comprising 24 +22% of the infarct area. A linear correlation was found between area of MO and signal voids ($R^2= 0.87$; $P= 0.002$). At 5 weeks, MO was observed in two out of 13 animals. Signal voids were identified in three out of seven animals. Ex vivo scanning showed signal voids on T2*-weighted scanning in all animals because of the presence of haemorrhage, as confirmed by histology. Signal voids interfered with the detection of iron oxide-labelled cells ex vivo (n= 21 injections).

Conclusion Haemorrhage in reperfused MI produces MRI signal voids, which may hamper tracking of iron oxide-labelled cells.

Introduction

Transplantation of cells after myocardial infarction (MI) has emerged as a promising therapy to restore heart function.¹⁻⁴ To evaluate cell engraftment, non-invasive tracking of cells with magnetic resonance imaging (MRI) has been proposed as a valuable tool. Cells labelled with iron oxide, paramagnetic probes cause a T2* signal void⁵ and can thus be detected up to single-cell resolution *in vitro*.⁶⁻⁸ *In vivo*, clusters of labelled cells could be detected after injection into infarcted myocardium of mouse,⁹⁻¹⁰ rabbit,¹¹ and pig hearts.¹²⁻¹⁷

However, in clinical practice, acute MI is treated by reperfusion therapy,¹⁸ aggravating microvascular obstruction (MO) and causing haemorrhage.^{19,20} Haemoglobin degradation products, such as methaemoglobin and haemosiderin, have strong magnetic susceptibility effects,²¹ which may mimic the signal voids caused by iron oxide-labelled cells.

We hypothesized that haemoglobin degradation products in reperfused MI produce signal voids that interfere with reliable iron oxide-labelled cell tracking. Therefore, we evaluated the MRI characteristics of subacute (1 week old) and chronic (5 weeks old) infarcts in a porcine model of reperfused MI and compared the MRI findings with histology of the infarct tissue.

Methods

Myocardial infarction

Experiments were performed in 23 Yorkshire–Landrace pigs (2–3 months old, ~25 kg). The study complied with the regulations of the Animal Care Committee of the Erasmus MC and the National Institutes of Health Publication 86–23, revised 1996. Animals were sedated (ketamine, 20 mg/kg IM and midazolam, 1 mg/kg IM), anaesthetized (thiopental, 12 mg/kg IV), intubated, and mechanically ventilated (mixture of oxygen and nitrogen, 1:2). Analgesia was maintained initially with fentanyl (12 mg/kg/min IV). Subsequently, animals underwent left coronary catheterization, followed by balloon occlusion of the left circumflex (LCx) coronary artery, proximal of the first margo obtusus branch. After 2 h, the balloon was deflated and the infarct reperfused, as confirmed by TIMI III flow on angiography. Anaesthesia was maintained with isoflurane (0.6–0.8%), starting after the occlusion of the LCx.

Magnetic resonance imaging

A 1.5 T MRI scanner with a dedicated four-element-phased array receiver coil was used (Signa CV/i; GE Medical Systems, Milwaukee, WI, USA). One week after MI, pigs were anaesthetized and ventilated as described earlier and underwent clinically applied,²² electrocardiogram (ECG)-gated cine, T2*-weighted, first-pass perfusion (FPP), and delayed enhancement (DE) MRI. The T2*-weighted sequence was applied in a subset of animals (n=8 and n=7 at 1 and 5 weeks, respectively) because of technical limitations of the scanner software at the start of the study. For detailed MRI protocols, see Supplementary material online. Breath-holding was achieved by interrupting the ventilation.

After scanning, eight animals were euthanized using an overdose of pentobarbital. Hearts were excised, immersed in saline, and scanned *ex vivo* using gradient echo (GE) and spin echo (SE) sequences with multiple echo times and flip angles to obtain T1-, proton density-, T2-, and T2*-weighted images (T1W, PDW, T2W, and T2*W, respectively). For detailed MRI protocols, see Supplementary material online. The minimum time interval between *in vivo* scanning and sacrifice was at least 3 h, and in most cases, 12 h (overnight), to make sure that all gadolinium-DTPA had been washed out.

One animal died following the 1 week scan. Five weeks after infarction, the remaining 14 animals underwent a follow-up MRI using a similar imaging protocol as at 1 week. In one animal, at 1 week and again at 5 weeks, no vascular access could be assured during scanning for injection of contrast; therefore, in this animal, no FPP and DE scans could be obtained. In one animal at 1 week, FPP scanning was not reliable for the assessment of MO owing to movement artefacts; therefore, it was not included in the analysis. Three infarct specimens were scanned a second time after standard paraffin embedding. Finally, of three animals, no *ex vivo* scans could be obtained because of technical limitations during scanning.

In order to compare signal voids induced by the presence of iron oxide-labelled cells and haemoglobin degradation products, *ex vivo* scanning was repeated after local injections with either 0.1, 1, or 4 x 10⁶ iron oxide-labelled human umbilical vein endothelial cells. A total of 21 injections were performed in four subacute and three chronic infarct specimens. Cells were labelled as described previously,⁸ resulting in ~9.2 pg iron per cell, and fixed in 4% formaldehyde.

A flowchart (Figure 1) summarizes the protocol and the number of animals studied at each time point.

Image analysis

MR images were analysed using Cine Display Application Version 3.0 (GE Medical systems, Milwaukee, WI, USA). Signal voids were identified on mid-papillary, single-slice T2*W scans, and expressed as a percentage of the infarct area as defined by DE MRI. Signal void volumes were calculated by multiplying their area by slice thickness. MO was identified on mid-papillary, single-slice FPP images as an area of persistent subendocardial hypoenhancement.²³ MI was identified on DE images as an area with delayed hyperenhancement and its size was expressed as a percentage of the left ventricular (LV) wall volume.

Contrast-to-noise ratio (CNR) was measured in the T2*W *in vivo* and *ex vivo* scans at 1 and 5 weeks, according to the relation $[CNR=(SI_{myo} - 2 SI_{void})/SD_{noise}]$, where SI_{myo} represents signal intensity of remote or infarcted myocardium, SI_{void} , signal intensity of signal voids, and SD_{noise} , standard deviation of background noise measured in the air outside the pig.

Total haemorrhagic areas were measured at mid-papillary levels in PD-T2*W *ex vivo* scans using Clemex Vision PE analysis software (Clemex Technologies, Longueuil, Canada) and expressed as a percentage of the total infarct area.

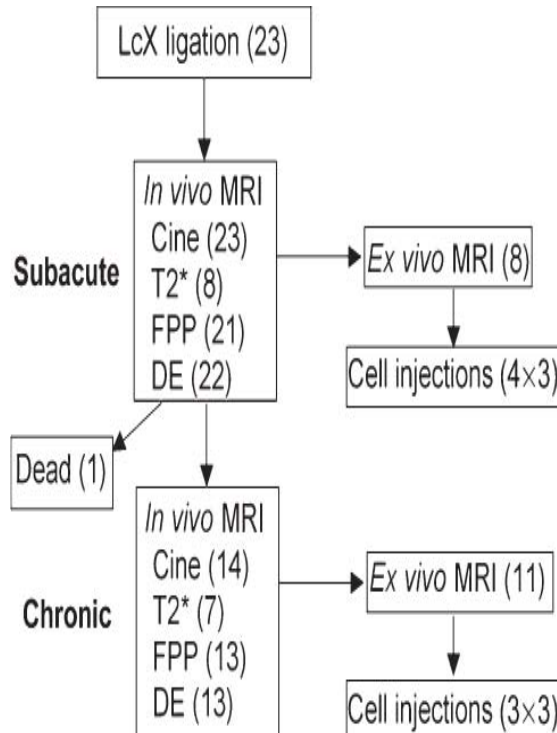


Figure 1 Flowchart of the study protocol. Numbers between brackets indicate the number of animals or specimens used at a certain time point.

Histology

Hearts were transversally cut in ~1 cm thick slices and stained with 1% triphenyltetrazolium chloride (37°C, 15 min; Sigma, St Louis, MO, USA) and subsequently with Prussian blue (PB), which stains haemosiderin deposits deep blue. After standard paraffin embedding, 5 mm serial sections were cut in the same plane as the MRI scans. Sections were stained with haematoxylin eosin (HE) or von Kossa's (VK), or restained with PB. VK was counterstained with von Gieson (VG). This approach allowed for identification of fat (HE), calcium (VK), collagen (VG), as well as haemosiderin (PB). Staining was analysed and compared with matching MR images at the same location and imaging plane.

Statistical analysis

Data are reported as mean±SD. Data from subacute and chronic infarcts were compared using paired or unpaired t-testing as appropriate. The correlation between area of MO and signal voids was assessed using linear regression analysis, including all animals assessed by T2*W scanning. Proportions were compared using a z-test (SigmaStat software version 2.03; SPSS Inc., Chicago, IL, USA). Sample size was determined with the following assumptions: type I error of 0.05, power of 80%, an estimated proportion of animals with an in vivo MRI detectable haemorrhage-induced signal void of 35%, based on the literature, with the assumption that a proportion of 5% would not be relevant. Therefore, eight animals would yield 80% power to detect a significant proportion of animals with such a signal void. On the basis of pilot studies,

the proportion of ex vivo detected signal voids was estimated to be 90%. A value of $P < 0.05$ (two-tailed) was considered statistically significant.

Results

In vivo MRI

In subacute infarcts, signal voids could be identified in five out of eight animals, using the T2*W sequence (Figure 2). In the remaining three animals, signal voids were either not observed (n=2) or could not be reliably discerned from the air–heart interface susceptibility artefact (n=1). The size of the signal voids was $0.53 \pm 0.51 \text{ cm}^3$. The area of signal voids comprised $24 \pm 22\%$ of the infarct area. MO was observed in 17 out of 21 animals, comprising $35 \pm 23\%$ of the infarct area (Table 1). A linear relationship was found between the area of signal voids on T2*W scans and the area of MO on the corresponding FPP scans at 1 week ($R^2=0.87$; $P=0.002$; $n=8$). Infarct size was $25 \pm 6\%$ of total LV wall volume (n=22). CNR between remote myocardium and areas of signal voids was 27 ± 16 and between infarcted, non-haemorrhagic

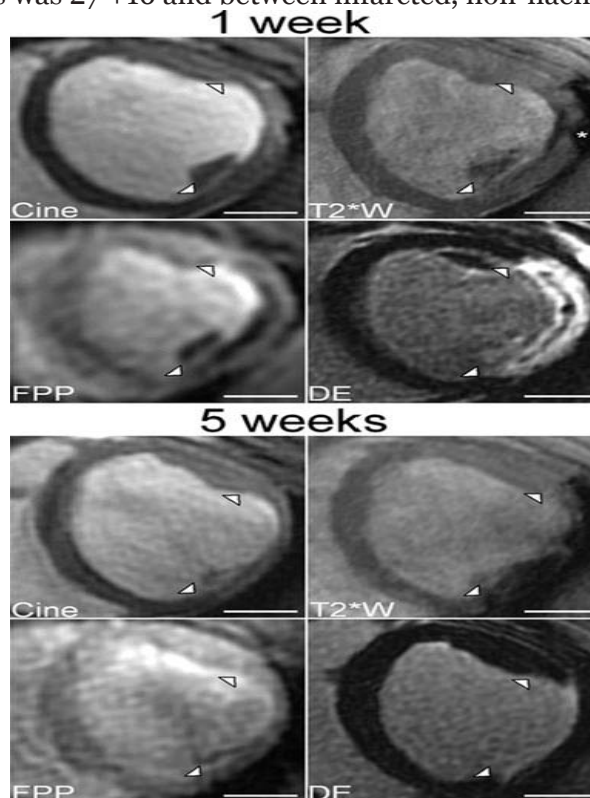


Figure 2 In vivo scans of one animal at 1 week (subacute) and 5 weeks (chronic) after infarction. Depicted are the end-diastolic frames of cine, T2*W, FPP, and DE scans at the same level. The infarct area is indicated by white arrows. In the T2*W image, endo- and epicardial rims of signal voids are present at 1 week. The artefact caused by the heart–air interface is indicated by an asterisk. The rims of signal voids correspond with a zone of hypo-perfusion in the FPP scan at 1 week, indicating MO. Furthermore, a zone of persistent hypo-enhancement can be appreciated in the DE scan within the hyperenhanced infarct area. At 5 weeks, the area of signal voids in the T2*W image takes up a larger part of the infarct area. Neither MO nor an area of persistent hypo-enhancement is observed in the FPP or DE scans. Bar indicates 2 cm.

Table 1: Results of MRI scanning

	Subacute infarcts (# of animals)	Chronic infarcts (# of animals)	P-value
<i>In vivo</i> MRI			
LV wall volume (cm ³)	63±15 (23)	85±13 (14)	0.00006
Infarct volume (%of LV volume)	25±6 (22)	15±5 (13)	0.00003
Animals with FPP defect	17 (21)	2 (13)	0.0007
FPP defect area (% of infarct area)	35±23 (21)	13±31 (13)	0.02
Animals with T2* signal void	5 (8)	3 (7)	NS
Area of T2* signal void (% of infarct area)	24±22 (8)	15±19 (7)	NS
CNR signal void vs. infarct area	34±11 (5)	23±6 (3)	NS
<i>Ex vivo</i> MRI			
Area of T2* signal void (% of infarct area)	42±5 (8)	19±7 (11)	0.00001
CNR signal void vs. infarct area	17±9 (8)	14±8 (11)	NS
CNR cells (4x10 ⁶) vs. infarct area	18±4 (4)	15±1 (3)	NS

myocardium, and areas of signal voids 34 ±11 (n=5).

In chronic infarcts, an area of signal voids could be identified in three out of seven animals, comprising 15 ±19% of the infarct area. MO was identified in two out of 13 animals, comprising 13 ±31% of the infarct area (P=0.0007 and 0.02 vs. 1 week, respectively; Table 1). Infarct size was 15 ±5% (P=0.00003 vs. 1 week; n= 13). CNR between remote myocardium and areas of signal voids was 34 ±21 and between infarcted, non-haemorrhagic myocardium, and areas of signal voids was 23 ±6(n= 3).

Ex vivo MRI and histology

In subacute infarcts, the ex vivo high-resolution scans showed rings of magnetic susceptibility-induced signal voids on T1W and PDW scans (Figure 3). The size of the signal voids increased with a longer TE (T1-T2*W). The rings surrounded large hyperintense areas on T1W scans, which appeared hypointense on T2W and PD-T2*W scans. At histology, these rings of signal voids corresponded with blue deposits on PB staining and surrounded large areas of erythrocytes.

In chronic infarcts, ex vivo scans showed magnetic susceptibility-induced signal voids on T1W, PDW, T2W, and T1-or PD-T2*W scans throughout the infarct area (Figure 4). Hyperintense areas were observed on T1W scans, which appeared hypointense on T2W and T1-or PD-T2*W scans (data not shown). Furthermore, hyperintense areas were observed on T2W scans, which appeared hypointense on T1W scans (data not shown). At histology, areas of signal voids matched the pattern of blue haemosiderin deposits after PB staining (Figure 5). No correlation was found with collagen, fat, or calcium deposits.

Total haemorrhagic areas at mid-papillary level as a percentage of the total infarct area as determined by T2*W MRI were significantly larger in subacute than in chronic infarcts (P=0.00001; n=8 and 11, respectively; Table 1).

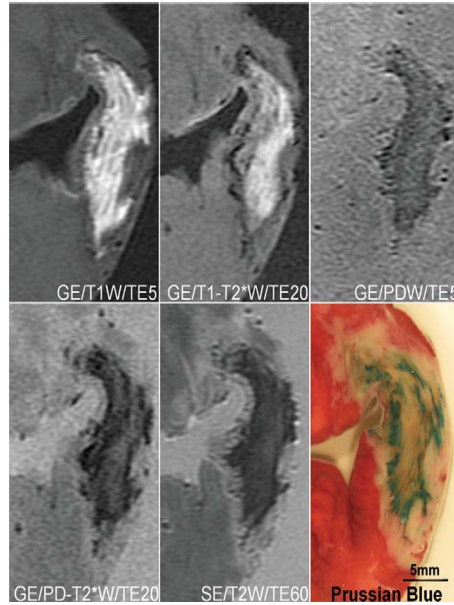


Figure 3 Ex vivo scans 1 week after infarction using different types of tissue contrast: T1W, PDW, T2W, and T2*W with a TE of 5, 20, or 60 ms (TE5, TE20, or TE60, respectively). Either a GE or an SE sequence was used. A ring of black signal voids is identified best in the T1W scan with a TE of 20 ms (T1–T2*W). It corresponds with the blue haemosiderin deposits in the PB image. The ring surrounds a hyperenhanced area on T1W scans, which is hypoenhanced on SE/T2 and PD–T2*W scans, corresponding with methaemoglobin within intact erythrocytes.

Post-mortem injections with iron oxide-labelled cells could be located in remote, non-infarcted myocardium. CNR between depots of 4×10^6 labelled cells and infarcted, non-haemorrhagic myocardium was 18 ± 4 in subacute infarcts ($n=4$) and 15 ± 1 in chronic infarcts ($n=3$; Table 1). This was comparable with the CNR between haemorrhage-induced signal voids and infarcted, non-haemorrhagic myocardium in subacute infarcts (17 ± 9 ; $n=8$) and chronic infarcts (14 ± 8 ; $n=11$; Table 1). As a cause, in the infarct region, none of the injection sites could be reliably located and discerned from haemorrhage-induced signal voids (Figure 6).

Discussion

Myocardial infarct reperfusion and haemorrhage

Reperfusion of MI is known to induce progressive MO, also described as the ‘no-reflow’ phenomenon.¹⁹ As shown in both animal and clinical studies, MO is followed by the development of haemorrhage, probably due to loss of microvascular integrity.^{20,24} The extent of the haemorrhagic area has been shown to correlate with the size of MO,²⁰ which was also observed in the present study.

Haemorrhage and MRI appearance

Few studies have been performed to evaluate the extent of the haemorrhagic area after reperfusion of MI using MRI.^{24–26} One study demonstrated the presence of

haemorrhage by SE imaging within 72 h after reperfused MI in dogs.²⁵ Hypointense lesions corresponding with haemorrhage were found in 14 out of 16 animals. These lesions were not found in non-reperfused animals. Furthermore, in two clinical studies, MRI was performed shortly after infarct reperfusion. The first study of 24 patients using GE and contrast-enhanced imaging showed hypointense areas within the infarct region in 38% of patients by both techniques.²⁴ In the second study, 39 patients were imaged using a T2*W GE sequence and haemorrhage could be identified as a hypointense zone within the infarct region in 33% of patients.²⁶ Because the two latter studies were done in patients, no histological comparison was possible. Furthermore, MRI was performed, on average, 6 days after MI, which is much shorter than the follow-up of 5 weeks used in the present study.

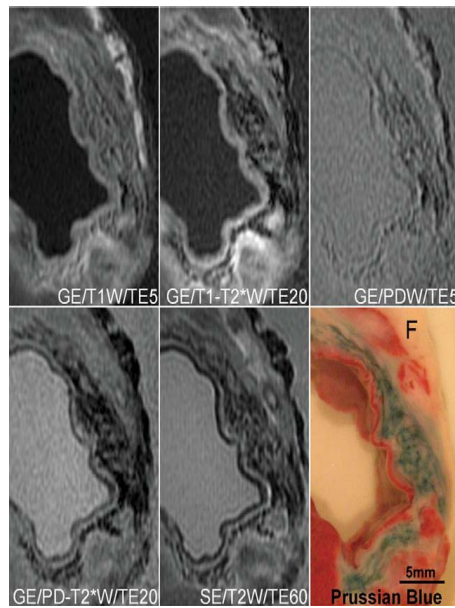


Figure 4 Ex vivo scans 5 weeks after infarction using various types of tissue contrast as described in Figure 3. Magnetic susceptibility-induced signal voids are observed throughout the infarct. Their size increases with T2*-weighting (TE 20 ms). Furthermore, signal voids correspond with blue haemosiderin deposits in the PB image. Epicardial fat, indicated by F, causes a hyperintense signal on the T1W scan and a hypointense signal on T2 and T2*W scans.

In contrast with intramyocardial haemorrhage, MRI appearance of intracranial haemorrhage has been given extensive attention.²¹ Intracranial haemorrhage causes accumulation of deoxyhaemoglobin within hours. Within days, deoxyhaemoglobin is oxidized to methaemoglobin, which causes T1 and T2 shortening owing to its paramagnetic properties and magnetic susceptibility effect.²⁷⁻²⁸ Therefore, the presence of methaemoglobin within intact erythrocytes causes hyperintense signals on T1W scans and hypointense signals on T2W scans, a pattern observed in the present study in subacute infarcts. With further degradation, haemosiderin deposits are formed,²¹ which remain chronically present.²⁹ Haemosiderin has a high magnetic susceptibility effect and thereby causes T2 shortening, resulting in signal voids on T1W, T2*W, and T2W images surrounding the brain haemorrhage from 2

weeks onwards, the so-called ‘ring’ pattern. In the present study, the same ring pattern was observed in subacute infarcts in the ex vivo scans. This difference in time course might be due to the higher in-plane resolution of ex vivo scanning, allowing early detection of such a pattern.

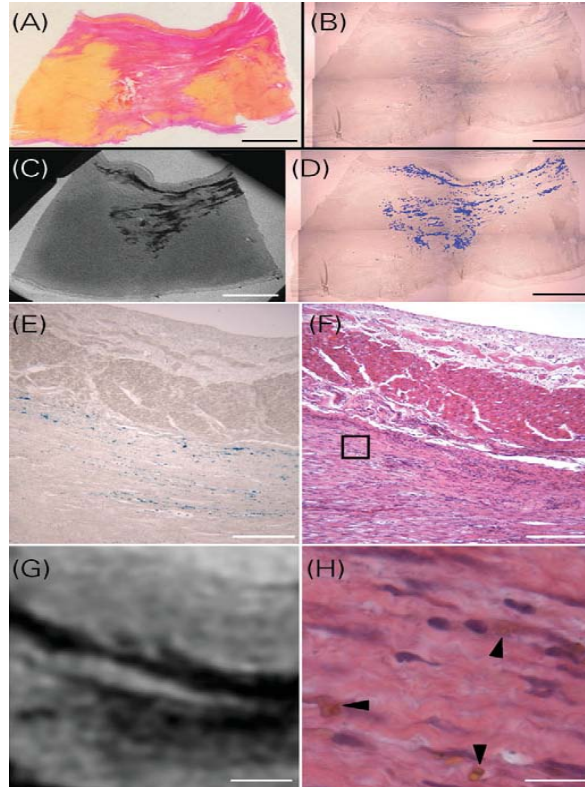


Figure 5 A tissue block from the infarct border of a 5-week-old infarction was scanned at high-resolution ex vivo. (A) shows the VK (calcium) and VG's (collagen) staining. Red staining corresponds with collagenous (scar) tissue. Yellow staining corresponds with muscle fibres. Black calcium deposits were not observed in this section. In (B), a serial section is shown after PB staining. (C) shows the corresponding slice from the MRI T2*W data set. (D) shows the same section as in (B); however, blue regions are artificially enhanced. MRI signal voids correspond with blue haemosiderin particles and not with calcium, fat, or collagenous tissue. (E) shows the same section as in (B) at higher magnification. Blue haemosiderin deposits can be appreciated. (F) shows a serial section after HE staining. (G) shows the corresponding region in the image of (A). Area of signal voids corresponds with blue haemosiderin deposits in (E). (H) shows the boxed region in (F) at higher magnification; haemosiderin deposits are visible as brownish particles (black arrows). Bar indicates 4 mm in (A–D), 400 μ m in (E–G), and 40 μ m in (H)

Iron oxide-labelled cell detection by MRI

Detection of iron oxide-labelled cells within MI has been described for mice^{9,10} and rabbit¹¹ models. Recently, several studies showed the feasibility of using iron oxide-labelled cells for clinically relevant, catheter-based delivery and cell tracking within MI in pigs. Infarcts were created by permanent coil occlusion^{16,17} or a 60–90 min balloon occlusion, followed by reperfusion of the infarct artery.^{12,13,15} Cells were injected immediately after infarction^{12,14} or into 1-day-,¹⁷ 1-week-,¹⁵ or 4-week-¹³ old infarcts.

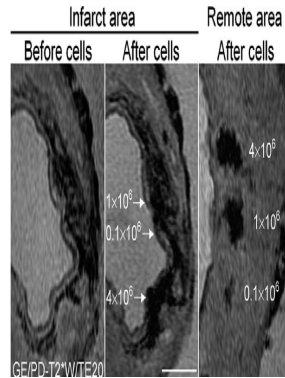


Figure 6 The left panel shows the GE/PD-T2*W/TE20 scan, depicted in Figure 4, before injection with iron oxide-labelled cells. The middle panel shows the same slice after injection with 0.1, 1, or 4×10^6 iron oxide-labelled cells. The right panel shows a similar series of injections in remote, non-infarcted myocardium. Although the cell injections create larger areas of signal voids in the middle panel, their precise location cannot be determined because of the signal voids induced by the presence of haemoglobin degradation products. Bar indicates 0.5 cm

None of these studies mentioned the presence of MO or haemorrhage within the infarct centre. In contrast, in the present study, MO was present in 17 out of 21 animals in subacute infarcts, and signal voids were identified in all animals on the ex vivo scans corresponding with haemorrhage on histology. The high frequency of MO and haemorrhage could possibly be explained by the longer occlusion times used in our study (i.e. 2 h vs. 60 or 90 min),^{12,13,15} approximating the time to reperfusion in the clinical setting more closely. The frequency of MO in the present study is indeed comparable with the frequency in patients reperfused early after MI.²² Despite the longer occlusion times, it has been shown that haemorrhage already occurs in the pig heart after coronary occlusions more than 45 min.³⁰

In a previous study, examining iron oxide-labelled cell detection in a mouse cryoinfarction model,¹⁰ the presence of 'spontaneous' signal voids within the infarct region was discussed. These signal voids were attributed to necrosis and fibrosis within the infarct scar. However, a recent study showed that cryoinfarction results in large areas of haemorrhage,³¹ which have most likely caused those signal voids. Furthermore, the problem of those spontaneous signal voids was purportedly solved by using a combination of PD- and T2*-weighted scanning: the areas with signal voids that were exclusively due to the tissue lesions would lead to similar signal void sizes in both imaging modalities. In contrast, the size of the signal voids generated by the presence of labelled cells was proposed to increase on T2*-weighted scans, thereby making unequivocal detection possible. However, Figures 3 and 4 clearly illustrate that the usefulness of this method could not be demonstrated in the present study, as the size of the haemorrhage-induced signal voids increased with a longer TE.

In studies of spinal cord regeneration by transplanted iron oxide-labelled cells,³²⁻³³ interference of haemorrhage with cell detection has been described as an important confounding factor. In one study, the discrimination between cells and haemorrhage was made by assessing the 'blooming' effect induced by iron oxide-labelled cells, where the distortion of the magnetic field occurs over a greater area than

the presence of the contrast agent.³² In another study, the use of imaging sequences less susceptible to haemorrhage-induced signal voids was proposed as a solution.³³

For cell detection *in vivo*, a certain number of labelled cells are necessary to obtain sufficient contrast with background tissue. For MI, the smallest number of cells needed for detection was reported to be 10^5 cells/150 mL,¹⁴ generating signal void volumes of 0.36 cm^3 . This study however was performed in a model of permanent occlusion in pigs. In three studies of porcine, reperfused infarct models, the number of cells per injection exceeded 28×10^6 .^{12,13,15} In the present study, the haemorrhage-induced signal voids in the *in vivo* scans had a mean total size of $0.53 \pm 0.51 \text{ cm}^3$ in subacute infarcts, and MRI of haemorrhage within reperfused MI therefore would possibly obscure detection of cell groups of 10^5 cells. Furthermore, CNR of signal voids identified on the T2*W *in vivo* scans were similar to the values previously reported for groups of iron oxide-labelled cells using similar scanning sequences.¹⁴ Finally, the *ex vivo* injections of iron oxide-labelled cells in the present study generated signal voids with a CNR similar to the haemorrhage-induced signal voids, thereby interfering with detection of the injected cells.

The presence of haemorrhage and visualization with longer TEs are important in relation to the injection route, as visualization of labelled cells was reported with local injections,¹²⁻¹⁷ although intracoronary injections have been used in most human studies.³ Using iron labelling to track these cells, which will presumably spread over a larger area, requires sequences with long TE, and the artefacts described in the present study are to be expected.

Study limitations

Because it is a very subjective process to match the image locations of *in vivo* scans with the locations of *ex vivo* scans on the basis of anatomical landmarks only, and because the slice thickness of *in vivo* scans was 6 or 8 mm compared with 0.8 mm of *ex vivo* scans, we chose to describe *in vivo* and *ex vivo* findings separately. Therefore, our data do not allow for a direct comparison between *in vivo* and *ex vivo* scans.

In the present study, a model of reperfused MI was used, causing large areas of haemorrhage. Therefore, it is not clear whether there is a difference in haemorrhage-induced artefacts in reperfused vs. non-reperfused infarcts in porcine models *in vivo*, although in similar canine models, no haemorrhage was observed when perfusion was not reinstated.²⁵

Only intramyocardial injections were performed in the present study using fixed, iron oxide-labelled cells, which were imaged after tissue preparation. Future studies are required to investigate whether haemorrhage-induced signal voids cause similar interference with cell detection after intracoronary injection *in vivo*.

Conclusion

The present study demonstrates that haemorrhage in reperfused MI produces MRI signal voids, which may interfere with reliable tracking of iron oxide-labelled cells.

Acknowledgements

This study was supported by ZON-MW Agiko stipend 920-03-191 (to E.J.B.) and by an ISHLT 2003 Research Fellowship Award (to E.J.B.).

References

1. Orlic D, Kajstura J, Chimenti S, Jakoniuk I, Anderson SM, Li B, Pickel J, McKay R, Nadal-Ginard B, Bodine DM, Leri A, Anversa P. Bone marrow cells regenerate infarcted myocardium. *Nature* 2001;410:701–705.
2. van den Bos EJ, Thompson RB, Wagner A, Mahrholdt H, Morimoto Y, Thomson LE, Wang LH, Duncker DJ, Judd RM, Taylor DA. Functional assessment of myoblast transplantation for cardiac repair with magnetic resonance imaging. *Eur J Heart Fail* 2005;7:435–443.
3. Schachinger V, Assmus B, Britten MB, Honold J, Lehmann R, Teupe C, Abolmaali ND, Vogl TJ, Hofmann WK, Martin H, Dimmeler S, Zeiher AM. Transplantation of progenitor cells and regeneration enhancement in acute myocardial infarction: final 1 year results of the TOPCARE-AMI Trial. *J Am Coll Cardiol* 2004;44:1690–1699.
4. Smits PC, van Geuns RJ, Poldermans D, Bountiokos M, Onderwater EE, Lee CH, Maat AP, Serruys PW. Catheter-based intramyocardial injection of autologous skeletal myoblasts as a primary treatment of ischaemic heart failure: clinical experience with six-month follow-up. *J Am Coll Cardiol* 2003;42:2063–2069.
5. Yeh TC, Zhang W, Ildstad ST, Ho C. Intracellular labeling of T-cells with superparamagnetic contrast agents. *Magn Reson Med* 1993;30:617–625.
6. Foster-Gareau P, Heyn C, Alejski A, Rutt BK. Imaging single mammalian cells with a 1.5 T clinical MRI scanner. *Magn Reson Med* 2003;49:968–971.
7. Shapiro EM, Skrtic S, Sharer K, Hill JM, Dunbar CE, Koretsky AP. MRI detection of single particles for cellular imaging. *Proc Natl Acad Sci USA* 2004;101:10901–10906.
8. Zhang Z, van den Bos EJ, Wielopolski PA, de Jong-Popijus M, Bernsen M, Duncker DJ, Krestin GP. In vitro imaging of single living human umbilical vein endothelial cells with a clinical 3.0 T MRI scanner. *MAGMA* 2005;18:175–185.
9. Himes N, Min JY, Lee R, Brown C, Shea J, Huang X, Xiao YF, Morgan JP, Burstein D, Oettgen P. In vivo MRI of embryonic stem cells in a mouse model of myocardial infarction. *Magn Reson Med* 2004;52:1214–1219.
10. Kustermann E, Roell W, Breitbart M, Wecker S, Wiedermann D, Buehrle C, Welz A, Hescheler J, Fleischmann BK, Hoehn M. Stem cell implantation in ischaemic mouse heart: a high-resolution magnetic resonance imaging investigation. *NMR Biomed* 2005;18:362–370.
11. van den Bos EJ, Wagner A, Mahrholdt H, Thompson RB, Morimoto Y, Sutton BS, Judd RM, Taylor DA. Improved efficacy of stem cell labeling for magnetic resonance imaging studies by the use of cationic liposomes. *Cell Transplant* 2003;12:743–256.
12. Kraitchman DL, Heldman AW, Atalar E, Amado LC, Martin BJ, Pittenger MF, Hare JM, Bulte JW. In vivo magnetic resonance imaging of mesenchymal stem cells in myocardial infarction. *Circulation* 2003;107:2290–2293.
13. Garot J, Untersee T, Teiger E, Champagne S, Chazaud B, Gherardi R, Hittinger L, Gueret P, Rahmouni A. Magnetic resonance imaging of targeted catheter-based implantation of myogenic precursor cells into infarcted left ventricular myocardium. *J Am Coll Cardiol* 2003;41:1841–1846.
14. Hill JM, Dick AJ, Raman VK, Thompson RB, Yu ZX, Hinds KA, Pessanha BS, Guttman MA, Varney TR, Martin BJ, Dunbar CE, McVeigh ER, Lederman RJ. Serial cardiac magnetic resonance imaging of injected mesenchymal stem cells. *Circulation* 2003;108:1009–1014.
15. Baklanov DV, Demuinck ED, Thompson CA, Pearlman JD. Novel double contrast MRI technique for intramyocardial detection of percutaneously transplanted autologous cells. *Magn Reson Med* 2004;52:1438–1442.
16. Karmarkar PV, Kraitchman DL, Izbudak I, Hofmann LV, Amado LC, Fritzges D, Young R, Pittenger M, Bulte JW, Atalar E. MR-trackable intramyocardial injection catheter. *Magn Reson Med* 2004;51:1163–1172.
17. Dick AJ, Guttman MA, Raman VK, Peters DC, Pessanha BS, Hill JM, Smith S, Scott G, McVeigh ER, Lederman RJ. Magnetic resonance fluoroscopy allows targeted delivery of mesenchymal stem cells to infarct borders in swine. *Circulation* 2003;108:2899–2904.

18. Giugliano RP, Braunwald E, The TIMI Study Group. Selecting the best reperfusion strategy in ST-elevation myocardial infarction: it's all a matter of time. *Circulation* 2003;108:2828–2830.
19. Rochitte CE, Lima JA, Bluemke DA, Reeder SB, McVeigh ER, Furuta T, Becker LC, Melin JA. Magnitude and time course of microvascular obstruction and tissue injury after acute myocardial infarction. *Circulation* 1998;98:1006–1014.
20. Reffelmann T, Kloner RA. Microvascular reperfusion injury: rapid expansion of anatomic no reflow during reperfusion in the rabbit. *Am J Physiol Heart Circ Physiol* 2002;283:H1099–H1107.
21. Bradley WG Jr. MR appearance of hemorrhage in the brain. *Radiology* 1993;189:15–26.
22. Baks T, van Geuns RJ, Biagini E, Wielopolski P, Mollet NR, Cademartiri F, Boersma E, van der Giessen WJ, Krestin GP, Duncker DJ, Serruys PW, de Feyter PJ. Recovery of left ventricular function after primary angioplasty for acute myocardial infarction. *Eur Heart J* 2005;26:1070–1077.
23. Lund GK, Stork A, Saeed M, Bansmann MP, Gerken JH, Muller V, Mester J, Higgins CB, Adam G, Meinertz T. Acute myocardial infarction: evaluation with first-pass enhancement and delayed enhancement MR imaging compared with 201Tl SPECT imaging. *Radiology* 2004;232:49–57.
24. Asanuma T, Tanabe K, Ochiai K, Yoshitomi H, Nakamura K, Murakami Y, Sano K, Shimada T, Murakami R, Morioka S, Beppu S. Relationship between progressive microvascular damage and intramyocardial hemorrhage in patients with reperfused anterior myocardial infarction: myocardial contrast echocardiographic study. *Circulation* 1997;96: 448–453.
25. Lotan CS, Bouchard A, Cranney GB, Bishop SP, Pohost GM. Assessment of postreperfusion myocardial hemorrhage using proton NMR imaging at 1.5 T. *Circulation* 1992;86:1018–1025.
26. Ochiai K, Shimada T, Murakami Y, Ishibashi Y, Sano K, Kitamura J, Inoue S, Murakami R, Kawamitsu H, Sugimura K. Hemorrhagic myocardial infarction after coronary reperfusion detected in vivo by magnetic resonance imaging in humans: prevalence and clinical implications. *J Cardiovasc Magn Reson* 1999;1:247–256.
27. Vymazal J, Brooks RA, Patronas N, Hajek M, Bulte JW, Di Chiro G. Magnetic resonance imaging of brain iron in health and disease. *J Neurol Sci* 1995;134:19–26.
28. Anzalone N, Scotti R, Riva R. Neuroradiologic differential diagnosis of cerebral intraparenchymal hemorrhage. *Neurol Sci* 2004;25:S3–S5.
29. Hardy PA, Kucharczyk W, Henkelman RM. Cause of signal loss in MR images of old hemorrhagic lesions. *Radiology* 1990;174:549–555.
30. Garcia-Dorado D, Theroux P, Alonso J, Elizaga J, Botas J, Fernandez-Aviles F, Soriano J, Munoz R, Solares J. Intracoronary infusion of superoxide dismutase and reperfusion injury in the pig heart. *Basic Res Cardiol* 1990;85:619–629.
31. van den Bos EJ, Mees BM, de Waard MC, de Crom R, Duncker DJ. A novel model of cryoinjury-induced myocardial infarction in the mouse: a comparison with coronary artery ligation. *Am J Physiol Heart Circ Physiol* 2005;289:H1291–H1300.
32. Dunning MD, Lakatos A, Loizou L, Kettunen M, French-Constant C, Brindle KM, Franklin RJ. Superparamagnetic iron oxide-labeled Schwann cells and olfactory ensheathing cells can be traced in vivo by magnetic resonance imaging and retain functional properties after transplantation into the CNS. *J Neurosci* 2004;24:9799–9810.
33. Dunn EA, Weaver LC, Dekaban GA, Foster PJ. Cellular imaging of inflammation after experimental spinal cord injury. *Mol Imaging* 2005;4:53–62.

Chapter 10

Summary and conclusions

Amber D. Moelker, MSc

Department of Experimental Cardiology, Thoraxcenter, Erasmus MC, Rotterdam, the Netherlands

Summary and conclusions

Coronary heart disease and heart failure continue to be significant burdens to healthcare systems in the Western world and are predicted to become so in emerging economies. Despite mixed results in both experimental and clinical studies, stem cell therapy is a promising option for patients suffering from myocardial infarction or patients with chronic heart failure after myocardial infarction. However, many issues in the field of cellular cardiomyoplasty still need to be resolved. This thesis describes the experiments performed in a pre-clinical model in swine with reperfused myocardial infarction aiming at addressing several of these issues.

Chapter two of this thesis shows that infarct size in swine can be measured accurately with multislice computed tomography, as compared to the “golden standard” histology. This study showed that myocardial viability can be assessed with multislice computed tomography. Furthermore, since we used magnetic resonance imaging in chapter three and four, we showed that for purposes of infarct size assessment multislice computed tomography compares well with magnetic resonance imaging, which is described in chapter three. Measurement of infarct size in patients with acute myocardial infarction is clinically relevant because infarct size is predictive of left ventricular function and geometric configuration and, hence, long-term clinical outcome. Information on infarct size obtained with multislice computed tomography would enhance the diagnostic armamentarium of physicians who lack access to cardiac magnetic resonance imaging or encounter patients who have contra indications to undergo magnetic resonance imaging.

The review of umbilical cord blood derived cells in the fourth chapter of this thesis shows a great potential of these cells to regenerate damaged myocardium. These cells can easily be obtained in large numbers and are not harvested from diseased individuals, therefore they have a great differentiation and proliferation capacity. Moreover, they do not raise ethical difficulties question, as do embryonic stem cells. In chapter five, the effect of umbilical cord blood cells is assessed with magnetic resonance imaging in a porcine model of myocardial infarction. There was no positive effect on left ventricular function or infarct size four weeks after injection of intracoronary administration of the umbilical cord blood cells, which what not very surprising since only a few of the injected cells survived. Therefore, the immunogenic status of these cells is not fully understood yet. However, this study shows that cultured umbilical cord blood cells should be used with caution when applied intracoronary, since their large cell size result in occluded blood vessels, thereby causing micro infarctions. Hence, it cannot be excluded that a possible positive effect of the umbilical cord blood derived cells was obscured by the induction of micro infarctions caused by the mode of administration. Therefore intracoronary application is not suitable for these cells. Although intracoronary injection is an easy and less invasive technique to administer cells post myocardial infarction, intramyocardial injection was shown to result in positive effects by Kim et al.

In contrast to the cells used in the initial experimental rodent studies, bone marrow derived mononuclear cells are the most common used cells in clinical trials. In chapter six the capacity of mononuclear cells and unselected bone marrow in a pre-clinical porcine model of reperfused myocardial infarction is evaluated. Our model closely mimics the clinical setting of myocardial infarction with regards to the route of administration and timing of stem cell therapy given in clinical trials. Four weeks after treatment with mononuclear cell injection a decrease in infarct size is observed as measured with magnetic resonance imaging. This was not observed after injection of unselected bone marrow. Histology showed that there was a trend towards more calcifications in the infarct area after the injection of unselected bone marrow. However, there was no beneficial effect of mononuclear cell or unselected bone marrow therapy on left ventricular function after myocardial infarction. Our results after mononuclear cell injection do not differ from those of the clinical trial performed in Leuven, Belgium by Janssens et al.

All clinical trials used the method of intermittent balloon occlusion during intracoronary injection of cells through the wire lumen of the balloon catheter, based on the assumption that this would yield increased adhesion of the injected cells to the vascular wall during the no-flow period, thereby leading to a higher cell engraftment. However, in our previous studies we used a selective probing injection catheter without interruption of blood flow. Therefore, we tested these different injection techniques in chapter seven. We observed no differences in the number of bone marrow mononuclear cells engrafted in the myocardium when applied through these two catheters (probing or balloon catheter). Therefore, the lack of effect on left ventricular function of bone marrow derived mononuclear cells in our study (which was described in chapter six), cannot be explained by the injection technique used.

Since cultured umbilical cord blood cells can cause micro infarctions when administered intracoronary in healthy myocardium (chapter five), we investigated in chapter eight whether cultured bone marrow derived mononuclear cells could cause micro infarctions four days after injection in healthy myocardium. We found that this was the case for cultured cells, but not for freshly isolated cells. Cultured cells are larger in size compared to freshly isolated cells, which result in the obstruction of the microcirculation. Although clinical trials suggest that intracoronary stem cell injection is safe, cultured stem cells should be used with caution when applied intracoronary.

The labeling of injected cells with iron to be able to track them *in vivo* with magnetic resonance imaging is assessed in chapter nine. This study showed that due to the hemoglobin breakdown products containing iron which is present in hemorrhagic areas in the reperfused infarct, iron labeling of intramyocardially injected cells is not suitable to track the stem cells after injection.

Future directions

Future studies are required to investigate whether hemorrhage induced signal voids cause similar interference with cell detection with magnetic resonance imaging after intracoronary injection in reperfused myocardial infarctions or after injection in non-

reperfused infarcts. Gadolinium may be a more suitable marker than iron to track cells *in vivo* with magnetic resonance imaging in reperfused myocardial infarctions.

It should be further investigated what the effect of injection of cultured cells is, when applying a different mode of administration, for example intramyocardial cell injection.

The effect of the stem cells used in our model seems to be disappointing compared to earlier study results in small rodents. It is possible that in our model bone marrow derived mononuclear cells will have a positive effect on left ventricular function in time. Therefore, in new experiments, swine should be monitored for a longer follow-up time, e.g. 2, 3, 6 and 12 months. For these experiments miniature swine should be used.

Differentiation of bone marrow derived stem cells *in vitro* towards cardiomyocytes is an option to enhance the effect of stem cell therapy in large mammals. However, it should always be tested whether these cultured cells induce microinfarctions when applied intracoronary. Pre-differentiation into cardiomyocytes might prevent the differentiation of injected cells into fibroblasts or inflammatory cells. The pre-differentiation might replace scar tissue by viable cardiomyocytes, and this might enhance the effect on infarct size on left ventricular function *in vivo* after injection. However, if the new cardiomyocytes are not able to survive in ischemic tissue, it should be investigated whether additional cytokine injections are needed to induce angiogenesis in the infarct tissue to enhance cell survival.

Patients benefit from optimal pharmacological treatment after myocardial infarction. Over time, ejection fraction will increase and infarct size will decrease in patients suffering from myocardial infarction due to remodeling which is influenced by optimal pharmacological treatment. Therefore, in a pre-clinical porcine model of myocardial infarction the combination of optimal pharmacological treatment and stem cell therapy could be tested to evaluate the additional effect of stem cell therapy on the recovery of function, infarct size and the remodeling after myocardial infarction.

However first, in animal models, it is necessary to determine the optimal cell number required to obtain optimal effects of the cells on infarct size and left ventricular function. It should be investigated how to access the cells (e.g. bone marrow aspiration versus cytokine mobilization), and whether they should be expanded *ex vivo*. Second, it should be determined which cell type will have maximal clinical effects. Third, the optimal delivery method will have to be determined. Finally, understanding the mechanism of cardiac regeneration in animals will shed a light on the optimal therapy for patients. The potential effect of stem cell therapy in patients should finally be assessed in large, randomized, placebo-controlled, double-blind clinical trials.

Chapter 11

Samenvatting

Amber D. Moelker, MSc

Department of Experimental Cardiology, Thoraxcenter, Erasmus MC, Rotterdam, the Netherlands

Samenvatting

Ondanks vele tegenstrijdige resultaten in zowel experimentele als klinische studies is stamcel therapie een veelbelovende optie voor patiënten met een myocard infarct, mede omdat er weinig alternatieve behandel methoden zijn voor patiënten met hartfalen.

In hoofdstuk twee van dit proefschrift is aangetoond dat je met “multislice computed tomography” nauwkeurig infarct grootte kan bepalen in varkens, dit is vergeleken met infarct grootte gemeten met histologie. Dit is de eerste studie die aantoont dat je met behulp van “multislice computed tomography” myocardiale viabiliteit kan meten. Aangezien het bepalen van infarct grootte van een acuut reperfusie infarct met behulp van “magnetic resonance imaging” ook nog onduidelijk was, is in hoofdstuk drie ook aangetoond dat “multislice computed tomography” ook goed te vergelijken is met “magnetic resonance imaging”, die we in hoofdstuk vijf en zes hebben gebruikt, als het gaat om infarct grootte.

In het review verhaal over navelstreng bloed cellen in hoofdstuk vier van dit proefschrift wordt de potentie van deze cellen om een infarct te regenereren duidelijk. Deze cellen kunnen makkelijk in grote aantallen gekweekt worden en ze zijn niet geogst van zieke donoren, waardoor ze een grote differentiatie en delings capaciteit hebben. Bovendien zijn er geen ethische bezwaren tegen het gebruik van deze cellen zoals bij embryonale stamcellen. In de studie beschreven in hoofdstuk vijf is met behulp van “magnetic resonance imaging” het effect van navelstreng bloed cellen bekeken in een varkensmodel met een myocard infarct. Er bleek geen positief effect te zijn op linker ventrikel functie of infarct grootte vier weken na injectie van de navelstreng bloed cellen, wat niet onverwacht was aangezien er maar een paar cellen overleeft waren. Hieruit bleek ook dat de immunogene status van deze cellen nog niet volledig is begrepen. Bovendien laat deze studie zien dat je voorzichtig moet zijn bij intracoronaire toediening van gekweekte navelstreng bloed cellen, omdat ze door de cel grootte bloed vaten kunnen verstoppen, wat kan leiden tot microinfarcten.

In tegenstelling tot de cellen die de eerste experimentele knaagdier studies gebruikten, zijn mononucleaire cellen uit het beenmerg de meest gebruikte cellen in klinische studies. In hoofdstuk zes wordt de capaciteit van deze cellen in een pre-klinisch varkens infarct-reperfusie model geëvalueerd. Ons model immiteert de klinische bepalingen van een myocard infarct en de route van toediening en het tijdstip van stamcel therapie in klinische studies. Vier weken na behandeling is er een verkleining van het infarct, gemeten met behulp van “magnetic resonance imaging”, waarneembaar. Er was echter geen effect van deze cel therapie op de linker ventrikel functie na het hartinfarct.

In alle voorgaande studies hebben we een probing katheter gebruikt om de cellen intracoronair toe te dienen, maar in de klinische studies is een ballon catheter gebruikt. Alle klinische studies gebruiken de onderbroken ballon occlusie tijdens cel injectie door het lumen van de ballon met de achterliggende gedachte dat de cellen sneller aan de vaatwand hechten tijdens deze periode zonder bloedstroom, wat zou

leiden tot een verhoogd aantal cellen dat in het infarct blijft hangen. We hebben in hoofdstuk zeven deze verschillende injectie katheters getest. Er was echter geen verschil in het aantal beenmerg mononucleaire cellen in het hart na injectie door deze twee katheters.

Omdat gekweekte navelstreng bloed cellen micro infarcten veroorzaken na intracoronaire injectie in gezond hartweefsel, hebben we in hoofdstuk acht onderzocht of gekweekte mononucleaire cellen uit het beenmerg ook micro infarcten veroorzaken, vier dagen na injectie in gezond hartweefsel. Dit blijkt het geval te zijn voor de gekweekte cellen, maar niet voor vers geïsoleerde cellen. Het moet nu verder onderzocht worden wat het effect is van een ander route van toediening, bij voorbeeld intramyocardiaal, voor gekweekte cellen.

De mogelijkheid om geïnjecteerde cellen met ijzer te labelen en *in vivo* te volgen met behulp van “magnetic resonance imaging” is bepaald in hoofdstuk negen. Door het in het reperfusie-infarct al aanwezige ijzer, blijkt ijzer-labeling geen goede optie om stamcellen te volgen na injectie.

Toekomstige studies

Voor het labelen van cellen moet in de toekomst worden onderzocht of wellicht gadolinium een betere methode is.

Tevens moet worden onderzocht of er na langere vervolging van mini-varkens wel een verbetering in linker ventrikel functie optreedt na injectie van beenmerg mononucleaire cellen.

Pre-differentiatie van de te injecteren cellen in een cardiovasculair fenotype zou er ook toe kunnen leiden dat er wel een verbetering in linker ventrikel functie optreedt na injectie van deze cellen na een myocard infarct.

Omdat patiënten profiteren van een optimale behandeling met medicijnen na een infarct, moet het onderzocht worden in een groot proefdier model wat het extra positieve effect van stamcellen bovenop de conventionele medische behandeling is. Uiteindelijk zal stamcel therapie in patiënten moeten worden onderzocht in grote, gerandomiseerde, placebo-gecontroleerde, dubbel-blinde studies.

Chapter 12

Over de Auteur

Over de auteur

Amber Dahvynya Moelker werd op 20 augustus 1979 in Rotterdam geboren. Zij groeide op in Roosendaal en behaalde haar VWO diploma in 1998 bij het Norbertus College te Roosendaal. Van 1998 tot 2002 studeerde zij Biologie aan de Universiteit Leiden. Een korte afstudeerstage werd gevolgd aan de “Kent State Unversity” in OHIO, USA in samenwerking met de Cleveland Clinic waarbij adulte en neonatale rat en muis myocyten geïsoleerd en in kweek gezet werden. De afstudeerstage betrof het ontwikkelen en opzetten van een muizen model voor het testen van stamcel transplantatie en cytokine injectie ter behandeling van hartfalen ten gevolge van een hartinfarct bij de afdeling Cardiologie van het LUMC te Leiden onder begeleiding van Prof. A. van der Laarse.

Vanaf september 2002 doet Amber promotie onderzoek naar stamcel therapie bij varkens met een myocard infarct. Dit onderzoek is ondergebracht bij het Thoraxcentrum van het Erasmus MC, de vakgroep Experimentele Cardiologie onder leiding van Prof. Dr. W. J. van der Giessen.



Chapter 13

Dankwoord

Dankwoord

Allereerst wil ik mijn promotores *Prof. dr. van der Giessen* en *Prof dr. Duncker* bedanken omdat zij mij de gelegenheid hebben geboden om bij de afdeling experimentele cardiologie te promoveren op een heel interessant en maatschappelijk relevant onderwerp.

Van mijn collega's van de afdeling experimentele cardiologie wil ik *Rob* graag bedanken omdat hij altijd klaar stond om technische problemen op te lossen of in no time moeilijke varkens catheteriseerde. *Carla* wil ik bedanken voor de snelle bestellingen die ze altijd deed en het begrip die alleen wij tweeën delen voor bepaalde buien die soms in de lucht hangen. Ik wil *Vincent* en *Kim* vooral bedanken voor de gein en gezelligheid die zij voor mij bij deze afdeling creëerden, zonder jullie zou het een stuk saaier zijn op de afdeling. *Miranda* wil ik ook bedanken, je hebt dezelfde grote passie als ik en gelukkig bleef je in de buurt werken. In mijn eerste jaren kon ik altijd erg goed praten met *Reier*; ik heb je gemist! *Marcel* wil ik bedanken voor alle nauwkeurige verwerkingen van de afgenomen beenmerg puncties. Ik vond het altijd zeer prettig om met je samen te werken. Het was altijd erg handig dat ik bij te weinig handen een student van *Daphne* kon lenen, bedankt hiervoor. In mijn eerste jaren hebben *Ewout* en *Wendy* geholpen met de experimenten, soms zelfs tot in de zeer late uren (02.30 uur 's nachts kan ik me zelfs voor de geest halen), hiervoor wil ik jullie bedanken. Ook *Ilona* was altijd bereid om te helpen op de OK met de varkens of door immuno's te doen, hiervoor mijn dank.

Van de afdeling radiologie wil ik *Piotr* en *Robert-Jan* bedanken die in eerste instantie zelfs in het weekend en de late avonduren hebben geholpen bij het opzetten van het MRI model voor varkens. En uiteraard gaat mijn grootste dank naar *Timo* die voor mij tientallen varkens gescand heeft, het was altijd erg gezellig tijdens het scannen.

Van de afdeling klinische genetica wil ik met name *Bert* bedanken voor het gebruik van de fluorescentie microscopen. Hij was altijd bereid om mij te helpen met zijn uitgebreide kennis van de fluorescentie.

Ik wil *mijn ouders* bedanken omdat zij het mogelijk gemaakt hebben om te gaan studeren en te promoveren. Ik hoop dat jullie allebei trots op me zijn.

Mijn paranimfen *Thierry* en *Olwen* wil ik bedanken, onder andere voor alle gezellige film avonden. Ik hoop dat er nog vele zullen komen.

Ricardo wil ik bedanken voor alle steun die hij me afgelopen tijd gegeven heeft. Hij is ondertussen erg belangrijk in mijn leven geworden.

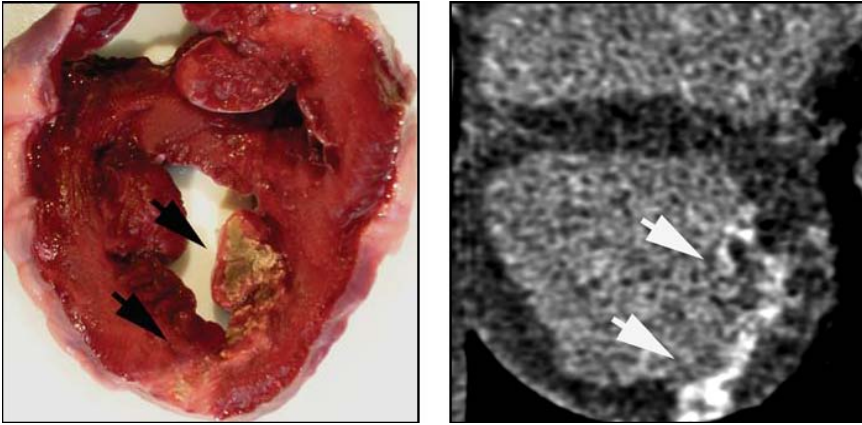
Ook wil ik *Amigo*, *Bentolino*, *Mary* en *Gill* toch ook even vermelden. Zij vormen de grote passie in mijn leven en maken mijn leven heel rijk.

Amber

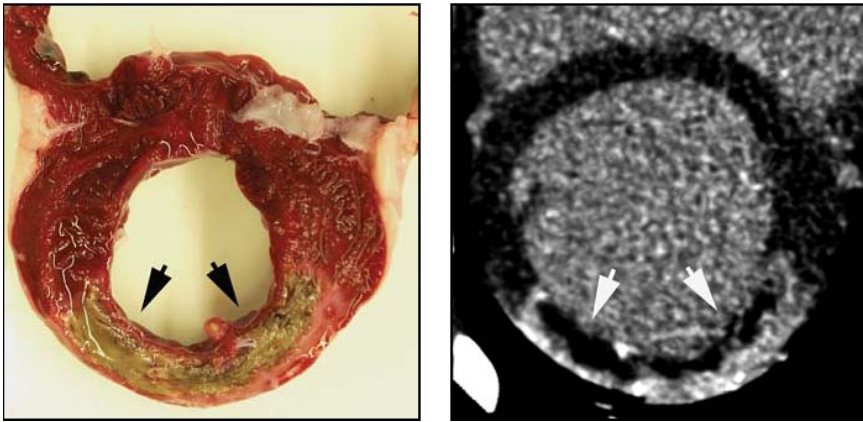
Chapter 14

Colour section

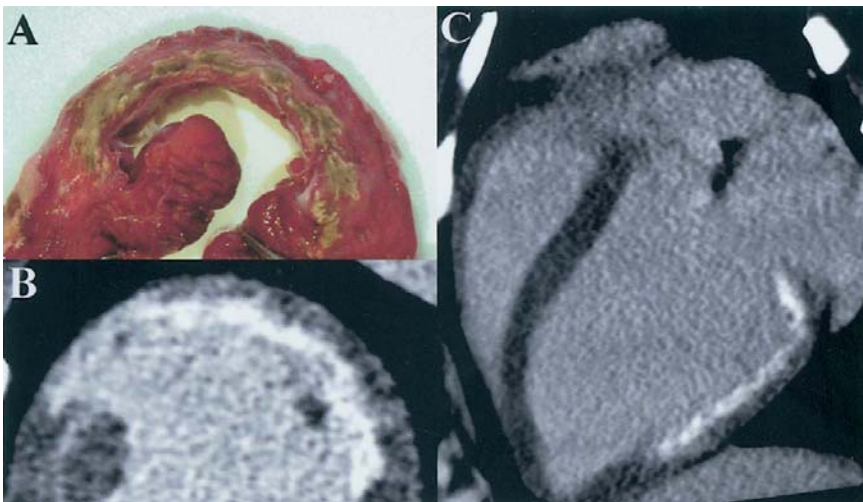
Colour section



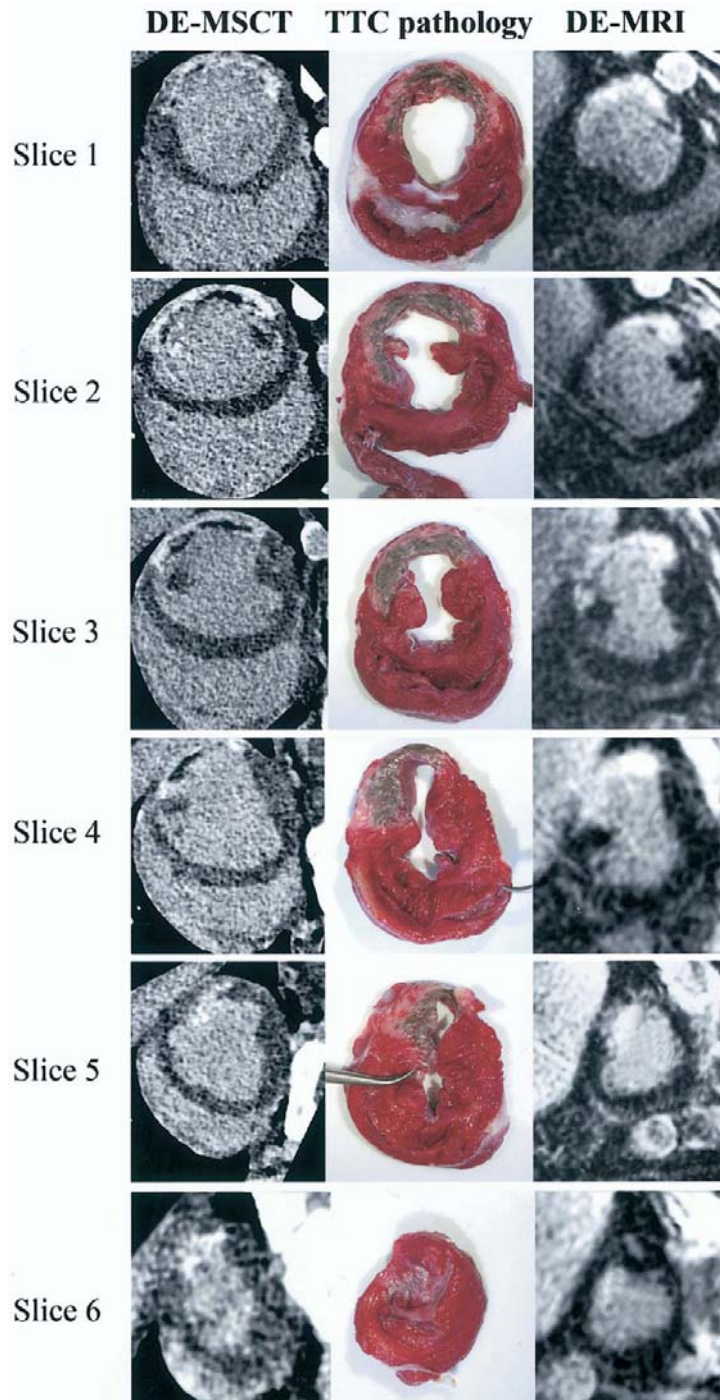
Chapter 2, Figure 1



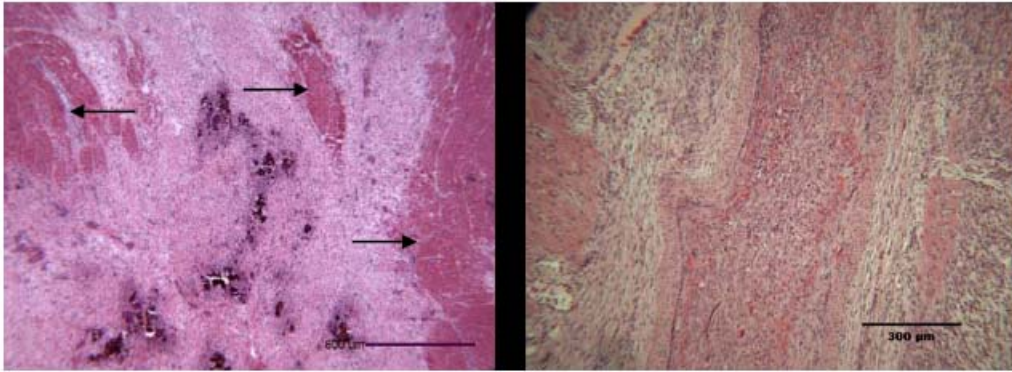
Chapter 2, Figure 2



Chapter 3, figure 2



Chapter 3, Figure 1

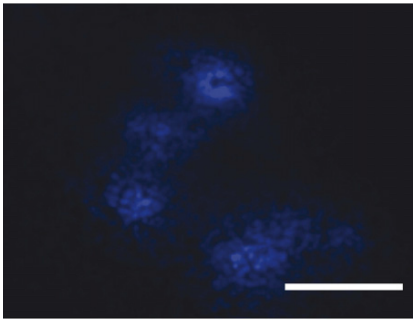


A.

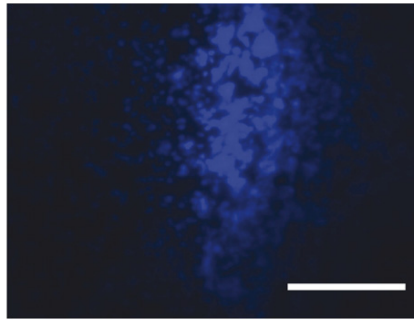
B.

Chapter 4, Figure 1

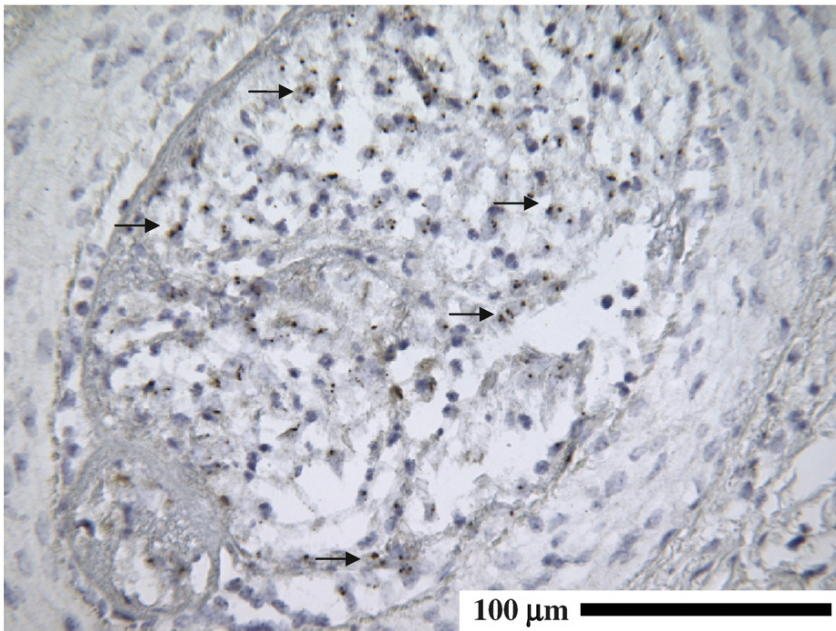
A.



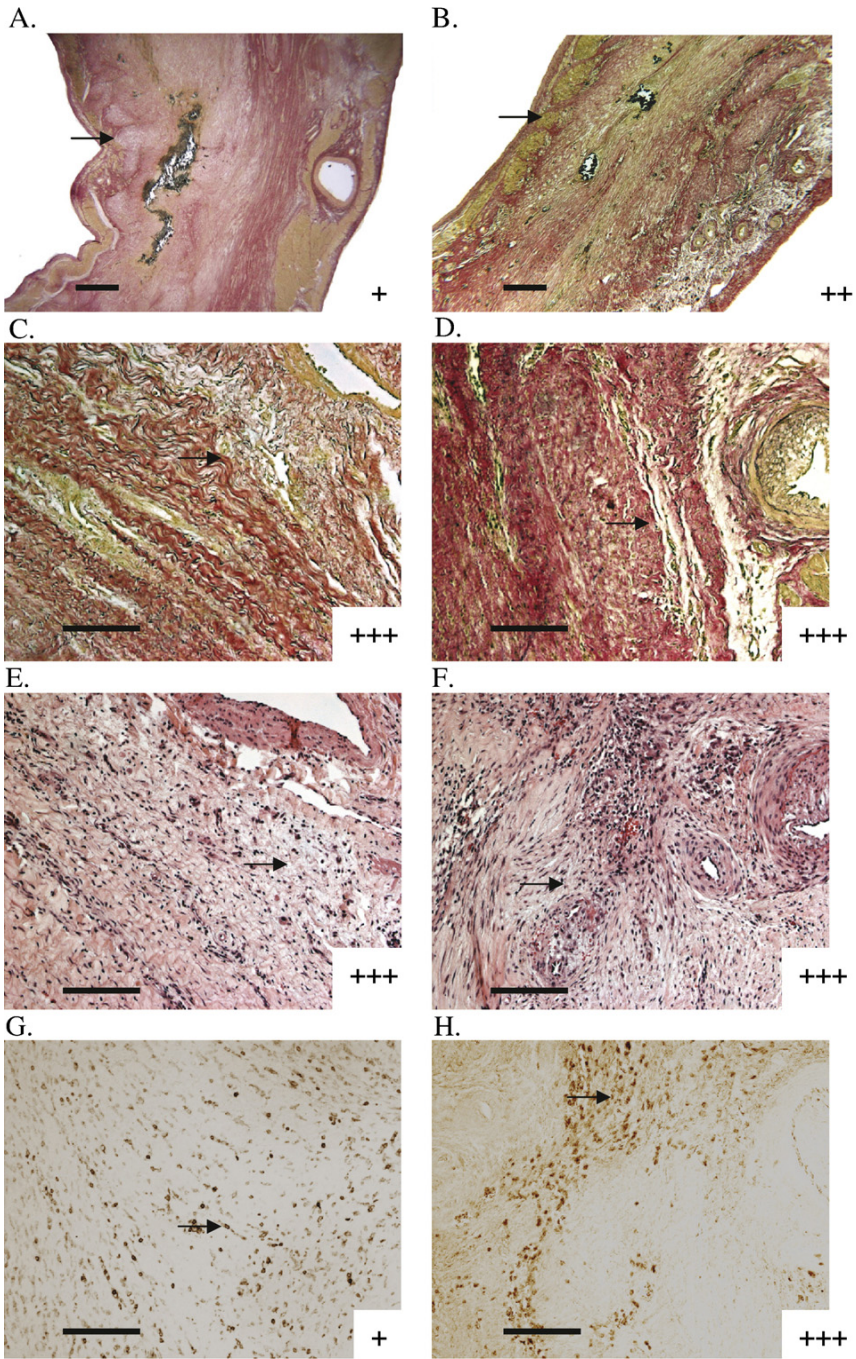
B.



C.

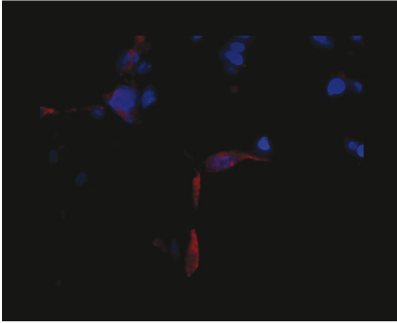


Chapter 5, figure 1

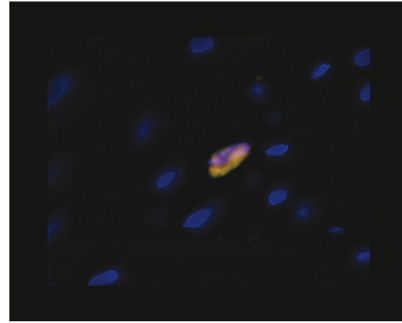


Chapter 5, figure 4

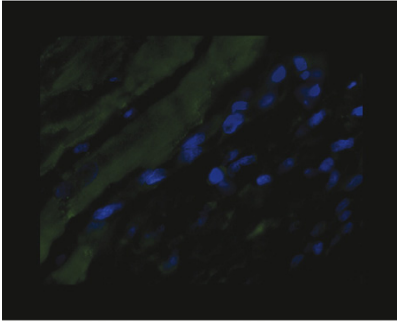
A. VWF



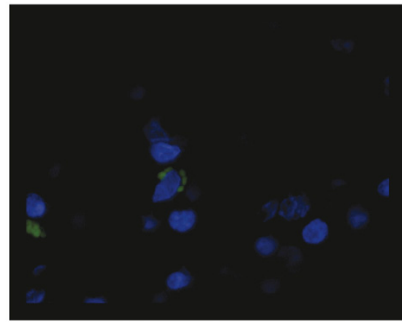
B. CD45



C. Troponin T

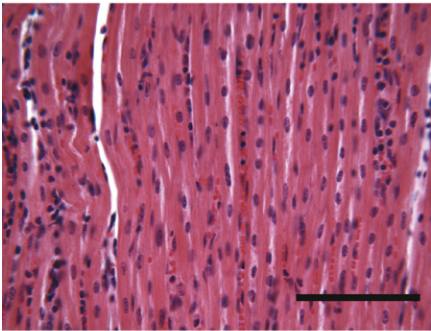


D. Human mitochondria

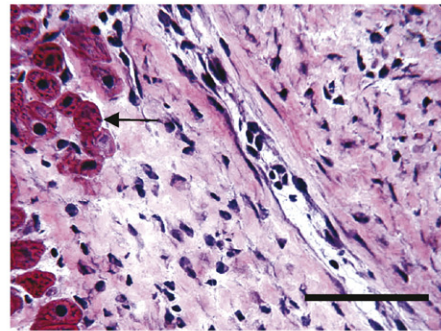


Chapter 5, figure 6

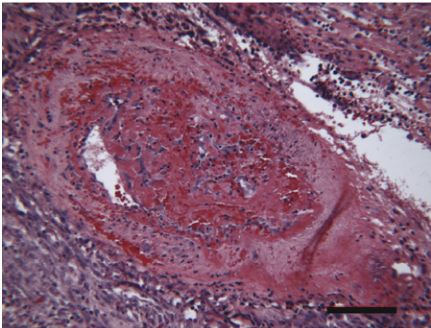
A.



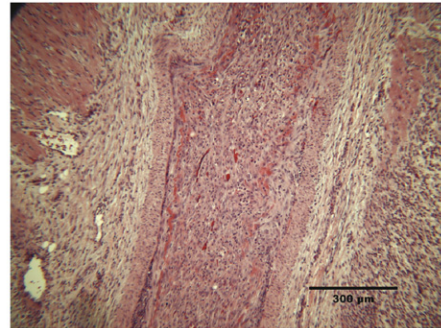
B.



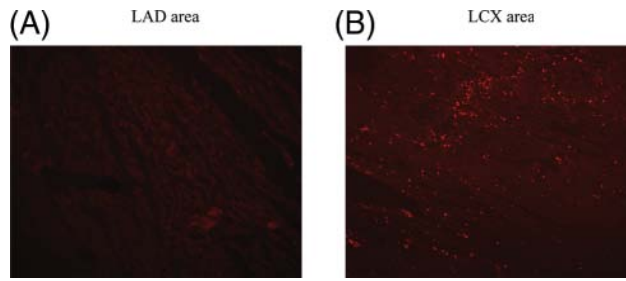
C.



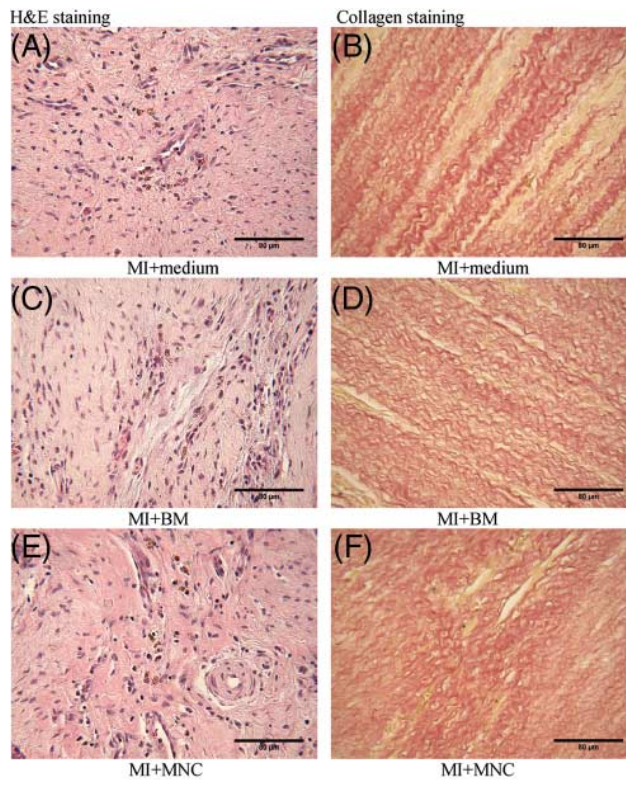
D.



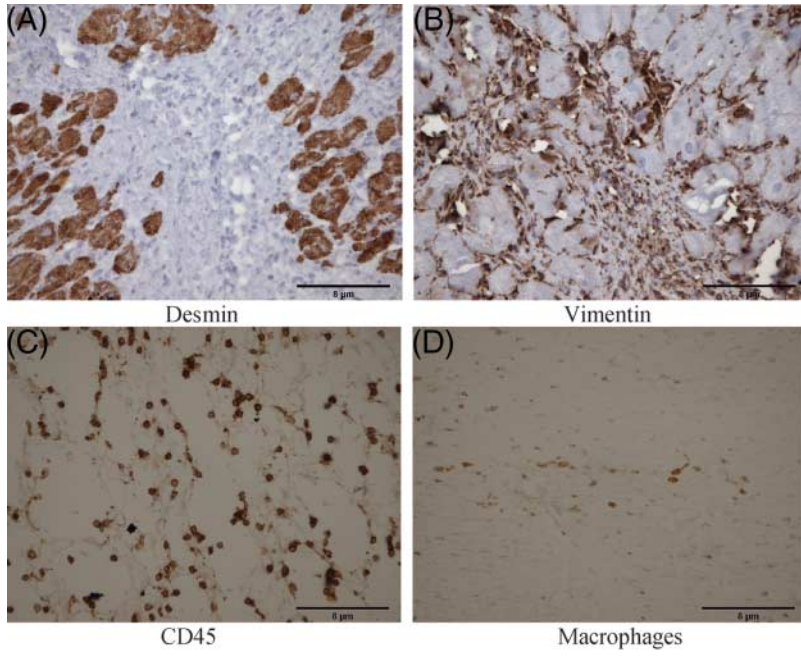
Chapter 5, figure 7



Chapter 6, figure 1



Chapter 6, figure 5

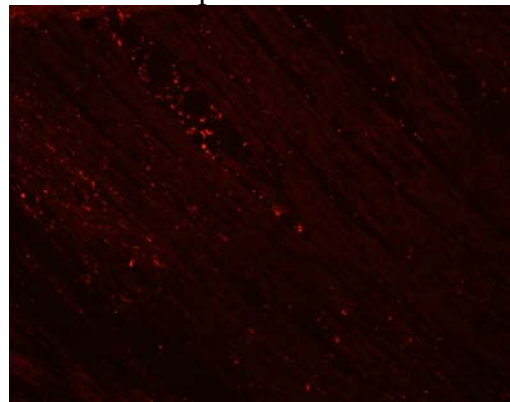
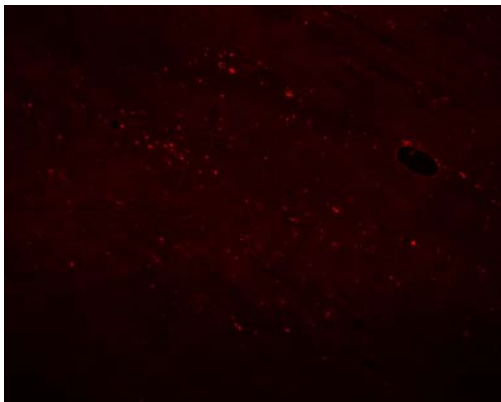


Chapter 6, figure 6

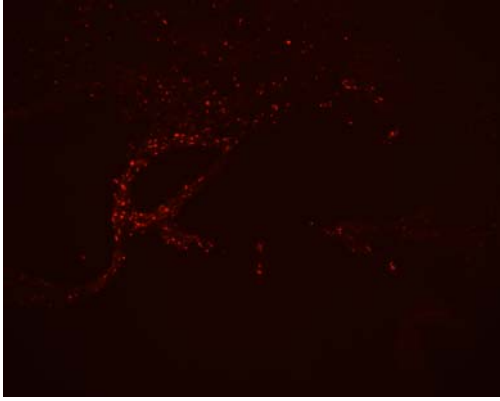
Normal flow

Interrupted flow

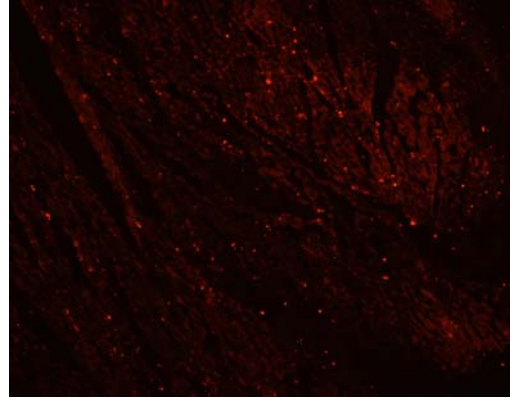
1,5h



4d

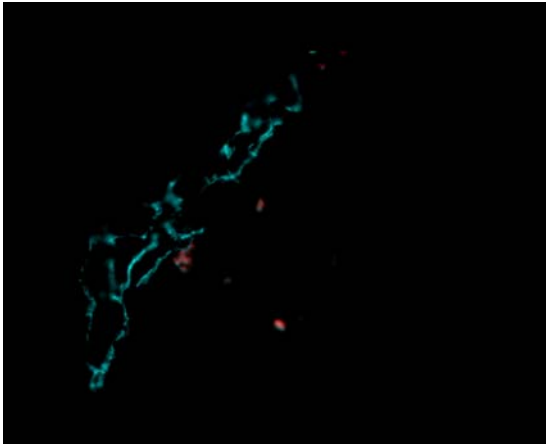


C.

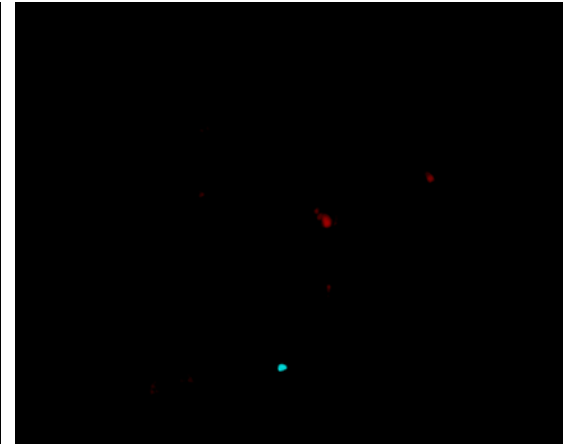


D.

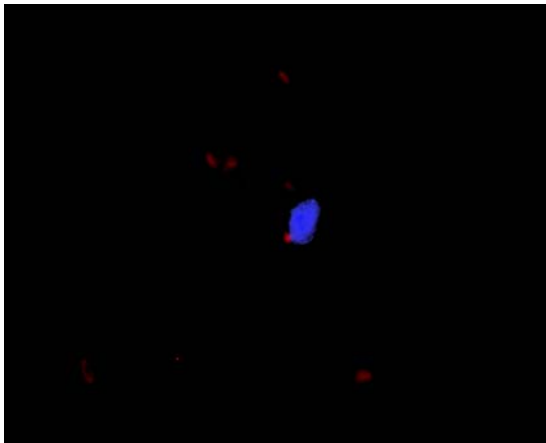
Chapter 7, Figure 1



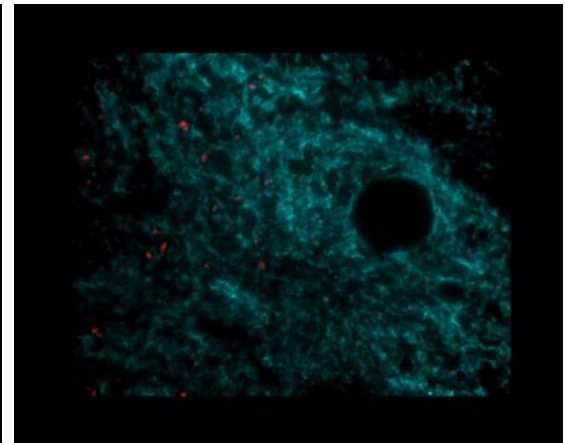
A.



B.

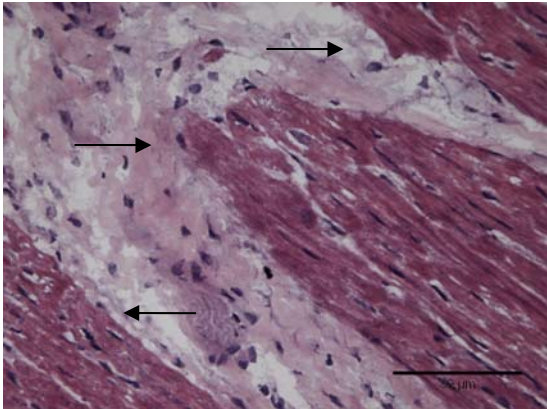


C.

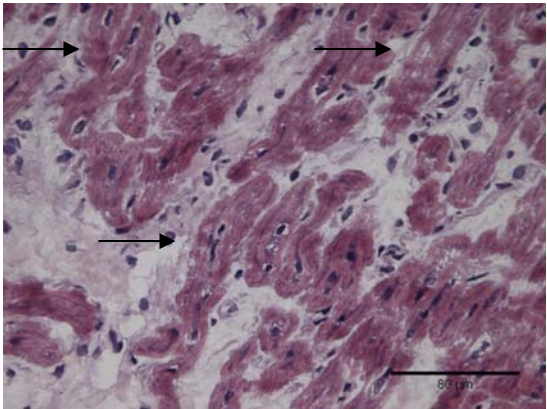


D.

Chapter 7, Figure 2



B.

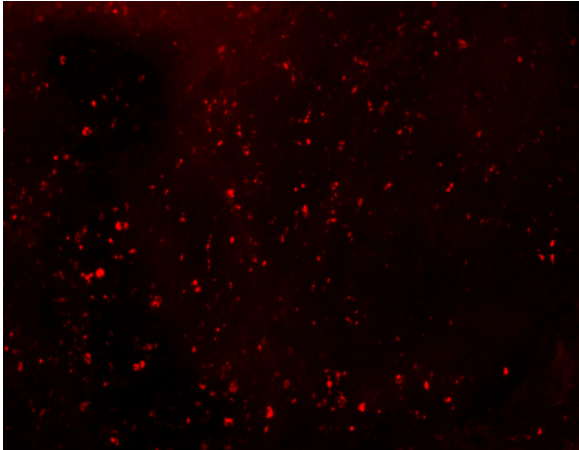


B.

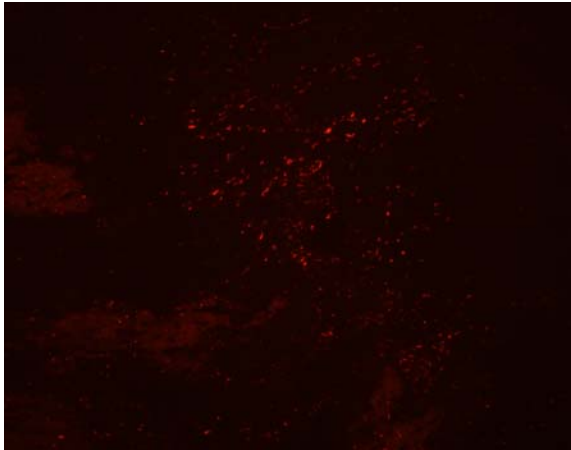
Chapter 8, Figure 2

Fresh MNC

Cultured MNC

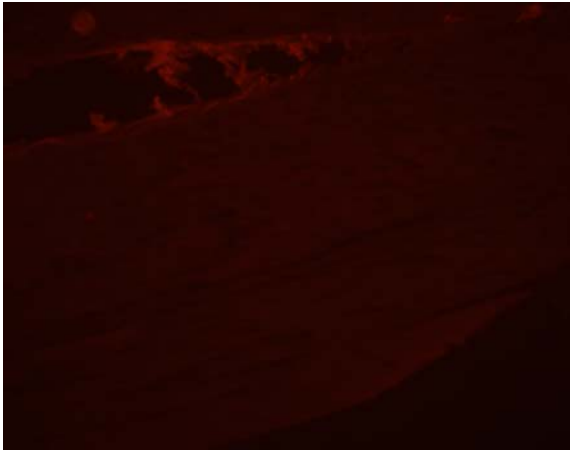


A.

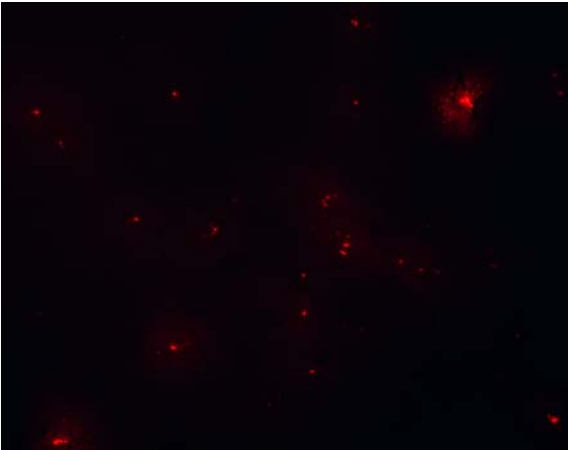


B.

LCX



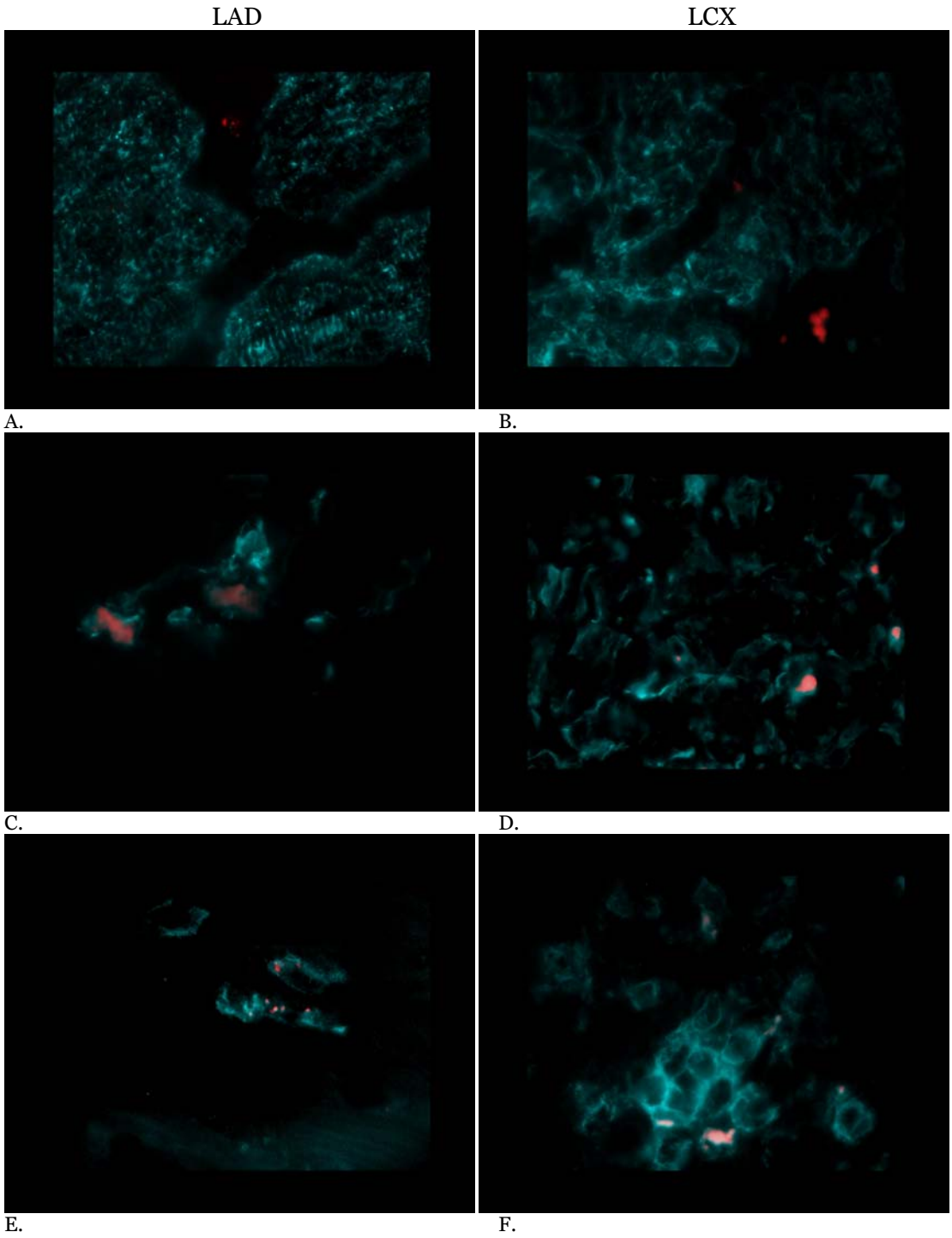
C.



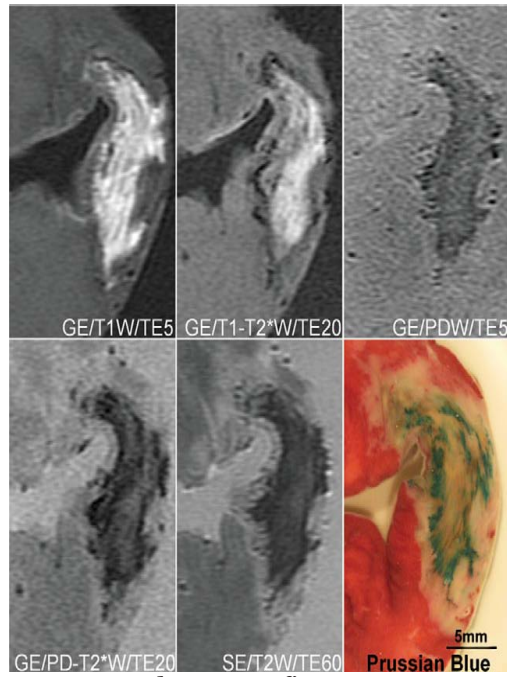
D.

LAD

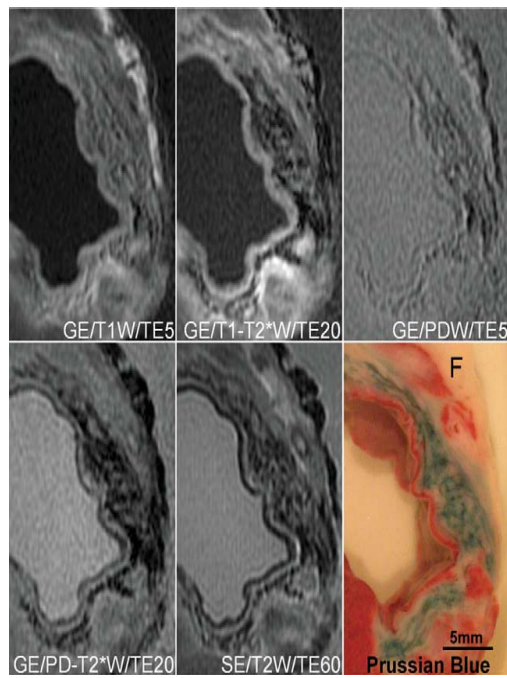
Chapter 8, Figure 3



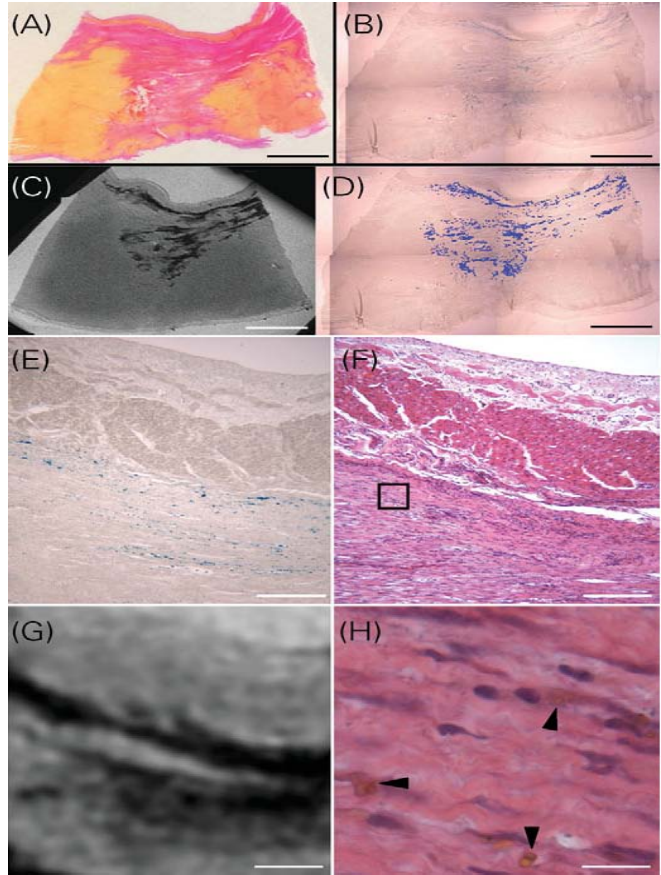
Chapter 8, Figure 4



Chapter 9, figure 3



Chapter 9, Figure 4



Chapter 9, Figure 5



